Energy, Exergy, Cost and Environmental Impact Assessments of Thermal Power Plants Integrated with Calcium Looping Process

Submitted in partial fulfillment of the requirements for the award of the degree of

DOCTOR OF PHILOSOPHY

in

CHEMICAL ENGINEERING

by

B. BASANT KUMAR PILLAI

(Roll No.716166)

Under the supervision of

Dr. A. SARATH BABU

Professor (Supervisor)

&

Dr. V. RAMSAGAR

Associate Professor (Co-supervisor)

DEPARTMENT OF CHEMICAL ENGINEERING

NATIONAL INSTITUTE OF TECHNOLOGY

WARANGAL- 506004, INDIA.

March 2023

NATIONAL INSTITUTE OF TECHNOLOGY WARANGAL
Warangal – 506004, Telangana, INDIA.

CERTIFICATE

This is to certify that the thesis entitled **"Energy, Exergy, Cost and Environmental Impact Assessments of Thermal Power Plants Integrated with Calcium Looping Process"** being submitted by **Mr. B. BASANT KUMAR PILLAI (Roll No.716166)** for the award of the degree of Doctor of Philosophy (Ph.D) in Chemical Engineering to the National Institute of Technology, Warangal, India is a record of the bonafide research work carried out by him under my supervision. The thesis has fulfilled the requirements according to the regulations of this Institute and in my opinion has reached the standards for submission. The results embodied in the thesis have not been submitted to any other University or Institute for the award of any degree or diploma.

Date: 27-03-2023

Dr. A. SARATH BABU
Thesis Supervisor
Professor,
Department of Chemical Engineering
National Institute of Technology
Warangal-506004, Telangana State
INDIA

DECLARATION

This is to certify that the work presented in the thesis entitled **"Energy, Exergy, Cost and Environmental Impact Assessments of Thermal Power Plants Integrated with Calcium Looping Process"** is a bonafide work done by me under the supervision of **Prof. A. Sarath Babu** and was not submitted elsewhere for award of any degree.

I declare that this written submission represents my ideas in my own words and where others' ideas or words have been included, I have adequately cited and referenced the original source. I also declare that I have adhered to all principles of academic honesty and integrity and have not misrepresented or fabricated or falsified any idea/data/fact/source in my submission. I understand that any violation of the above will be a cause for disciplinary action by the Institute and can also evoke penal action from the sources which have thus not been properly cited or from whom proper permission has not been taken when needed.

B. BASANT KUMAR PILLAI

(Roll No.716166)

Acknowledgements

I am extremely indebted to my guide **Dr. A. Sarath Babu,** Professor and my co-guide **Dr. V. Ramsagar**, Associate Professor, Department of Chemical Engineering, National Institute of Technology, Warangal for giving me the opportunity to work under them. Their expertise and knowledge have helped immensely in carrying out the research work. Without their motivation and continuous encouragement, this research would not have been successfully completed.

I am grateful to the university authorities, **Prof. N.V. Ramana Rao**, Director, NIT Warangal and other top officials who gave me an opportunity to carry out the research work. I also sincerely thank **Dr. S. Srinath**, Head, Chemical Engineering Department, NIT Warangal and **Dr. Shirish H Sonawane,** Professor and former Head, Chemical Engineering Department, NIT Warangal for their continuous support towards carrying out the research work and for providing necessary facilities in the department.

I would like to give my special thanks to **Dr. P. V. Suresh**, Professor, Department of Chemical Engineering, NIT Warangal for his personal guidance, constructive criticism and his extensive discussions about the work which helped in shaping of the thesis.

I wish to express my sincere and whole-hearted thanks and gratitude to Doctoral Scrutiny Committee (DSC) members, **Dr. S. Vidyasagar**, Associate Professor, Department of Chemical Engineering, **Dr. D. Jaya Krishna**, Professor, Department of Mechanical Engineering, NIT Warangal for their kind help, encouragement and valuable suggestions for successful completion of research work. I would like to express heart-felt thanks to former DSC member **Prof. Y. Pydi Setty**, Department of Chemical Engineering, NIT Warangal for his encouragement, motivation, care and support.

I sincerely acknowledge S. Gajanan Dattarao, Mukul Anand, D. Kiran, Shailesh Sikharwar, Abdul Gaffar and Bidesh for their support and feedback in this research work. I would like to express my deepest thanks to Chaithanya Sudha, for her constant support in each phase of my doctoral study. I want to thank my parents and brother for their presence in each moment. I am grateful to them for their never-ending love, patience and encouragement.

Date: 27/03/2023 **B. BASANT KUMAR PILLAI**

Abstract

In the study, the biomass, coal and natural gas fired power plants were integrated with single and double calcium looping configurations to explore the efficient carbon capture and sequestration/utilization/hydrogen co-generation options. These integrated configurations are systematically analyzed based on overall energy, exergy, environmental and cost parametric indicators. The performance of proposed carbon capture and sequestration power plant configurations were compared with their respective reference biomass, coal and natural gas fired power plants. The carbon capture integrated coal fired power plant was further extended to explore an efficient electricity and hydrogen co-production scheme. Similarly two different carbon capture and utilization configurations namely (i) conventional dry reforming based dimethyl ether production unit coupled with double calcium looping integrated natural gas fired combined cycle power plant and (ii) Solar energy aided dimethyl ether production unit coupled with double calcium looping integrated natural gas fired combined cycle power plant were explored for DME production and power cogeneration.

The results from the comparative assessment indicates that the biomass, coal, natural gas fired power plants integrated with double calcium looping CO_2 capture scheme have superior energy, exergy and environmental performance than the single calcium looping integrated power plant configurations. The research work also reveals that the levelized cost of electricity and levelized product of hydrogen for the hydrogen production unit coupled with conventional calcium looping integrated coal fired power plant were 69.40 €/MWh and 2.34 €/kg, while hydrogen production unit coupled with double calcium looping integrated coal fired power plant configuration has 58.51 €/MWh and 2.11 €/kg respectively. Finally, to improve the energy and exergy efficiency of calcium looping integrated natural gas fired combined cycle power plant and make the process environmentally sustainable, the captured CO_2 is utilized for dimethyl ether production. Compared to a conventional dry reforming based dimethyl ether production process, the integration of solar energy aided dimethyl ether production with double calcium looping integrated natural gas fired combined cycle power plant configuration has less levelized cost of electricity and levelized product cost of dimethyl ether. The outcome of this study can provide the basis for potential improvement of biomass and fossil fuel fired power plants integrated with calcium looping based on CO_2 capture based on thermodynamic, environment and cost analysis.

Keywords: Calcium looping, Carbon capture and sequestration, Carbon Capture and Utilization, Carbon Capture and hydrogen co-production, Dimethyl ether production

Table of contents

List of Figures

List of Tables

Nomenclature

Greek Letters

λ	exergy destruction ratio
η	energy efficiency
φ	multiplication factor
ψ	exergy efficiency

Subscripts

aux	auxiliary power consumptions
b	biomass
bp	biomass fired power plants
c	coal
$C1$	base case configuration
Ci	proposed configuration
CO_2cap	CO_2 captured
CO_2e	CO_2 emission
CO_2ut	CO_2 utilized
$comp$	air compressors
cp	coal fired power plants
$dest$	destruction
dme	dimethyl ether
dnp	dimethyl ether production and calcium looping units integrated natural gas fired combined cycle power plant
dpu	input stream of natural gas supplied to the dimethyl ether production unit
$genCO_2$	CO_2 generated
$gross$	gross output
H_2	hydrogen
hcp	hydrogen production and calcium looping units integrated coal fired power plant
i	yearly project interest rate
in	input
N	power plant life
net	net output
ng	natural gas
ngp	natural gas fired combined cycle power plants
o	overall
out	output
$pump$	pumps
s	solar energy input stream

Acronyms

ASS	air separation system
BFPP1	standalone biomass fired power plant
BFPP2	conventional calcium looping integrated biomass fired power plant
BFPP3	double calcium looping integrated biomass fired power plant

C	carbon
c_F	cost of exergy associated with the fuel
CA	CO_2 emission avoided cost
$CaCO_3$	calcium carbonate
CaO	calcium oxide
CC	overall cost
CCaLU	conventional calcium looping unit
CCE	CO_2 capture efficiency
CCHC	carbon capture and hydrogen cogeneration
CCS	carbon capture and sequestration
CCU	carbon capture and utilization
CD	cost associated with exergy destruction
CFPP1	Indian coal fired power plant
CFPP2	conventional calcium looping integrated coal fired power plant
CFPP3	double calcium looping integrated coal fired power plant
CH_4	methane
CSP	concentrated solar power
CU	CO_2 compression unit
CUE	CO_2 utilization efficiency
DCaLU	double calcium looping unit
DME	dimethyl ether
DMESR	dimethyl ether synthesis reactor
DNGFCPP1	conventional dry reforming based dimethyl ether production unit coupled with double calcium looping integrated natural gas fired combined cycle power plant
DNGFCPP2	solar energy aided dimethyl ether production unit coupled with double calcium looping integrated natural gas fired combined cycle power plant
DPU	dimethyl ether production unit
DRR	dry reforming reactor
DSU	dimethyl ether separation unit
E	energy
Ex	exergy
f	exergoeconomic factor
FC	fuel cost
GHG	greenhouse gas
GPGU	gas power generation unit
h	latent heat of vaporization
H_2	hydrogen
HCFPP1	hydrogen production unit coupled with conventional calcium looping integrated coal fired power plant
HCFPP2	hydrogen production unit coupled with double calcium looping integrated coal fired power plant
HCU	H_2 compression unit

HHV	higher heating value
HPT	high pressure turbine
HPU	hydrogen production unit
HRSG	heat recovery steam generator
IGCC	integrated gasification combined cycle
IPT	intermediate pressure turbine
LCOE	levelized cost of electricity
LHV	lower heating value
LPCD	levelized product cost of dimethyl ether
LPCH	levelized product cost of hydrogen
LPT	low pressure turbine
m	mass flowrate
MC	maintenance cost
MEA	mono-ethanolamine
n	unit or component
N_2	nitrogen
NGFCPP1	natural gas fired combined cycle power plant
NGFCPP2	conventional calcium looping integrated natural gas fired combined cycle power plant
NGFCPP3	double calcium looping integrated natural gas fired combined cycle power plant
O_2	oxygen
ORC	organic rankine cycle
RCa.C	CaO circulation rate per unit of CO_2 in flue gas
S	sulphur
SCE	specific CO_2 emission
$SCEx$	specific exergy
SPGU	steam power generation unit
T	temperature of the absorber in concentrated solar power system
T_o	reference (atmosphere) temperature
TCR	total capital requirement
UA	thermal capacity
VAR	vapor absorption refrigeration
w	mass fraction of moisture
W	work
Z	cost associated with capital investment

CHAPTER 1

INTRODUCTION

Chapter 1

Introduction

Energy plays a very critical role in the socio-economic development of any country. It is a well-known fact that human beings are the most intelligent species on earth and have invented different products for improving their quality of life. All these products directly or indirectly require energy and because of this per capita energy requirement increases gradually. The world's total energy consumption in the year 1973 was only 6098 Mtoe that has grown tremendously to 14282 Mtoe by the year 2018 (IEA., 2020c). The data reveals that as the industrial revolution has proliferated across different nations, the world energy consumption and demand also increased collectively. At present, a major part of this energy demand is fulfilled by fossil fuels such as coal, oil and natural gas. Fossil energy plays an important role in the near future, since fossil fuels have a higher energy density than renewables and have established technologies for harvesting energy.

In this 20^{th} century, while the energy consumption of countries like the USA and Germany have shown the largest downturns, China has become the major energy consumer that is utilizing more than three-quarters of the world's total energy (Looney, 2020). India is also one of the major developing economies in the world, where energy needs are rising at a rapid pace (Singh et al., 2017). A significant part of this need is fulfilled by fossil fuel based power plants such as coal and natural gas fired combined cycle power plants (Singh and Sharma., 2016; Lakshmi et al., 2019). Nonetheless, these fossil fuels are also a major source of Greenhouse Gas (GHG) emissions i.e., mostly carbon dioxide (CO_2) that causes climate change. Therefore, in order to limit climate change, India is adopting policies and exploring various carbon mitigation techniques.

Generally, renewable energy technologies are considered to be the best substitutes to solve this problem of GHG emissions. However, it has been found out that fossil fuels will continue to dominate for a fair period of time because of the less competitiveness of renewable energy technologies as compared to the conventional sources of energy such as natural gas and coal (Rafiee et al., 2018). Carbon capture and sequestration (CCS), Carbon capture and utilization (CCU) and carbon capture and hydrogen cogeneration (CCHC) techniques are few sustainable approaches which can be easily integrated with fossil fuel fired power plants for minimization of greenhouse gas emissions. In addition to that, India being an agricultural based country produces

a significant amount of biomass (considered as a carbon neutral fuel) that can be used for rural electrification via biomass-based power plants. Coupling biomass power plant with CO_2 capture is a promising option to enable a 'carbon neutral' technology to a 'carbon negative' technology. Thus, there is a greater need to identify the viability of CCS/CCU/CCHC techniques in coal, natural gas and biomass fired power plants for India. These techniques not only will help to build a sustainable way of energy generation along with renewables in India but will also majorly contribute to the whole world to mitigate the greenhouse gas emissions.

The rest of this chapter is organized as follows, section 1.1 explains the current status on fossil energy (coal, natural gas) and biomass energy share in electricity generation in India and across the world. Section 1.2, presents the recent greenhouse gas emission trends in India and across the world and possible mitigation opportunities. Section 1.3, details the most potential CO_2 mitigation techniques such as CCS,CCU and CCHC. The motivation and objectives behind the proposed research are highlighted in section 1.4 and 1.5. At the end, a broad outline and organization of the thesis is presented in section 1.6.

1.1 Overview of coal, natural gas and biomass energy based power plants

In this section, the importance of coal, biomass and natural gas fired power plants in electricity generation in India and the world is highlighted. The presented statistics will help to understand the dominance of these energy sources in power generation. Subsequently, the presented CO_2 emission statistics will highlight the environmental impact.

1.1.1 Energy from coal fired power plants - Status in World and India

Coal fired power plants generate electricity by burning coal as fuel. Generally, in this system, the heat energy developed from coal combustion is used to generate steam at very high pressure. The turbine is powered by high-pressure steam, which ultimately turns the generator and produces electricity. Since the operation of the world's first coal fired power plant in the year 1882 by Thomas Edison in New York (Xu et al., 2018; Parsons., 2015), the rapid progress in its technology has paved the way for the establishment of a large number of coal fired power plants worldwide for power generation. Today the coal fired power plants are categorised into four types i.e., circulating fluidised bed combustion, pressurised fluidised bed combustion, integrated gasification combined cycle (IGCC) and pulverised coal fired power plants. These can be further

classified into subcritical, supercritical, advanced supercritical and ultra-supercritical types based upon the operating steam pressure (Lako., 2004). Among all these categories, the pulverised CFPPs are widely used around the world. Currently there are around 2,425 active coal fired power plants, around the world, producing 2,000 GW of electricity and releasing 15 billion tonnes per year of CO_2 into the atmosphere (Desjardins., 2019). As per the International Energy Outlook report, the global energy demand is going to increase continuously in the 21st century.

A majority of this energy consumption is going to be in highly populated countries like Brazil, China and India (IEO., 2016). India's coal consumption in 2018 contributes to around 45% of the country's total energy consumption (as shown in Fig. 1.1A) and is the second largest coal consuming country after China. In India as on 2020, the coal fired power plants account 55% of the total installed capacity (i.e., around 370 gigawatts), while renewable energy accounts for 24% only as shown in Fig. 1.1B. Major reasons for dependency on coal fired power plants are: the abundant availability of coal in the country at a low cost, technology availability, and the ability to consistently meet the base load demand (EIA India., 2020). Keeping all this in view, it is very much clear that the coal fired power plants are going to play a prominent role at present and in near future to meet India's electricity demand. Having said that, it is also quite evident from the literature mentioned earlier (Desjardins., 2019), that these coal-fired power plants are also major emitters of greenhouse gases mainly CO_2.

1.1.2 Energy from gas fired power plants – Status in World and India

Gas fired power plant is another fossil fuel-based power plant that produces electricity by using natural gas as fuel. Likewise in coal fired power plant, in this system the chemical energy of natural gas is initially transformed into heat energy, then to mechanical energy and at last into electrical energy. Initially, the growth in gas power technology was not significant. However, during the world wars, the need for innovations in aircraft technology, manufacturing and engineering advancement has provided this technology with major upgrades (Harvey et al., 2022).

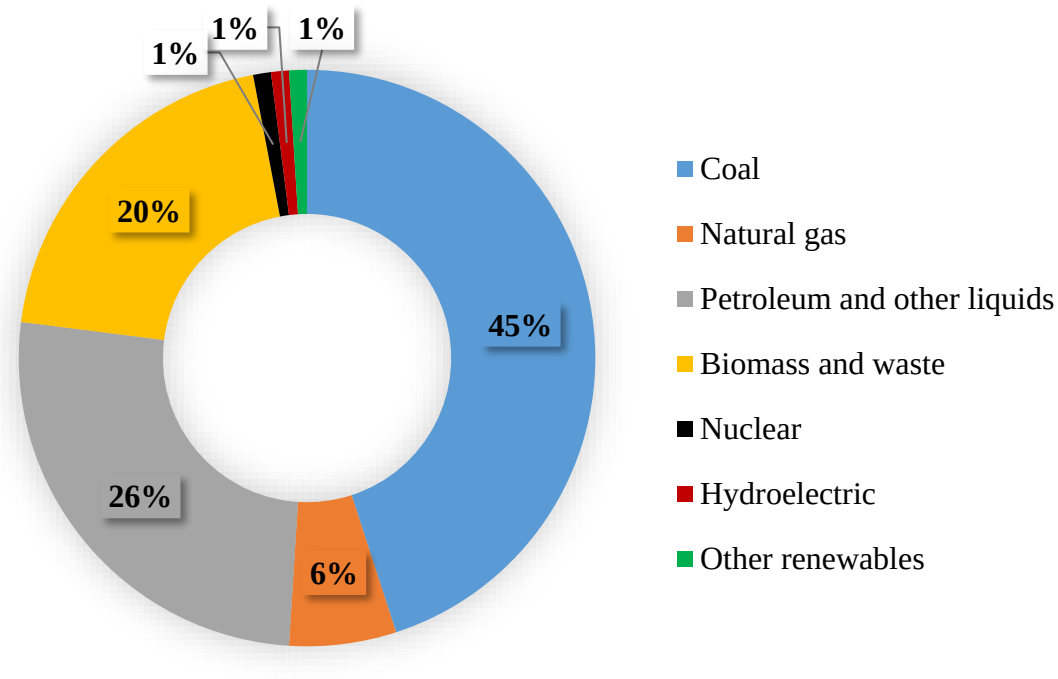

(A)

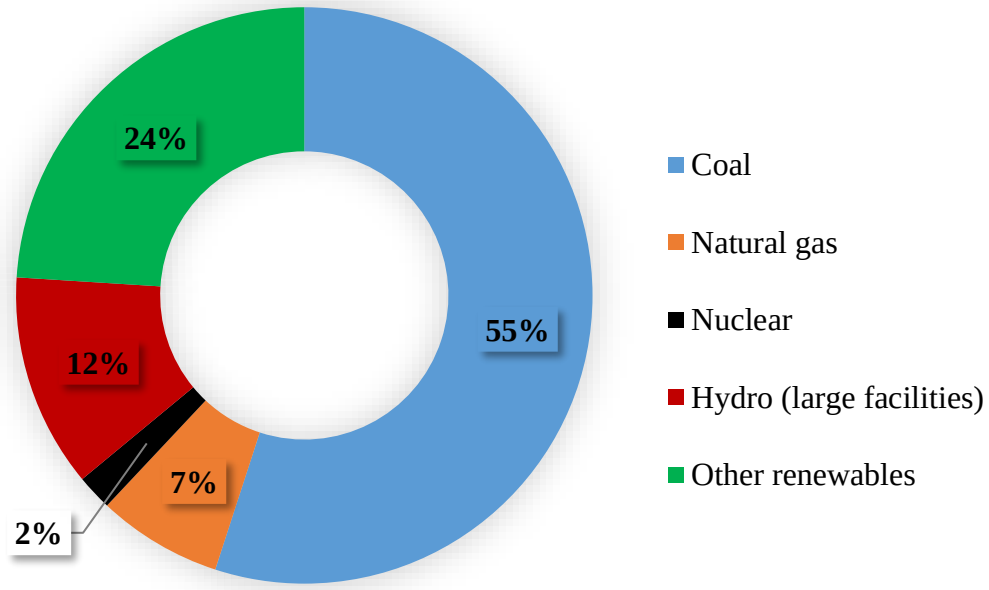

(B)

Fig. 1.1 (A) Total energy consumption in India, 2018 (B) Installed power capacity in India, June 2020 (Source: EIA India., 2020)

The first commercial use of gas power technology for electricity took place in Neuchâtel, Switzerland around the year 1939-1940. Thereafter, it took around 21 years to develop a gas fired power plant based on a combined cycle i.e., both gas and steam-based cycles. The plant was built in Korneuburg, Austria in the year 1961 with an electricity generation capacity of 75 MW. Since then, the technology of natural gas fired combined cycle power plants has improved rapidly. Currently, the natural gas fired combined cycle power plant emits lower greenhouse gas emissions and have higher thermal efficiency as compared to fossil fuel-based power plants (Miser., 2015). It has been predicted that the world's total power generation demand will significantly rise to 34,290 TWh by 2030 and around 21% of this power generation is expected from natural gas fired combined cycle power plants (Hu and Ahn., 2017). Fig. 1.2 indicates the projection of the total World's energy consumption in 2050 when compared with the year 2018. It shows that in the next few decades, the energy share of natural gas is going to be more consistent after nuclear energy. This is due to its more compatibility with carbon capture and utilization and storage technologies that either store or reuse the exhaust CO_2 emissions when compared with coal power plants (Outlook., 2019). On the other hand, renewable energy replaces coal energy utilization in power sector (EIA., 2019).

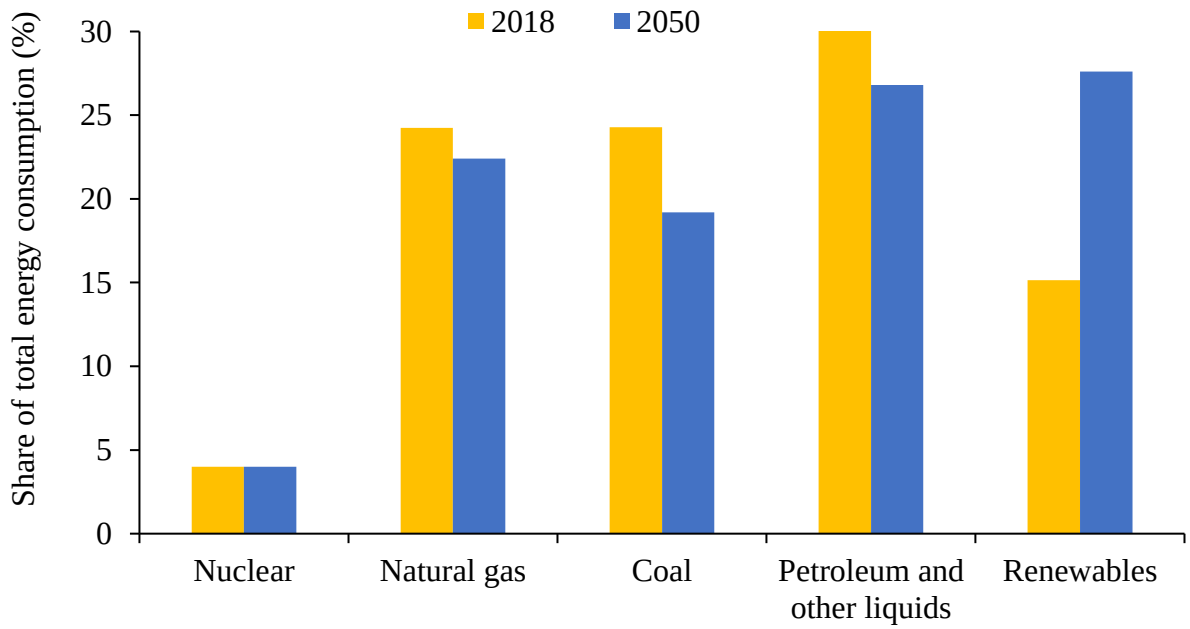

Fig. 1.2 Projection of total world's energy consumption in 2018 and 2050 year (Source: EIA., 2019)

From India's perspective, it was found out that the share of natural gas in the energy sector is around 6% while the total installed power capacity based on gas energy contributes 7% approximately in 2018 (Fig. 1.1). However, as part of cleaner fuel utilization for energy production the country is aiming to increase its natural gas share to 15% of total energy consumption by the year 2030 (EIA India., 2020). The discoveries of shale gas reserves in Krishna-Godavari, Cauvery and Cambay basins (Negi et al., 2017) have paved the way to exploit the available native hydrocarbon resource for natural gas fired combined cycle power generation.

1.1.3 Biomass fired power plants – Status in World and India

Biomass is often regarded as a carbon neutral fuel (Gądek & Kalisz., 2018). In addition, it is one of the renewable energy sources, which decreases the consumption of fossil fuels for electricity generation. Wood as a main source of biomass has fueled the global economy for thousands of years. After the industrial revolution it was slowly replaced with commercial fuels such as coal, gas and oil. However, the difficulties in the acquisition of fossil fuels due to the geopolitical, economic and environmental issues after the world wars have brought back the prominence of bioenergy in the world (Lewis., 1981). Since then, bioenergy is growing optimistically along with other renewable energies.

A growth of 5% in bioenergy was observed in the electricity sector in the year 2019. However, by the year 2030, it is expected to grow at a slightly higher rate i.e., 6% annually (IEA., 2020a). The reason is that various countries are implementing new policies to generate sustainable energy in the future. Countries like China and Germany are promoting the energy from waste (EfW) technique for electricity generation by using municipal solid waste. On the other hand, predominantly agricultural based countries like India and Brazil are primarily focusing on bagasse as a biomass resource for the production of biofuel and electricity generation (IEA., 2020a; Arasto et al., 2017).

In recent times, India is facing a threat to the human and environment due to burning of biomass in the farm fields and has gained a lot of public attention. One possible solution to eradicate this problem is the installation of decentralized biomass-based power plants in rural areas. This not only helps to meet electricity demand locally but also is a medium to dispose of the agricultural waste sustainably (Kaur., 2020). Fig. 1.3 represents the share of various renewable

energies for power generation in India. At present, biomass power plants contribute to around 12% of total energy after wind and solar power i.e., 44% and 39%. India has the potential to produce 26,000 MW of power from agriculture residue-based biomass. A major share of around 8000 MW is contributed by bagasse alone (MNRE., 2020).

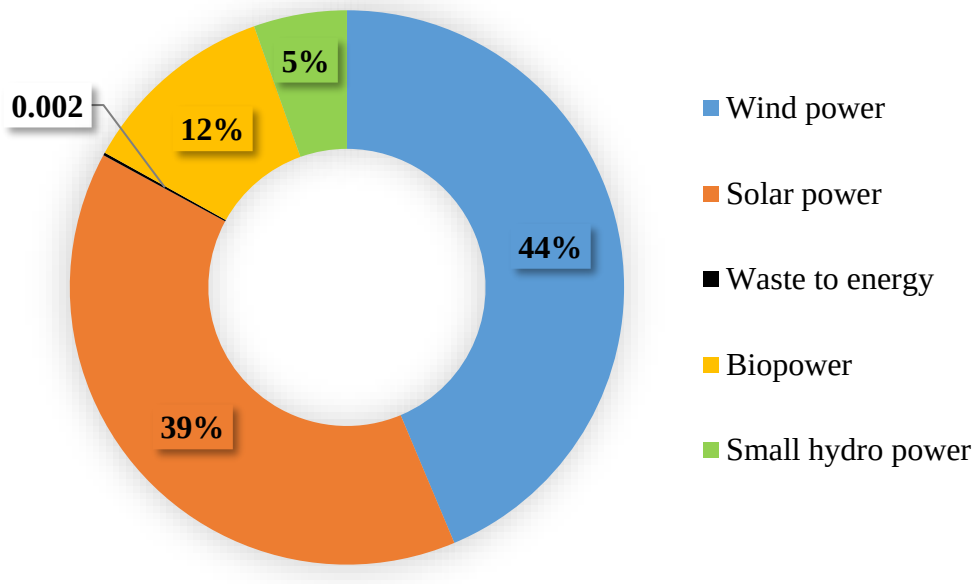

Fig. 1.3 Share of different installed grid connected renewable power in India, Dec 2019 (Source: MNRE., 2020)

1.2 Status of greenhouse gas emission and mitigation opportunities in India and the World

Climate change due to global warming has emerged as a very important concern around the world. It is believed that the increasing accumulation of these GHGs is the major cause of global warming. Most of the GHGs (most commonly CO_2) are released into the environment due to the utilization of fossil fuels such as coal, oil and natural gas in the energy generation process. As per the Global Energy Review report published by IEA in March 2022, the annual CO_2 emissions consistently are decreasing in the developed countries such as USA, European Union and Japan as shown in Fig. 1.4A. Few countries had very low CO_2 emissions in 2021 due to the COVID pandemic.

The CO_2 emissions in developing countries such as India and China continue to grow annually, as shown in Fig. 1.4B. The above facts clearly signify that today the cause of GHG

emissions problem is not just owned by developed and developing countries but has become a worldwide concern. To achieve net zero carbon emissions by 2050, any fossil fuel based power plants must be integrated with a suitable CCS or CCU technology (IEA., 2021). At present, a number of mitigation strategies are being adopted globally to reduce the GHG emissions after the Paris agreement signed in the year 2015 that legally binds the nations all over the world to keep global warming below 2 $^{\circ}$C by the end of 21st century (Schurer et al., 2018). The first and most common approach adopted by many countries is reforestation i.e., planting trees on a large scale that reduces atmospheric CO_2 concentration through photosynthesis.

To minimize the anthropogenic greenhouse gas emissions into the atmosphere, IEA., (2015) proposed several alternatives along with their potential as shown in Fig. 1.5. From the data it can be observed that the improvement of existing process energy efficiencies can play a major role in mitigating the CO_2 emissions, which also improves the process sustainability in terms of reduced operating cost, environmental impact and waste. In the power sector, switching from fossil fuel-based energy sources to clean energy (zero CO_2 emission) sources such as renewables and nuclear energy can have considerable impact on CO_2 mitigation. These advanced technologies enable a significant reduction of GHG emissions into the atmosphere and are considered to be the best alternative against fossil fuel-based power plants. However, it has also been reported that switching completely to renewables from fossil fuels even by the year 2050 is not possible (IEA., 2021). Hence, currently the developing countries are exploring the integration of CO_2 capture technologies with thermal power plants. This minimum retrofitting can make the power production from thermal power plants as environmentally sustainable and viable option to meet the base load demand in most of the countries. The captured CO_2 after this modification in power plants was either sequestrated directly into the geological storages such as depleted oil fields, gas fields and saline aquifers or else utilized for the production of value-added products such as chemicals and biofuels. Currently, researchers are actively working on synthesizing different CCS & CCU configurations, enhancement of first-generation technologies' efficiency and effective integration of CCS & CCU units with thermal power plants.

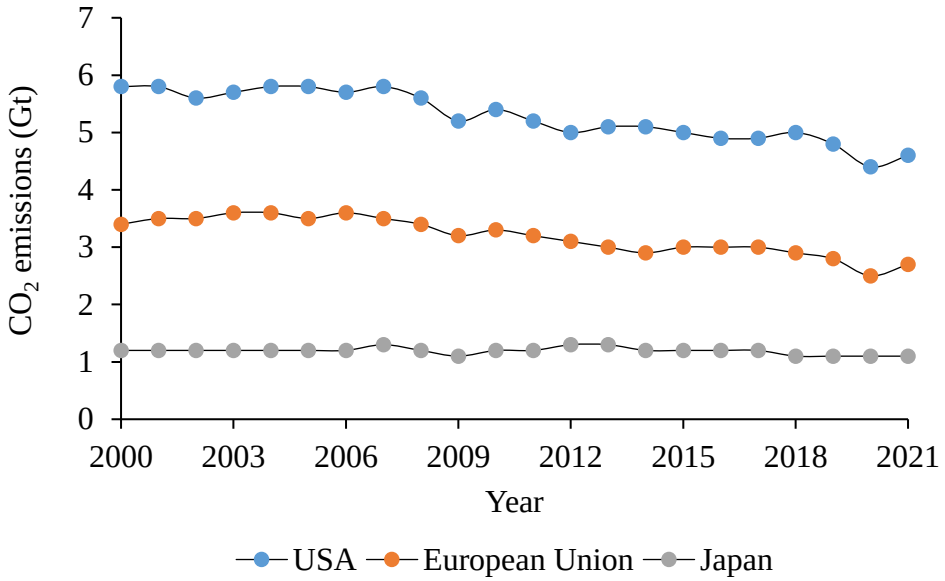

(A)

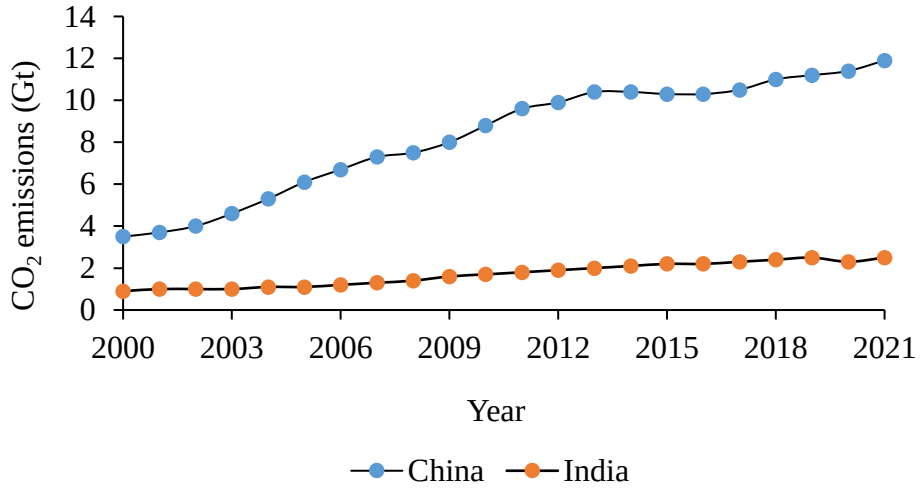

(B)

Fig. 1.4 Annual CO_2 emissions of the (A) developed countries and (B) developing countries between the years 2000 and 2021

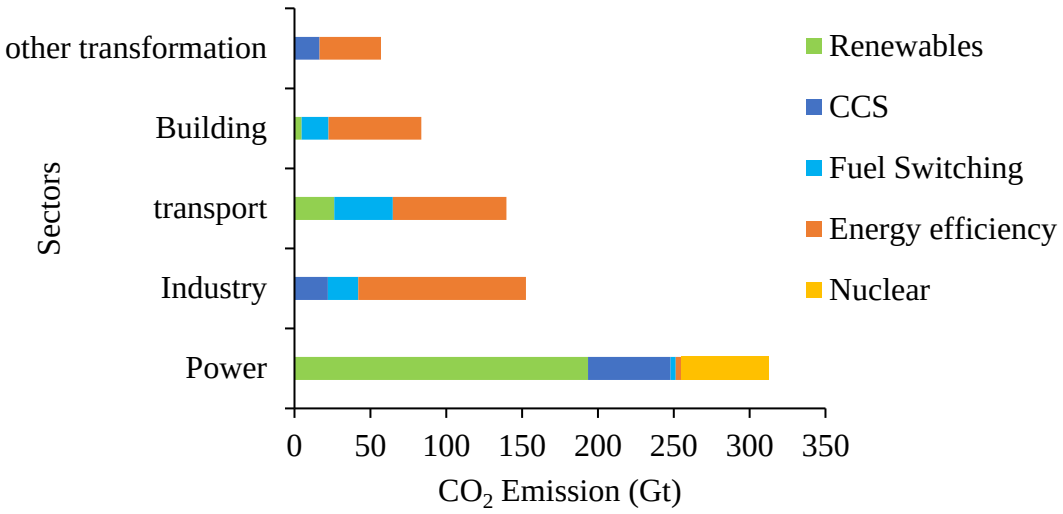

Fig. 1.5 CO_2 emission reduction targets and the means to achieve them (Source: IEA., 2015)

1.3 The most potential CO_2 mitigation techniques such as carbon capture and sequestration, carbon capture and utilization and carbon capture and hydrogen co-generation

In this section, the general information of the origin, current status and future prospects of CCS, CCU and CCHC technologies is discussed in detail. The discussion helps to derive the motivation for the present research work.

1.3.1 Carbon capture and sequestration (CCS)

CCS is a process where primarily the CO_2 is separated from other constituent components present in a mixture of gases and was further sent into deep geological storages e.g., depleted oil fields, gas fields and saline aquifers. The technology of CO_2 capture was available since the 1920s when the CO_2 present in natural gas reservoirs was separated from the saleable methane (CH_4) gas (IEAGHG., 2013). The first known CCS facility was built in the year 1971 in Texas in the form of a gas processing facility named Terrell Natural Gas Processing Plant. (Loria and Bright., 2021) The captured CO_2 in this case was used for Enhanced Oil Recovery (EOR). In the year 1977, this concept of CCS was extended and first considered in the thermal power plants with an aim to prevent CO_2 emissions into the atmosphere (IEAGHG., 2013). Since then, in the last four decades, the growth in this technology has been quite volatile.

In spite of that, it has been reported that by the year 2021, there are around 26 CCS plants in an operationally active condition, 34 CCS plants in a developmental phase, 2 CCS plants suspended operations and 4 CCS plants under construction around the world. A major portion of this growth in CCS plant numbers was observed in the last three years alone (Loria and Bright., 2021). This reveals that the concept of CCS is gaining more attention at present as a tool to mitigate GHG emissions around the globe. The key reason behind this CCS growth is the recognition of this technology as a sustainable alternative to integrate with thermal power plants for green energy production. As per the Sustainable Development Scenario of IEA, around 70 -100 new CCS plants are needed every year that can sequestrate 5,635 Mt per annum of CO_2 by the year 2050 in order to limit GHG emissions (IEA., 2019; Townsend and Gillespie., 2020). Therefore, to make this CCS process sustainable, researchers are focusing on the enhancement of process robustness and efficiency.

1.3.2 Carbon capture and utilization (CCU)

The CO_2 sequestration is an intermittent solution, and it has the unavoidable drawback in the form of leakage from geological storage units (Loria and Bright., 2021). The CCU addresses this issue by utilizing the captured CO_2 to create valuable products and thus enables a more economically attractive solution in terms of feasibility. The difference between CCU and CCS from CO_2 emitted facilities such as power plants is depicted in Fig. 1.6.

The idea of CCU actually started from the information obtained from the Keeling curve that reveals the amount of CO_2 in the atmosphere changes that annually corresponding to the seasonal variation of vegetation and the landmass difference between the southern and northern hemisphere of the earth (Keeling CD., 1960; Keeling CD., 1976). A concept of planting crops with C4 photosynthesis that enables higher CO_2 capture was then proposed further to utilize it for biomass related applications such as production of biochar (Harris et al., 2018). Over the years, the concept of CCU has further diversified and today the CCU technology is mainly distinguished in two pathways (Assche and Compernolle., 2021). These are called direct use pathways and indirect use pathways.

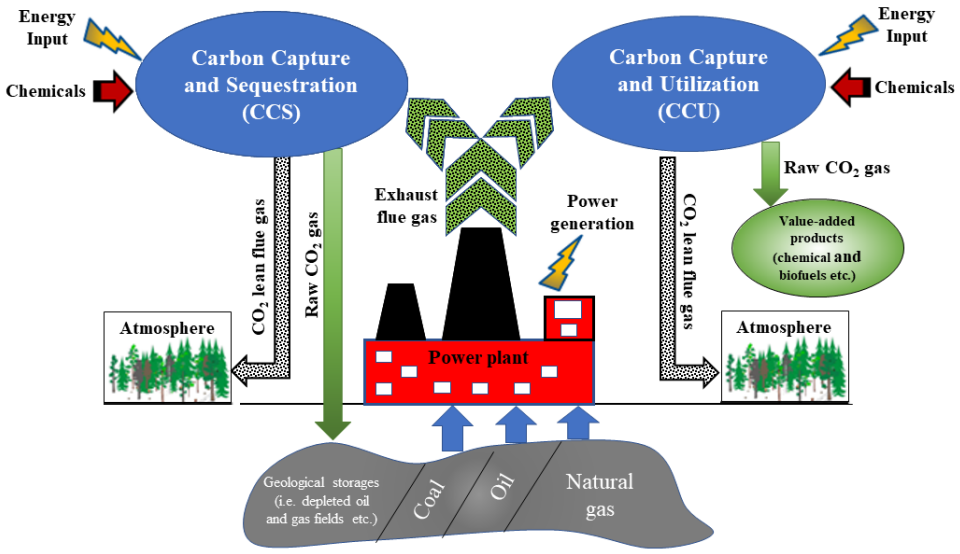

Fig. 1.6 Outline of CO_2 sequestration and CO_2 utilization strategy in power plants (Source: Pillai et al., 2022)

The direct use involves the utilization of captured CO_2 in those areas where the CO_2 as a molecule is not chemically altered. Some major examples of this include yield boosting applications such as algae, fertilizer (urea) etc. and heat transfer fluid applications such as refrigeration. On the other hand, indirect use pathways involve the utilization of captured CO_2 in the fields where it is converted into chemicals such as polymers, fuels such as methanol and CH_4 etc., building materials such as concrete or cement. The world's first industrial scale, low cost CCU facility was built in Tuticorin, India in the year 2016 with an aim to capture nearly 60,000 tons of CO_2 annually from coal fired power plants and to utilize it for producing sodium carbonate (soda ash) (Edie., 2021). However, most of the technologies linked with the development of CCU strategies are in the early stages of research. Nevertheless, it is well argued that CCU strategy is economically better than CCS, a major disadvantage with this is its capacity to store lower CO_2 both in terms of duration and physical scale against CCS strategy. In the near future, it is quite possible that the CCS and CCU technologies can co-exist and share a common infrastructure in most of the industrial plants for CO_2 mitigation (Tapia et al., 2016). Numerous, research works were also carried out to integrate renewable energy technology based on wind and solar energy

sources with CCU to establish a cost and eco-friendly energy supply system (Kim et al., 2019; Mikulčić et al., 2019; Ravikumar et al., 2020).

1.3.3 Carbon capture and hydrogen cogeneration (CCHC)

Apart from CCS and CCU strategy, CCHC technique is also an attractive alternative that can lead to a reduction of CO_2 emissions and production of green fuel. Generally, in a conventional hydrogen (H_2) production process, a CH_4 reforming/coal gasification followed by a water gas shift reaction was carried out to produce the H_2. Apart from the H_2, the gaseous mixture produced at the end of the process also consists of constituent gases such as CO_2, CH_4, hydrogen sulphide and nitrogen (N_2) etc. The H_2 was separated from other gases by means of H_2 purification unit. However, to enable carbon capture along with H_2 production, additional gas separation units must be installed by which high purity H_2 and CO_2 can be obtained.

As per the IEA report, in the year 2020, the pure H_2 demand is at around 70 Mt per year and most of it is produced from fossil fuels such as coal and natural gas. This makes the conventional H_2 production process emit a considerable amount of CO_2 (IEA., 2020b). H_2 is going to be a major source of fuel in the future, and it is predicted to replace fossil fuel completely, especially in the transport sector in long term. Therefore, several research efforts are being carried out by various countries to produce H_2 via non-fossil fuel-based sources. The amount of H_2 produced by gasification and electrolysis using renewable energy is expected to be between 12-38% of total production by 2050. In contrast, fossil fuels will account for around 58-81% of H_2 production by 2050 (Voldsund et al., 2016). In light of all the above arguments, producing H_2 from fossil fuels and capturing CO_2 can make this technology green and sustainable.

1.3.4 Carbon capture technologies and the concept of the calcium looping process

In the previous sections, the feasibility of various CO_2 mitigation strategies, such as CCS, CCU and CCHC as well as their integration with thermal power plants, were discussed in general. A CO_2 capturing system is an integral part of all these three strategies. The effectiveness of CO_2 capture systems plays a very critical role in assessing the energy, ecological and economic performance of the thermal plant. Numerous CO_2 capture technologies along with several demonstration projects were investigated with an aim to capture CO_2 from power plants on a commercial scale (Rackley., 2010). Presently pre-combustion, post-combustion and oxy-fuel

combustion are the most dominant CO_2 reduction strategies (Li and Fan., 2008; Míguez et al., 2018).

The post combustion amine scrubbing with mono-ethanolamine (MEA) solvent was one among the matured CO_2 capture technologies (MacDowell et al., 2010). However, the process is expensive and solvent used is corrosive in nature are the major problems associated with this technology (Supap et al., 2006; Fytianos et al., 2016). The oxy-fuel combustion technology has enough technical competency for CO_2 capture. In this process, the fuel was combusted in the presence of oxygen and recycled CO_2. But the energy penalty associated with air separation system (ASS) to generate oxygen makes this technology highly energy intensive (Xiong et al., 2014). These unavoidable limitations indeed motivated the researchers to develop 2^{nd} generation CO_2 capture technologies aiming at lower energy and economic penalties.

From the last two decades, researchers focused on development of novel chemical looping technologies for CO_2 capture from thermal power plants. Currently, more attention is given to the chemical looping combustion of fossil fuels using metal oxides as oxygen carriers for oxy-fuel combustion and calcium looping technology for post combustion CO_2 capture as they have indistinctive advantage of low efficiency penalty (Perejón et al., 2016). Many successful demonstration projects on calcium looping all over the world proved its viability as CO_2 capture technology (Hanak et al., 2015). Its feasibility to retrofit the existing plants with less energy and economic penalty along with plant load flexibility makes it one of the sustainable CO_2 capture options (Hanak and Manovic., 2017b; Dieter et al., 2014; Berstad et al., 2012; Berstad et al., 2014). The concept of the calcium looping process was foremost proposed in the year 1999 (Duan et al., 2016). In this process, lime is used as a regenerated sorbent to capture CO_2 (Wu et al., 2017) as shown in Fig. 1.7. The basis of this process is the equilibrium reaction between calcium oxide (CaO) and CO_2 that generates calcium carbonate ($CaCO_3$) in the carbonator at a temperature between 600 ^{0}C and 700 ^{0}C. The unreacted lean CO_2 flue gas was then separated and $CaCO_3$ sorbent was transferred to the calciner to regenerate CaO and CO_2. This calcination reaction occurs in the temperature range of 850 ^{0}C to 950 ^{0}C (Zhai et al., 2016). The raw CO_2 collected can be further compressed for storage. During this repeated carbonation-calcination cycle, a part of deactivated calcium sorbent will be removed in the form of the purge. An equal amount of fresh $CaCO_3$ will have to be added as a make-up sorbent to compensate for the deactivated calcium

sorbents in the system (Wu et al., 2017). The kinetic reactions that occur in both carbonator and calciner reactors (Zhai et al., 2016) are as follows:

$$Carbonator: \ CaO + CO_2 \rightarrow CaCO_3 \qquad \Delta H_{25^0c} = -178.9 \ \frac{kJ}{mol} \tag{1.1}$$

$$Calciner: CaCO_3 \rightarrow CaO + CO_2 \qquad \Delta H_{25^0c} = +178.9 \ \frac{kJ}{mol} \tag{1.2}$$

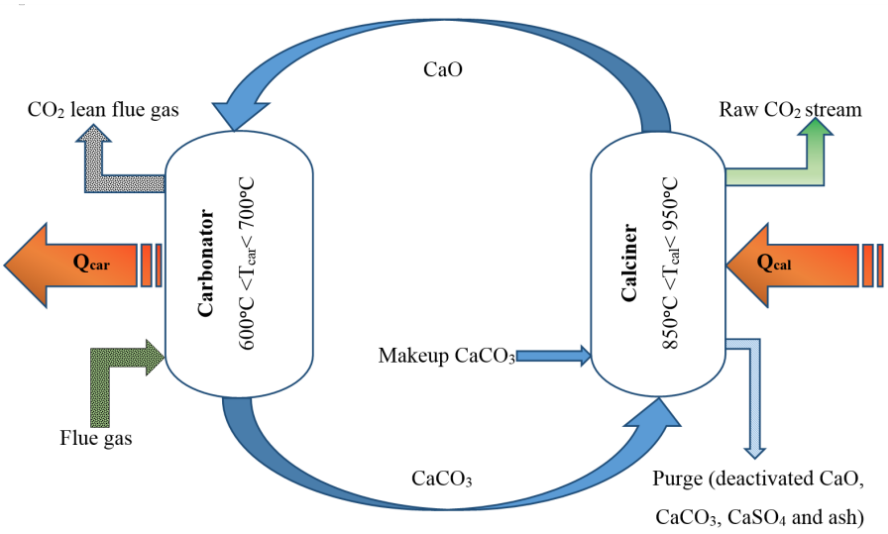

Fig. 1.7 Outline of calcium looping process (Source: Pillai et al., 2019)

1.4 Motivation behind the proposed research

From the above overview, it is clear that at present, and also in the near future, developing countries such as China, India, and Brazil will rely heavily on fossil fuels for their power supply. At the same time, India is also a signatory to the Paris Convention, and the policies and regulations have to meet this international commitment. To satisfy the international commitment, it is critical to determine the scope of CCS, CCU, and CCHC that are technically and economically appropriate for India's rising power generation. Furthermore, as an agriculture based country, India produces a substantial amount of biomass (a carbon neutral fuel) that can be used for rural electrification through biomass based power plants. Coupling biomass power plant with CO_2 capture is a promising option to enable a 'carbon neutral' technology to a 'carbon negative' technology. This will allow India to meet its GHG reduction targets while also supporting the rest of the world in minimizing the threat of climate change caused by GHG. Research on the integration of CCS, CCU, and CCHC with power plants has been undertaken over the years. However, there is still a

scope for performance enhancement by designing effective integration and cogeneration schemes. Further, limited studies are available in the literature on overall energy, exergy, cost and environmental assessment of thermal power plants integrated with second generation CCS and CCU technologies. To the best of our knowledge, no studies were reported on comprehensive performance assessment of thermal power plants integrated with calcium looping for CO_2 capture. Therefore, the main aim of the present research work is to propose novel thermal power plant configurations using different fuels for sustainable power and valuable products cogeneration along with CO_2 capture.

1.5 Objectives of the present work

A comprehensive literature review was carried out on sustainable thermal power technologies in general and integration of second-generation CO_2 capture technologies with thermal power plants in particular, to identify the research gaps. These were discussed in the next chapter. Based on the identified research gaps, the following objectives were formulated.

To propose a CCS, CCHC and CCU strategies for biomass, coal and natural gas fired power plants.

1. To synthesis and develop novel double calcium looping integrated coal, biomass and natural gas fired combined cycle power plants.
2. To explore the possibility of H_2 coproduction from double calcium looping integrated coal fired power plant and to evaluate its performance.
3. To integrate the solar energy coupled dimethyl ether (DME) production process and double calcium looping integrated natural gas fired combined cycle power plant for CCU.

To perform theoretical investigations of the above-mentioned configurations by using thermodynamic based methods with energy and exergy approaches:

1. To determine the mass, entropy, energy and exergy inputs and outputs to the system and from the system for each component, subsystem, as well as the overall system.
2. To investigate the energy and exergy losses of each component, subsystem and overall system.
3. To calculate the energy and exergy efficiencies of each subsystem and system.
4. To carry out parametric studies to investigate the effect of important variables on system performances.

5. To perform an exergoeconomic analysis to determine economic competitiveness and viability.
6. To assess the proposed configurations based on the energy, exergy, environmental and economic parameters.

1.6 Organization of thesis

The current thesis is composed of 5 chapters starting from the overall context of the work to its comprehensive conclusions and future perspectives. The content of these chapters is explained briefly as shown below:

Chapter: 1: This chapter describes the general aspects and the importance of the area of research work. It provides the general information of the origin and current status of the power plants that plays a major role in the energy sector of India and the world. It further elaborates concern of the greenhouse gas emissions by this energy sector and the importance of CCS, CCU and CCHC as a possible solution to curb it. At the end, it illustrates the motivation derived from overall discussion for this research work along with the proposed objectives.

Chapter: 2: A detailed literature review of different CO_2 capture technologies, calcium looping configurations integrated with power plants for CCS, calcium looping configurations integrated with power plants for CCHC as well as comparative performance of various CO_2 utilization technologies for CCU is reported in this chapter. It concludes by identifying the scope and research gaps from the literature review.

Chapter: 3: This chapter discusses the overall methodology, system description, analysis and modelling techniques that were used to carry out the studies for the accomplishment of the desired objectives. The formulae used to determine the energy, exergy, cost and environmental parameters were discussed in detail in this chapter. It also consists of the details of the data of validation results and operation conditions used for developing the aspenONE flowsheet models.

Chapter: 4: In this chapter, the developed biomass, coal, and natural gas fired power plants integrated with calcium looping were analyzed in terms of energy, exergy, environmental, and economic parameters. The performance of the proposed configurations was compared with conventional power plants. Further, the results obtained from the newly derived coal fired power plant configuration for CO_2 capture with coproduction of electricity and H_2 were compared against

a conventional calcium looping gasification and electricity coproduction configuration. In the context of CCU strategy, natural gas fired combined cycle integrated calcium looping power plants, coupled with conventional and solar energy DME production plants for CO_2 utilization, were also discussed. At the end, a comparative performance assessment of all the efficient calcium looping integrated power plants as a part of CCS, CCHC and CCU were discussed.

Chapter: 5: The overall conclusions drawn from this research work is illustrated in this chapter. The potential scope to extend this research work for future study is also included in this chapter.

CHAPTER 2

LITERATURE SURVEY

Chapter 2

Literature review

The Chapter 1 emphasized the importance of integrating CCS, CCU, and CCHC technologies with thermal power plants in order to mitigate CO_2 emissions. In this chapter, a review of the existing CO_2 capture and utilization technologies is presented along with the identified research gaps. The chapter is mainly divided into five sections. Section 2.1 provides an overall view on available CO_2 capture technologies with main emphasis on the working principle, integration feasibilities, technology readiness level, etc. Section 2.2 describes an overall view of different configurations adopted in calcium looping technologies for CO_2 capture. A comparative performance assessment of several calcium looping configurations developed over the years for various types of plants and fuels is included in this section. A review of different calcium looping based technologies for H_2 and power co-production along with CO_2 capture is presented in section 2.3. In section 2.4, literature review on the different processes that use CO_2 as a feedstock for DME synthesis is presented. At the end, the identified research gaps from the presented literature were highlighted in section 2.5.

2.1 Studies on carbon capture technologies

The origin and significance of CO_2 capture technologies has been described in Chapter 1. In this section, different CO_2 capture technologies under the classification of pre-combustion, oxy-combustion and post combustion are reviewed in detail. The presented literature helps to identify potential CO_2 capture technologies that can be effectively integrated with thermal power plants.

2.1.1 Pre-combustion CO_2 capture

Pre-combustion CO_2 capture is a technique where CO_2 is captured before the combustion process takes place, as shown in the Fig. 2.1. In this technology, the fuel is first converted into a combustible gas (syngas) that consists mainly of H_2 and CO gases. Steam reforming process is used to convert solid fuels such as coal and biomass, and partial oxidation process is used for the liquid and gaseous fuels. The corresponding reactions are as follows (Sifat and Haseli., 2019):

$$Steam\ reforming: \qquad C_xH_y + xH_2O \rightarrow xCO + \left(x + \frac{y}{2}\right) H_2 \tag{2.1}$$

$$Partial\ oxidation: \qquad C_xH_y + \frac{x}{2}O_2 \rightarrow xCO + \left(\frac{y}{2}\right)H_2 \qquad (2.2)$$

The CO gas produced during these processes is further converted into CO_2 by using steam in the water gas shift reaction, resulting in more H_2 production as shown in Equation 2.3.

$$Water\ gas\ shift\ reaction: \qquad CO + H_2O \leftrightarrow CO_2 + H_2 \qquad \Delta H_{25^0c} = -50.1\frac{kJ}{mol} \qquad (2.3)$$

Since this water gas shift reaction takes place at high pressure (Van Dijk et al., 2014; Sato T et al., 2004), it further enables the separation of the CO_2 at ambient temperature. The remaining gases (mainly H_2) are then sent for combustion to generate power in the power plant.

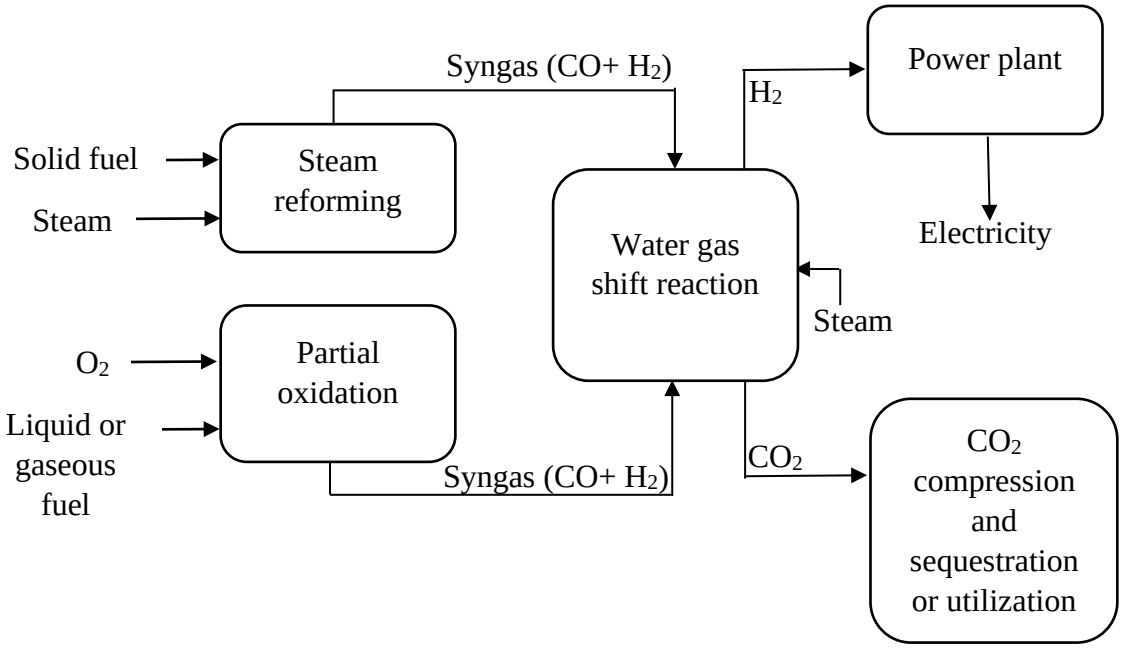

Fig. 2.1 General layout of pre-combustion CO_2 capture process (Source: Madejski et al., 2022)

Generally, most of the research work in pre-combustion CO_2 capture technology has been carried out on natural gas fired power plants. This is because other fuels such as coal or biomass require additional separation schemes to remove other contaminants produced during the gasification process (Jansen et al., 2015). A significant number of studies have been carried out in this area that reveal the potential and drawbacks of its integration with various power plants. Romano et al., 2010 integrated an auto thermal reforming-based pre-combustion CO_2 technique with the natural gas fired combined cycle power plant. It was found out that almost 91.6% of CO_2 was successfully captured, but the net energy efficiency of the integrated configuration was 8%

less than the reference natural gas fired combined cycle power plant. Moioli et al., 2014 carried out a thermodynamic performance assessment of air-blown gasification-based pre-combustion CO_2 technique integrated with an IGCC power plant. The results revealed that the energy penalty of the integrated configuration was 6.1% without CO_2 compression unit (CU) and 9.5% with CU with a CO_2 capture efficiency of around 87%. The research works from Romano et al., 2010 and Moioli et al., 2014 indicate that the pre-combustion CO_2 capture technology enables high CO_2 capture efficiency but at the expense of a high energy penalty. This is mainly due to the energy losses incurred during the chemical reactions in the overall CO_2 capture process. This ultimately induces a high economic cost to the power plant when integrated with this CO_2 capture technology.

A number of research investigations have been carried out to understand its economic aspect and scope for further improvement needed in this area (Franz et al., 2014, Xin et al., 2020, Roussanaly et al., 2020; Thimsen et al., 2011). Jansen et al., 2015 carried out a review on pre-combustion CO_2 capture technology and discussed in detail about the various advancements that have been carried out in this area. It was concluded that over the last decade, the development of pre-combustion CO_2 capture technology was very limited because most of the research was focused on post combustion CO_2 capture technology for the natural gas and coal fired power plants.

2.1.2 Oxy-combustion CO_2 capture

Oxy-combustion CO_2 capture technique is a method where fuel combustion happens in the presence of pure oxygen. A layout of this CO_2 capture process is shown in Fig. 2.2. In this technology, the oxygen is initially separated from other constituent components of the air by means of an ASS. The obtained pure oxygen is then sent for combustion with fuel in power plants. The products (flue gas) formed after combustion are mainly CO_2, water vapor and ash (in the case of coal, biomass etc.). At the end, the CO_2 is captured after removing the ash and water vapor by using an ash remover and CO_2 compression system. A part of the flue gas before compression is recycled back to the combustion chamber. It helps to regulate the flame temperature inside the combustion chamber as per its metallurgical constraints (Wu et al., 2018).

The Oxy-combustion CO_2 capture technique was adopted initially in industries with an objective to send N_2 free air that further enhances the performance in terms of energy consumption and productivity (Dugué., 2000; Charon., 2000). This is because a considerable amount of thermal

energy meant to be carried away by the flue gas gets lost in heating the N_2, and the formation of NO_x after combustion becomes an environmental concern (Gaber et al., 2021). This technology was later adopted for CO_2 capture in power plants and over the years it has been successfully demonstrated via large scale projects across the world to capture around 90% of the produced CO_2 emissions (Komaki et al., 2014; Koohestanian and Shahraki., 2021).

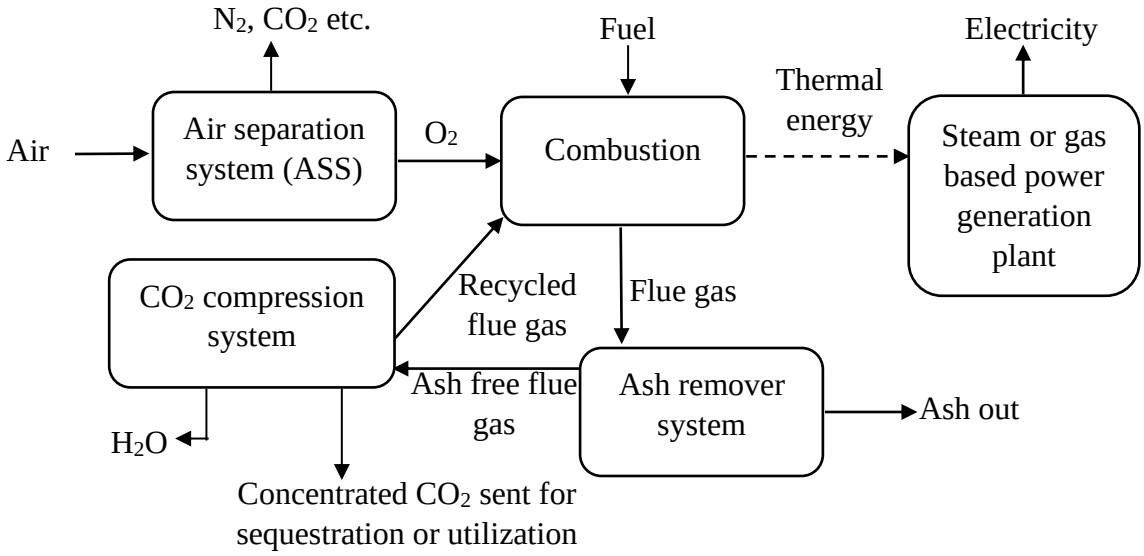

Fig. 2.2 General layout of oxy-combustion CO_2 capture process (Source: Zheng and Liu., 2017)

Contrary to the pre-combustion CO_2 capture technology which is preferred mostly for partially or completely natural gas fired power plants, a major advantage of the oxy-combustion CO_2 capture technology is that it can be easily retrofitted in all the fuels i.e., coal, biomass and natural gas fired power plants (Buhre et al., 2005; Valero and Usón., 2006; Khallaghi et al., 2020). However, a significant drawback in this technology is its use of an ASS that imposes almost 3 to 4% of energy penalty when integrated with the conventional power plants (Shah et al., 2013). This in overall, contributes as a major negative impact on the performance of the oxy-combustion CO_2 integrated power plants whose total energy penalty lies in the range of 7 to 11% (Escudero et al., 2016). Also, the need of a cryogenic-based refrigeration unit makes this technology economically less attractive (Mehrpooya et al., 2019). Therefore, in order to reduce the energy and economic penalty associated with the ASS of the oxy-combustion CO_2 capture technology, various research works are being carried out in this particular area (Pfaff and Kather., 2009; Brigagão et al., 2019).

2.1.3 Post-combustion CO_2 capture

Post combustion CO_2 capture is a technique in which the CO_2 is separated from the flue gas after the combustion of fuels such as coal, natural gas or biomass. A layout of this CO_2 capture process is shown in Fig. 2.3. In this technology coal, biomass or natural gas is combusted in the presence of air. The exhaust flue gas after energy recovery is sent to the CO_2 capture system. A majority of CO_2 gas present in the exhaust flue gas is separated and then passed to the CO_2 compression system for compression while the lean flue gas is emitted into the atmosphere. The concentrated CO_2 gas is at last sent for sequestration or utilization.

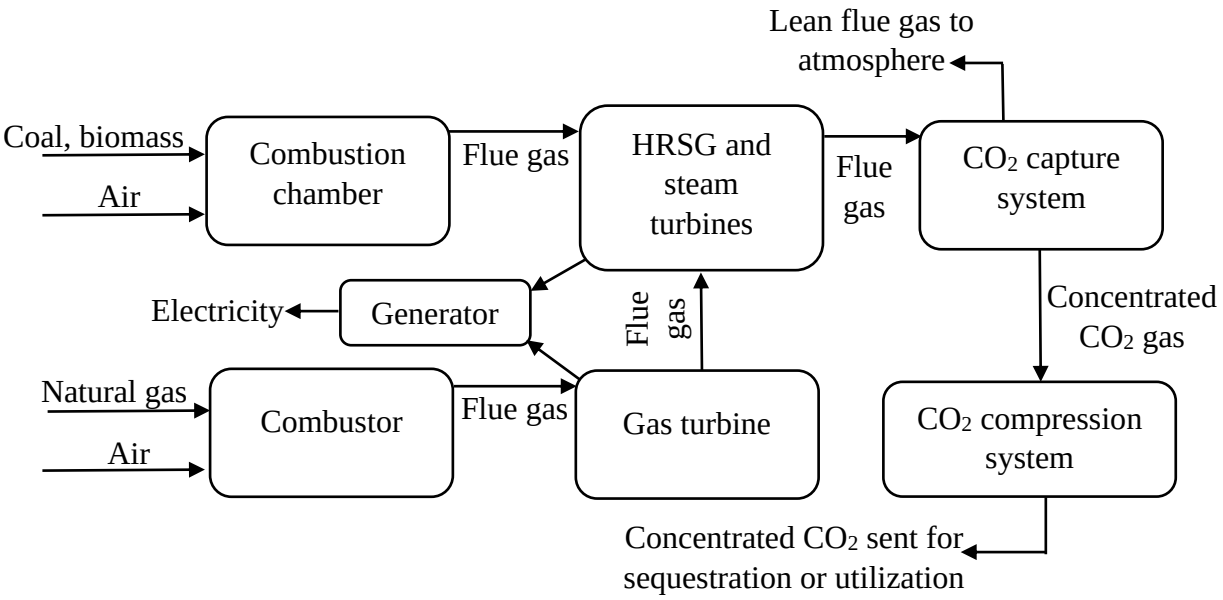

Fig. 2.3 General layout of post-combustion CO_2 capture process (Source: Koohestanian et al., 2021; Metz et al., 2005)

Among all the three CO_2 capture technologies, post combustion CO_2 capture technology is mostly preferred as compared to pre and oxy combustion CO_2 capture technologies. This is because of its 'end of pipe' concept (Wang et al., 2017) is seen as a more viable option that can be adopted in all the existing coal, biomass and natural gas fired power plants as well.

Numerous research works are being carried out to identify and explore the feasibility options of various post-combustion CO_2 capture methods (Chao et al., 2021). The most dominant and mature post-combustion CO_2 capture technology at present in the market is based on absorption of CO_2 using solvents such as amine scrubbing (Leung et al., 2014). However, these first-generation technologies have the following major bottlenecks: solvent degradation,

equipment corrosion, high energy penalty and high operational cost (Aaron and Tsouris., 2005; Chi and Rochelle., 2002; Aroonwilas and Veawab., 2007). Goto et al., 2013 carried out a review to understand the energy penalties of various post combustion CO_2 capture technologies integrated with coal fired power plants. It was observed that the energy penalty in most of the post combustion CO_2 capture technologies ranges (with CU) in between 8% and 12%. The review also stated that when solid sorbents-based CO_2 capture system was integrated to a 430 MW coal fired power plant, the electricity generation reduces to 346 MW only. On the other hand, when a MEA based CO_2 capture system was integrated with that same coal fired power plant, the net power output was reduced to 303 MW. This reveals that the performance of solid sorbents for CO_2 capture are superior as compared to the solvent-based methods.

The chemical and calcium looping technologies have become attractive options to capture CO_2 from thermal power plants because of their salient features such as easy retrofitting, low cost and less energy penalty. Both these second generation technologies have emerged as prominent options to capture CO_2 at large scale (Fennell and Anthony., 2015). However, some key advantages of calcium looping over chemical looping technology are the abundant sorbent availability at low cost especially in countries such as India and utilization of deactivated sorbent in other applications (Annual Report., 2017; Indian Bureau of Mines., 2017; Telesca et al., 2014). These features enable calcium looping technology as an attractive option to capture CO_2. However, there is still significant scope towards the development of efficient solid sorbents and technology integration with power plants to reduce the efficiency penalty.

2.2 Studies in calcium looping technologies for carbon capture

The general working principle of calcium looping process has already been explained in Chapter 1. A detailed review of the studies conducted to improve the performance of calcium looping configurations and their integration with coal, natural gas, and biomass fired power plants is presented in this subsection.

The concept of calcium looping process for CO_2 capture was foremost proposed in the year 1999 (Shimizu et al., 1999). There have been numerous technological improvements since then, making this option one of the potential alternatives for capturing CO_2 from power plants. A major issue with this technology is the short lifetime of sorbent because of its high deactivation rate, but

this deactivated sorbent can be reused as construction material (Markewitz et al., 2012). Most of the current research is focused on enhancement of sorbent performance and effective integration of calcium looping technology with power plants. Reactivation by hydration and development of synthetic sorbents seem to be prominent options to improve the reactivity and cyclic stability of sorbent (Blamey et al., 2010; Liu et al., 2012; Manovic and Anthony., 2010; Li et al., 2009). Hydration is a process where steam is used to improve the morphological features of sorbent particles in terms of surface area and pore size distribution. This can be achieved through the penetration and reactivation of the inner core of the spent sorbent by steam.

This process of reactivation saves cost and also improves SO_2 or CO_2 absorption capacity of the sorbent (Montagnaro et al., 2004; Montagnaro et al., 2006; Montagnaro et al., 2008). However, a major drawback with this process is its higher tendency for attrition of the particles due to poor connectivity and mechanical resistance (Coppola et al., 2014). Another way to reduce the susceptibility of CaO-based sorbent to sintering is by improving the sorbent stability. This can be achieved by high-active synthetic sorbents that are produced by doping of inert and refractory materials like Al_2O_3, MgO, La_2O_3, TiO_2 and SiO_2 to CaO based sorbents. The sintering resistance of an inert support is dependent upon the specific BET surface area, melting point and dispersion of the inert material in the sorbent (Hu et al., 2016). Generally, the investigation of reactivity decay, CO_2 sorption capacity and morphological behavior of sorbents (both natural and synthetic) are studied by analyzing its chemical interactions and crystalline phase changes that take place during subsequent intervals of calcination-carbonation cycles. Thermogravimetric (TGA), X-ray power diffraction (XRD) and scanning electron microscope (SEM) are some of the techniques that are used to study the behavior of sorbents in calcium looping (He et al., 2017; Wu et al., 2010; Benitez-Guerrero et al.,2018).

A compromise must be arrived between improving the sorbent performance and increasing its cost, which means a relatively practical, scalable, and inexpensive method for long term reactivity of sorbents, should be found. Li et al., 2009 proposed a calcium sorbent which was prepared by rice husk ash and CaO hydration together. The synthetic sorbent exhibited higher carbonation conversions and less sintering effects as compared with natural CaO sorbent. The above studies signify the possibility of realizing enhanced sorbent performance, and thus positions the concept of calcium looping CO_2 capture integrated power plants a step ahead as compared to

power plants integrated with other CO_2 capture technologies, especially in countries such as India, which are self-sufficient in limestone deposits and available at low market cost.

Several intensification strategies have also been proposed in the last decade for reducing calcium looping technology's energy penalty by (i) minimizing the ASS power consumption, (ii) eliminating the ASS requirement and (iii) retrieving the maximum possible thermal energy. A summary of various research works on the post combustion calcium looping configurations integrated with different plants for CO_2 capture is highlighted in Table 2.1. Most of the energy integrated schemes demonstrated are based on Oxy-Cal in which an ASS is an essential component (Berstad et al., 2012; Zhang and Liu., 2014; Mantripragada and Rubin., 2014; Duan et al., 2016; Hanak and Manovic., 2016). He et al., 2017 carried out research work to assess the effect of ash on calcium looping technology. The chemical interaction of sorbents with ash in calcium looping technology reveals that the ash creates a blockage in the pores of sorbents and thus restricts its ability to capture CO_2. In addition, it also results in higher energy consumption in calciner. The study reveals that higher ash content in coal results in lower CO_2 capture and a higher energy demand in calcium looping technology.

Table 2.1 Literature on post combustion calcium looping configurations integrated with different plants for CO_2 capture

Plant type	Fuel used	Calcium looping type	Highlights	Source
Natural gas fired combined cycle power plant	Natural gas	Oxy-CaL	Performance assessment of six energy integration strategies was examined. Energy penalty (%): 10 - 12.5 CO_2 capture efficiency (%): 90.3 - 92.4	Berstad et al., 2012
Coal fired power plant	Coal	Oxy-CaL	An analysis of lignite (coal) based fired power plant integrated calcium looping was presented. Energy penalty (%): 4.96	Vorrias et al., 2013

Coal fired power plant	Coal	Oxy-CaL	Coupled the concentrated solar power (CSP) with calcium looping integrated coal power plant to reduce fossil fuel energy. A higher overall energy penalty (9.63%) was observed due to lower CSP efficiency.	Zhang and Liu., 2014
Coal fired power plant	Coal	Oxy-CaL	A comparative techno-economic assessment of calcium looping and MEA integrated power plant was done. The energy penalty of MEA integrated power was found to be 11%, as compared to conventional coal fired power plant. MEA regeneration is an energy intensive process mainly responsible for higher energy penalty. However, the calcium looping integrated power plant has only 3% energy penalty.	Mantripragada and Rubin., 2014
Coal fired power plant	Coal, CH_4	Ca-Cu looping	Ca-Cu looping based CO_2 capture process was integrated with coal fired power plant and compared against calcium and amine based coal fired power plant. Energy penalty of Ca-Cu looping based CO_2 capture was found to be the lowest, i.e., 3.5%, however, economic analysis is not done.	Ozcan et al., 2015

Coal fired power plant	Coal	Oxy-CaL	The performance of a conventional calcium looping integrated coal fired power plant was analyzed with/without the recarbonation process. The net energy efficiency of the proposed configuration (with recarbonation process) was found to be 3.53% higher than the conventional calcium looping integrated coal fired power plant.	Duan et al., 2016
Coal fired power plant	Coal	Oxy-CaL	Integrated solar energy with calcium looping and coal fired power plant. The finding revealed an energy penalty of 13.44% as compared to conventional coal fired power plant. High energy consumption by ASS and CO_2 compression system are the major reasons.	Zhai et al., 2016
Coal fired power plant	Coal	Oxy-CaL	Replaced the conventional steam cycle with supercritical CO_2 cycle and integrated with calcium looping for CO_2 capture. Overall energy penalty reduced by 1% as compared to calcium looping integrated coal fired power plant.	Hanak and Manovic., 2016
Cement plant	Coal	Double calcium looping	Proposed a novel scheme of calcium looping for CO_2 capture from a typical cement plant. The configuration effectively captures 94% of CO_2 and eliminates the use of ASS.	Diego et al., 2016

On the other hand, the Ca-Cu looping and double calcium looping eliminates the use of ASS and thus have the potential to reduce the energy penalty significantly (Ozcan et al., 2015;

Diego et al., 2016). However, the advantage of double calcium looping over Ca-Cu looping is its ability to operate with single sorbent (calcium) that is widely available at low cost in many countries. This innovative approach endorses the double calcium looping configuration as an attractive alternative for CO_2 capture at bulk scale from power plants and other industries. It should also be noted that apart from the various energy integration strategies, the chemical properties of fuel also play a key role in overall plant performance, as indicated by Vorrias et al., 2013.

2.3 Studies on calcium looping for carbon capture and hydrogen production

It is most certain that H_2 is going to become a primary source of fuel in the future. At present it is used in a wide number of industries that deal with fertilizer production, electronics and petrochemicals (Ramachandran and Menon., 1998). Generally, in a conventional process, the H_2 is produced from fossil fuels by means of steam reforming, partial oxidation and water gas shift reactions, as explained in section 2.1.1. The production of H_2 in the pure form requires additional process steps for purification and storage.

Since CO_2 capture in a CCS strategy is a cost intensive process, the concept of producing H_2 along with CO_2 capture drives the whole process towards a more economically feasible solution. Apart from the CO_2 capture along with power production, calcium looping also provides an option to co-produce H_2 (Hanak et al., 2018). It has also been observed that cost and energy consumption incurred in process of H_2 production via calcium looping technology is considerably less as compared to the conventional H_2 production process (Connell et al., 2013; Wu et al., 2019). Although, the process of calcium looping based H_2 production technology is classified as an advanced application; the literature review indicates that this process of H_2 production was patented in the year 1931 (Dean et al., 2011). Over the last decade, most of the research in calcium looping has been focussed mainly in enhancing its feasibility to capture CO_2. However, some studies have also been carried out to co-produce H_2 along with CO_2 capture. A summary of the studies that were carried out for CO_2 capture and H_2 coproduction via calcium looping is given in the Table 2.2.

HyPr-RING is a patented technology developed in the early years of the 20th century in Japan that proposed the use of CaO to produce H_2 from hydrocarbons for power generation and simultaneous separation of the CO_2 effectively (Lin et al., 2002). This innovative approach

endorses the calcium looping configuration as an attractive option for CO_2 capture at bulk scale from power plants along with H_2 co-generation. The early studies, which investigated the potential of H_2 production via calcium looping using coal, biomass, and natural gas as raw materials, are reviewed by Florin and Harris., 2008; Dean et al., 2011. These reviews concluded that, more emphasis is needed on sorbent cyclic stability enhancement to make this technology viable. Over the last decade, several research works focused on synthesis of novel CaO based sorbents to enhance the structural stability, CO_2 capture efficiency and H_2 production rates (Zhao et al., 2014; Zhou et al., 2019; Ma et al., 2021). Energy integration also has a vital role in improvement of overall plant performance. A considerable number of energy integration strategies have also been proposed to enhance the energy efficiency. Chen et al., 2011 proposed a calcium looping based novel reactor configuration involving a compact fluidized bed for CO_2 capture and H_2 cogeneration. The parametric study revealed that the H_2 production rate and purity were reduced when pressure was increased from 1 bar to 10 bar. Shaikh et al., 2022 proposed a biomass-based calcium looping configuration for power generation and H_2 production to achieve a net zero or negative CO_2 emission. The results indicated that coproducing H_2 along with CO_2 capture is a more promising and market friendly approach than the calcium looping configuration that only captures CO_2 in a power plant. Both the schemes mentioned above require pure O_2 to function and needs an ASS that consumes more energy.

The concept of calcium-copper based looping configuration for CO_2 capture and H_2 co-generation described in the literature by Abanades et al., 2010; Martínez et al., 2013 and Fernández and Abanades., 2017 operates without an ASS. The cyclic oxidation-reduction reactions (by copper) of the chemical loop integrated along with calcium loop successfully helps to eliminate the requirement of ASS and reduce the energy penalty. However, it should be noted that the cost of copper used in the corresponding technology imposes an additional burden economically.

2.4 Studies on CO_2 utilization

The power production from thermal plants can be more attractive if the captured CO_2 is utilized for production of value-added chemicals rather than just sequestration (Wang and Demirel., 2018). The CO_2 utilization strategies have been explored widely for production of different useful chemicals, however most of these strategies are not fully matured (Dutta et al., 2017). The studies showed that the chemical and oil industry has the highest market potential for CO_2 utilization.

Table 2.2 Summary of different calcium looping configurations for H_2 co-production along with CO_2 capture

Source	Fuel used	Highlights
Lin et al., 2002	Coal	Developed an innovative H_2 production process that involves a calcium sorbent in a chemical loop. The experimental study proved that this process is better than other conventional ways of H_2 production.
Florin and Harris., 2008	Biomass	A review of calcium looping based H_2 production using biomass was done in this article. The sorbent cyclic stability enhancement is still a challenging task.
Dean et al., 2011	Coal, Biomass, Natural gas	The authors reviewed the performance of calcium looping for H_2 production and/or CO_2 capture in the power plant and cement industries. It was concluded that calcium looping could prove to be a low-cost technology for H_2 production and CO_2 capture. Yet, improvements need be made to enhance the regenerability of the sorbent for multiple cycles.
Abanades et al., 2010	Natural gas	Proposed a concept of calcium-copper based loop for H_2 production along with CO_2 capture. An experimental investigation is needed to assess the feasibility of the concept.
Chen et al., 2011	Coal	Proposed a novel reactor configuration that works on calcium looping for CO_2 capture and H_2 cogeneration. It was also found out that the H_2 production yield decreases as the operating pressure increases.
Martínez et al., 2013	Natural gas	Integrated the calcium copper loop with natural gas fired combined cycle power plant for H_2 production and CO_2 capture. An efficiency penalty of 8.1% was observed with a CO_2 capture efficiency of 90% when compared with the conventional natural gas fired combined cycle power plant.

Connell et al., 2013	Coal, Natural gas	A thermodynamic assessment was carried out for three process models based on calcium looping, conventional natural gas reforming and coal gasification technologies for H_2 production and electricity generation. Using calcium looping based process model, the cost of H_2 production and electricity generation was 9 -12% less than that of CO_2 capture and H_2 production with other process models.
Fernández and Abanades., 2017	Natural gas	A review on calcium copper looping process was carried out for the production of H_2 and/or electricity generation. It was observed that further investigation is needed to identify the best suitable synthetic sorbent on a commercial scale.
Hanak et al., 2018	Coal, Natural gas, Biomass	The feasibility of H_2 production from the calcium looping process was discussed as a part of the review in this work. It was noticed that the calcium looping based sorption enhanced steam reforming as a competent technology for H_2 production.
Wu et al., 2019	Coal, Biomass	An experimental investigation of calcium looping for high purity H_2 production and CO_2 capture was done in this work. The results revealed that a significant amount of energy consumption can be reduced at optimal desorption and sorption temperatures.
Shaikh et al., 2022	Biomass	Economic analysis of calcium looping process model for the production of electricity and H_2 was carried out using biomass as a fuel. The use of biomass in calcium looping lead to zero or net negative CO_2 emissions.

Several products such as methanol, oxy-methylene ethers, and DME can be made by utilizing the captured CO_2 from various plants (Koytsoumpa et al., 2018). Further, these products can also be utilized as feedstocks for synthesizing different chemicals, for example, DME can be used as a feed for producing methyl acetate, methyl sulfate, and green gasoline–based hydrocarbons, similarly methanol can be used to produce methyl tert-butyl ether, acetic acid,

olefins, etc. (Lee et al., 2021., Kung et al., 1994). Presently, the synthesis of DME with CO_2 utilization has gained a lot of attention, because it can be effectively utilized as an alternative fuel due to the following advantages such as better lower heating value (LHV) against methanol and ethanol and have high cetane number as compared to conventional diesel (Prasertsri et al., 2016; Park and Lee., 2014).

Generally, in a conventional process, the production of DME is carried out in two steps. In the first step, methanol is generated using syngas. Subsequently, methanol is dehydrated to produce DME (Lebarbier et al., 2012). However, a major drawback in this conventional process is the deactivation of the hydrophilic natured solid catalyst (gamma aluminum or modified gamma aluminum) that is used for methanol dehydration (Ivanova et al., 2015). This ultimately increases the overall cost of the conventional process. Dry reforming is a method that eliminates the complex methanol synthesis step by converting the gaseous mixture of syngas to DME directly (Schakel et al., 2016).

Various research articles demonstrated the ability of dry reforming process for the production of synthetic diesel, gasoline, H_2 etc. (Er-Rbib et al., 2012; Sun et al., 2011; Wang and Wang., 2009). Gangadharan et al., 2012 carried out an investigation to assess the economic and ecological impact of dry reforming in combination with steam reforming of CH_4. The results revealed that the combination of steam reforming and dry reforming of CH_4 is a more environmentally friendly approach as compared to standalone steam reforming of CH_4. However, more emphasis is needed to identify suitable catalysts that can improve the reforming efficiencies, reduce utility costs and CO_2 emissions. Luu et al., 2016 studied the direct CH_4 reforming process and bi-reforming process and compared these processes with the auto-thermal reforming process for the production of DME. For the same amount of CO_2 utilization, the CH_4 feed intake in direct CH_4 reforming and bi-reforming processes was 22.3% less as compared to the auto-thermal reforming process.

DinAli and Dincer., 2019b carried out a performance assessment of a cogeneration system integrated with solar energy for DME production and electricity generation. A chemical absorption method and a carbon hydrogenation process were used in this configuration to capture the emitted CO_2 and DME production, respectively. The overall energy and exergy efficiency of the integrated

system were found to be 28.75% and 32.54%, respectively. Similarly, a number of studies have also been reported with an aim for cleaner production of DME using solar energy (Martín., 2016; DinAli and Dincer., 2019a; DinAli and Dincer., 2019c). The above studies clearly reveal that the dry reforming based DME production is an energy-efficient. Also, integrating the DME production process with renewable energy technologies such as solar energy enables the entire process to be an environmentally friendly option. Therefore, it can be considered as a potential CO_2 utilization strategy to integrate with thermal power plants for sustainable power production.

2.5 Gaps identified in the literature

The literature review assisted in identifying the following research gaps:

1. Biomass is a potential fuel source for low capacity and grid independent power plants. The potential for electricity generation in rural regions using agricultural biomass as fuel, such as bagasse, is immense. Further, integration of this power plant with CO_2 capture and utilization technologies can make this configuration as carbon negative process. Preliminary studies are available in the literature on the use of calcium looping technology for CO_2 capture from biomass combustion. To make this technology sustainable and feasible at small scale power generation, an efficient integration of the fuel combustion, power cycle and CO_2 capture modules is necessary along with the energy, exergy, environmental and cost analyses.

2. The calcium looping CO_2 capture technology integration with coal-fired power plants is explored in the literature. However, feasibility study of different calcium looping technologies integration with coal-fired power plants, detailed analyses and performance comparison based on energy, exergy, environmental and cost parameters is not performed. In addition to CO_2 capture, there is potential to incorporate a H_2 production scheme in calcium looping integrated coal fired power plant. There have been limited studies that incorporated calcium looping technology for H_2 and electricity co-generation, as well as CO_2 capture. Further, there are no studies on double calcium looping integrated H_2 production using coal gasification.

3. In the literature, no studies have evaluated the performance of a natural gas fired combined cycle power plant integrated with different calcium looping technologies. An effective

integration of calcium looping technology with natural gas fired combined cycle power plant can be explored.

4. The literature study clearly suggests that dry reforming based DME production that utilizes CO_2 can be integrated with gas fired power plants. It also demonstrates that integrating this DME production unit (DPU) with solar energy could be an energy and environmentally friendly option. In this perspective, there is a great potential to propose a CO_2 utilization scheme by coupling a dry reforming based DPU and solar energy with the calcium looping integrated natural gas fired combined cycle power plant.

It is clear from the literature that there is a lack of studies on detailed performance assessment of biomass, coal, and natural gas power plants integrated with different calcium looping technologies based on energy, exergy, environmental, and economic factors. Development of novel cogeneration configurations and evaluating their performance against conventional power plant configurations will result in the utilization of these technologies in thermal power plants for the production of sustainable energy from biomass, coal, and natural gas.

CHAPTER 3

METHODOLOGY

Chapter 3

Methodology

This chapter aims to present a detailed description of the modeling and simulation methodologies used in order to achieve the objectives identified in the previous chapter. Section 3.1 describes the methodology adopted for the design of coal, biomass and natural gas based power plant configurations, which are integrated with CO_2 capture and utilization processes. The necessary unit models required to design the power plant configurations are simulated and validated against the literature results. By systematic integration of these unit models, different power plant configurations have been synthesized to explore the advantages of CO_2 capture, CO_2 utilization and cogeneration schemes. The conventional coal, biomass and natural gas fired combined cycle power plant configurations from the literature are reproduced and considered them as reference cases in the comparison studies. Section 3.2 presents the assumptions and mathematical equations used to evaluate the performance of the proposed configurations based on energy, exergy, environmental, cost and exergoeconomic analysis.

3.1 Systems description

As part of this project, different flowsheet configurations were constructed for coal, biomass and natural gas fired combined cycle fired power plants. Simulation environment, aspenONE v10.0, is used to develop plant layout, operating conditions (temperature, pressure, flow rates, fuel composition and unit efficiency) and key parameters. The conventional power plant configurations are simulated using the appropriate models and data from the published literature. The different plant types considered in the present study are grouped into the following five categories:

Category 1: Calcium looping for CO_2 capture in biomass fired power plants
Category 2: Calcium looping for CO_2 capture in coal fired power plants
Category 3: Calcium looping for CO_2 capture in natural gas fired combined cycle power plants
Category 4: Calcium looping for CO_2 capture, H_2 and electricity coproduction in coal fired power plants

Category 5: CO_2 utilization in double calcium looping integrated natural gas fired combined cycle power plants

Each category involves different cases defined as per the need of the objective, which are discussed in the below subsections. Steady-state simulations of all the cases of these categories are conducted with suitable models using aspenONE v10.0.

3.1.1 Category 1 – Calcium looping for CO_2 capture in biomass fired power plants

In this section, a step by step methodology was followed to derive three different biomass fired power plants configurations. First, double calcium looping and an organic rankine cycle (ORC) process flowsheets were simulated using aspenONE and validated with data published in the literature. Using these validated models, standalone biomass fired power plant (BFPP1) and calcium looping integrated biomass fired power plant configurations were synthesized. In the present study the biomass combustor was not integrated with gas turbine cycle because the configuration was designed at near atmospheric pressure. Further, the proposed grid independent power plant configurations operate is designed at near atmospheric pressure and operates at low capacity by utilizing the biomass available in rural areas. The amount of heat energy generation with such low fuel feed rate in the biomass combustor is more suitable to drive an ORC rather than a steam turbine. Similar studies on integration of ORC with biomass combustion are available in the literature (Al-Sulaiman et al., 2012; Quoilin et al., 2013; Ahmadi et al., 2013).

3.1.1.1 Model validation

Due to the lack of literature data for integrated calcium looping biomass fired and ORC based configurations, individual modules were validated separately and then integrated appropriately. The double calcium looping and ORC process unit models are adopted from Diego et al., 2016 and Ozdil et al., 2015 respectively. Fig. 3.1 and Fig. 3.3 show the process flowsheets for the double calcium looping and ORC unit models, respectively. The simulated results of these configurations and validation with source models are presented in Table 3.1 and Table 3.2. All the results indicate that the deviation is well in between ± 4%. Thus, the simulated results are in good agreement with the configurations obtained from the literature. The double calcium looping unit model is simplified into conventional single calcium looping model as shown in Fig. 3.2 by

eliminating the indirect heat transfer loop between combustor and calciner as shown in Fig. 3.1. This single calcium looping unit model is simulated by considering all other parameters as double calcium looping unit. The various models are then systematically integrated in terms of mass and energy to come up with effective power plant configurations, with or without CO_2 capture.

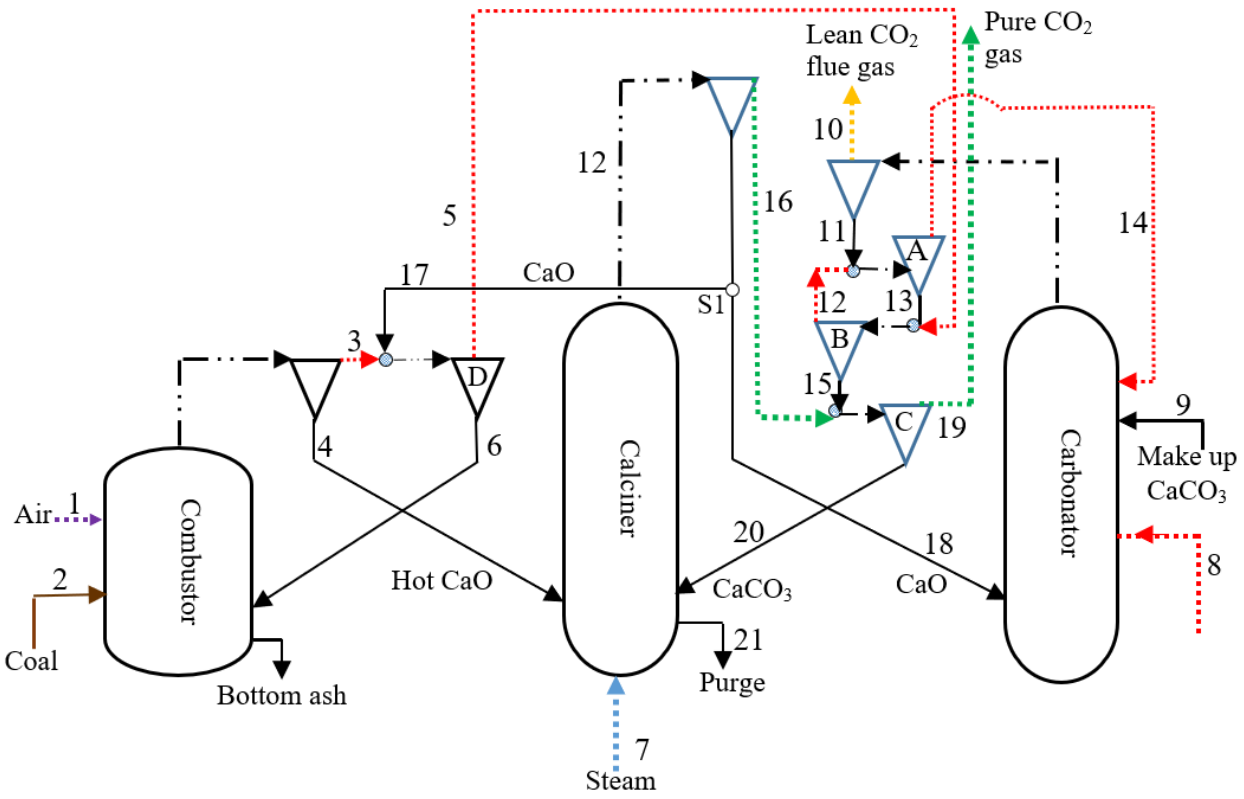

Legend

	Coal		Air
	Sorbent / bottom ash		CO_2 stream
	Lean CO_2 flue gas stream		Sorbent + Gas
	Steam		Mixer
	Flue gas		Cyclone separator

Fig. 3.1 Schematic layout of the double calcium looping configuration (Source: Diego et al., 2016)

Table 3.1. Validation of double calcium looping system based on main stream parameters

Stream ID	Source model	ASPEN model		Source model	ASPEN model	
	Temperature	Temperature	Error %	Molar flow	Molar flow	Error%
	°C	°C		kmol/s	kmol/s	
1	400	400	0.00	2.5	2.5	0.00
2	20	20	0.00	6.7	6.7	0.00
3	1030	1041	-1.07	2.6	2.61	-0.38
4	1030	1041	-1.07	1034.5	1035.3	-0.08
5	916	916	0.00	2.6	2.61	-0.38
6	916	916	0.00	1034.3	1034.9	-0.06
7	400	400	0.00	0.1	0.1	0.00
8	150	150	0.00	0.5	0.5	0.00
9	600	600	0.00	36.1	36.1	0.00
10	650	650	0.00	2.7	2.66	1.48
11	650	650	0.00	141.7	142	-0.21
12	780	782	-0.26	2.6	2.61	-0.38
13	698	700.8	-0.40	141.7	142	-0.21
14	698	700	-0.29	2.6	2.61	-0.38
15	780	782.9	-0.37	141.7	142	-0.21
16	904	904	0.00	0.9	0.9	0.00
17	904	904	0.00	1034.3	1034.9	-0.06
18	904	904	0.00	86.1	86.1	0.00
19	810	810	0.00	0.9	0.9	0.00
20	810	810.8	-0.10	141.7	142	-0.21
21	904	904	0.00	20.7	21.6	-4.35

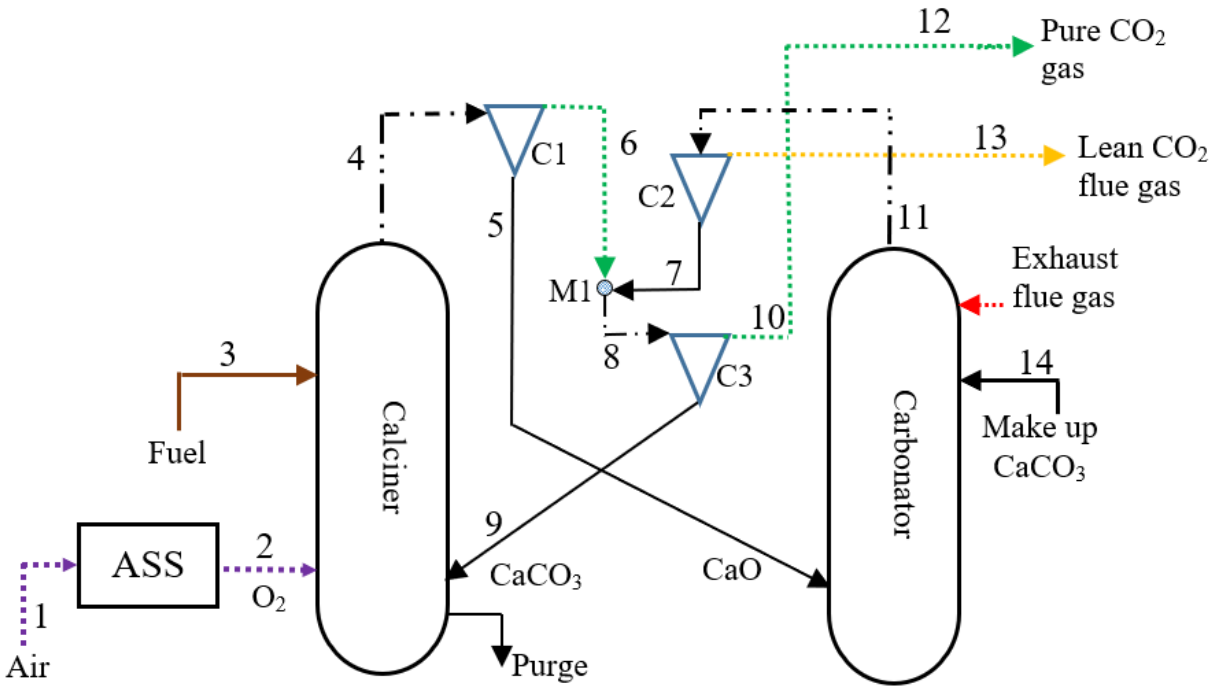

Legend

	Coal		Air
	Sorbent		CO_2 stream
	Lean CO_2 flue gas stream		Sorbent + Gas
	Flue gas		Mixer
	Cyclone separator		

Fig. 3.2 Schematic layout of the conventional (single) calcium looping configuration

Table 3.2. Validation of ORC based on main stream parameters

	Source model	ASPEN model		Source model	ASPEN model		Source model	ASPEN model	
Stream ID	Mass flowrate (kg/s)	Mass flowrate (kg/s)	Error %	Temperature (K)	Temperature (K)	Error %	Pressure (bar)	Pressure (bar)	Error %
1	13.48	13.48	0	400	400.00	0.00	2.7	2.7	0
2	13.48	13.48	0	356.9	366.90	-2.8	2.2	2.2	0
3	10.63	10.63	0	368.4	368.40	0.00	11.4	11.4	0

4	10.63	10.63	0	326	324.75	0.38	2.4	2.4	0
5	10.63	10.63	0	303	303.00	0.00	2.4	2.4	0
6	10.63	10.63	0	303.17	304.07	-0.3	11.4	11.4	0
7	110	110	0	300.5	300.50	0.00	1.37	1.37	0
8	110	110	0	305.4	303.97	0.47	1.37	1.37	0

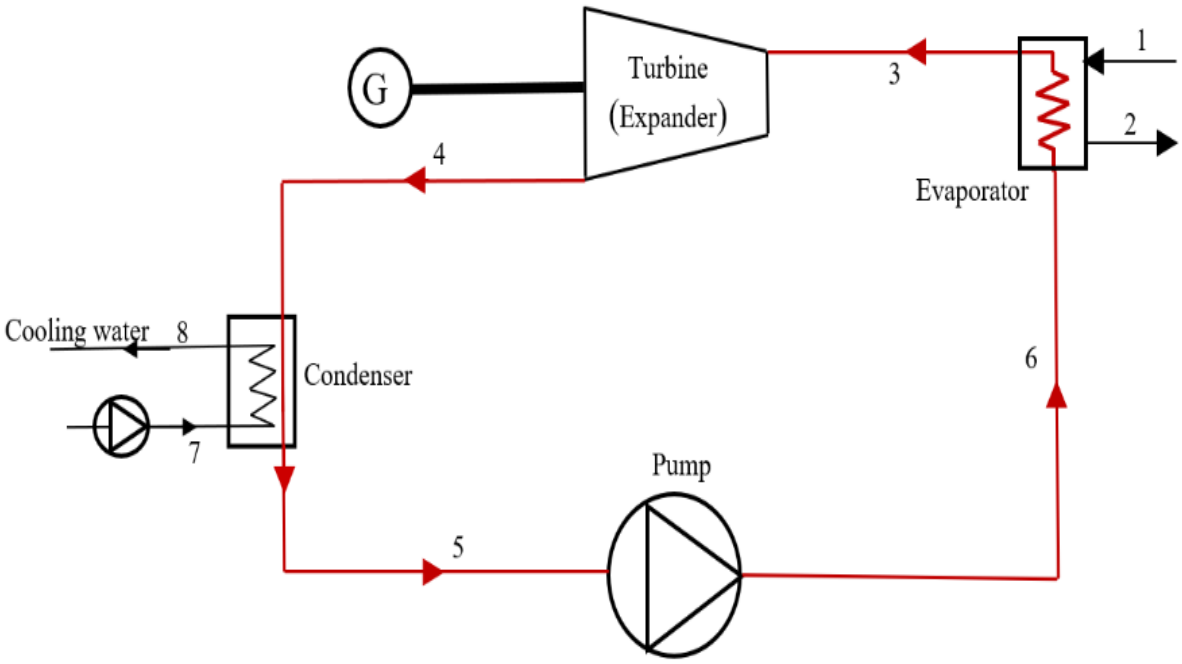

Legend

⟶	Organic (working) fluid	⏦	Heat exchanger
⟶	Water	G	Generator

Fig. 3.3 Schematic layout of ORC (Source: Odzil et al., 2015)

3.1.1.2 Standalone biomass-fired power plant (BFPP1)

The BFPP1 configuration is synthesized by integrating three major modules, i.e., combustor, thermal oil tank, and ORC unit for power generation as shown in Fig. 3.4.

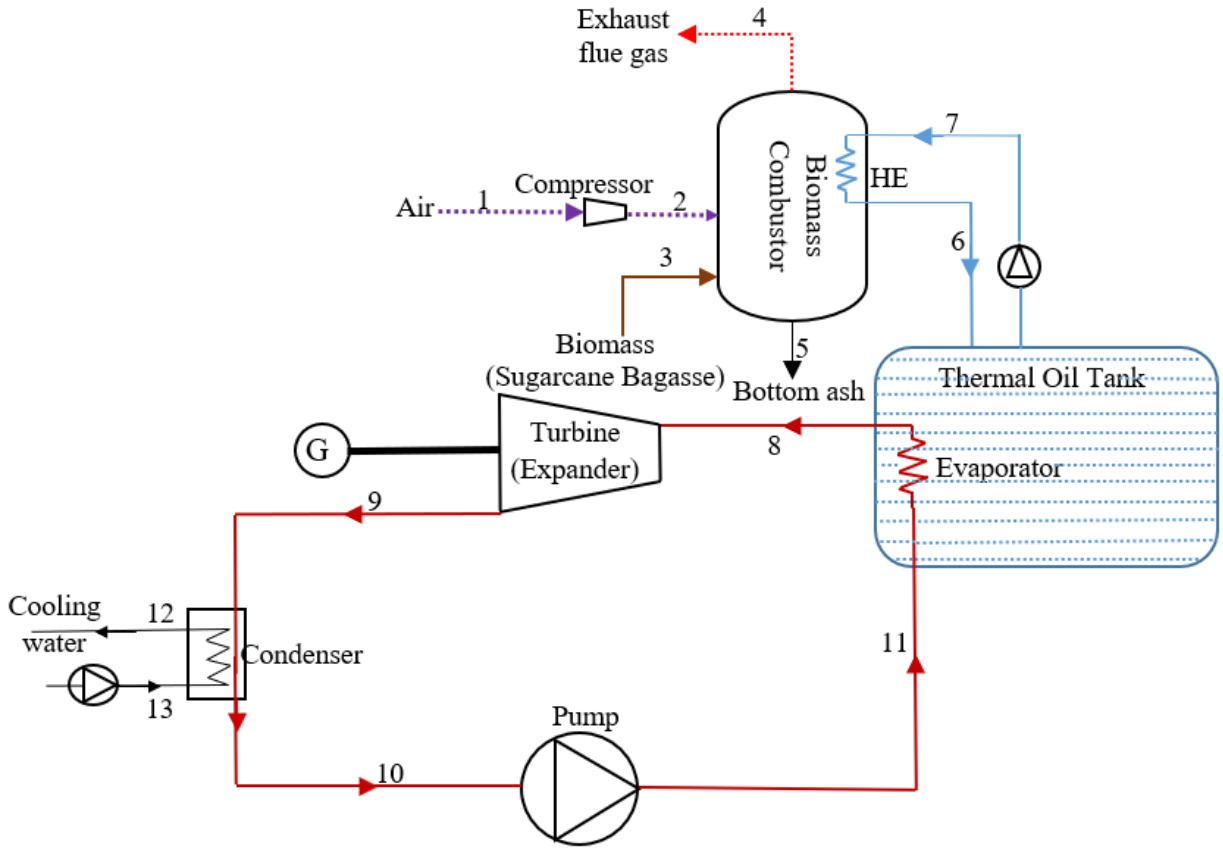

Legend

	Working fluid		Heat exchanger
	Thermal oil	G	Generator
	Fuel		Flue gas stream
	Air		Bottom ash

Fig. 3.4 Schematic layout of BFPP1

In this power plant configuration, the operating temperature of combustor was maintained at constant value by continuous supply of biomass (sugarcane bagasse) and 20% excess air. Excess air was supplied to ensure complete combustion of fuel. The hot flue gas generated during combustion exchanges heat with the thermal oil in a heat exchanger. This is done to avoid local overheating and to prevent the organic fluid (refrigerant) from becoming chemically unstable when comes in direct contact with hot flue gases of combustor (Algieri and Morrone., 2014). The ORC unit consists of a pump, an evaporator, a turbine/expander, and a condenser. The pump was initially used to compress the working (organic) fluid from a low pressure (2.4 bar) to high pressure liquid

(11.4 bar). The high-pressure liquid was then allowed to enter the evaporator where it evaporates by utilizing the energy available in thermal oil. This high-pressure vapor was then passed through the turbine to expand isentropically to a low-pressure vapor and generate electricity. Finally, this low-pressure vapor leaving the turbine was cooled, condensed and recirculated back into the cycle.

3.1.1.3 Conventional (single) calcium looping integrated biomass fired power plant (BFPP2)

The proposed BFPP2 configuration mainly consists of three sub systems: biomass combustion, calcium looping, and ORC. The schematic diagram is shown in Fig. 3.5. The biomass was initially combusted in the presence of air to generate the hot flue gas. The thermal oil extracted heat from the hot flue gas in the heat exchanger (HE1), and its temperature was increased to 374 ^{0}C. It was then passed through the heat exchanger (HE2) to recover the maximum possible high-grade energy available in the carbonator. The exhaust flue gases leaving the combustor were sent to the calcium looping unit where the CO_2 gas was separated through the carbonation and calcination cycle. An ASS is used to generate the O_2 required for the combustion of biomass in the calciner. The remaining energy from the concentrated CO_2 stream and lean flue gas leaving the calcium looping unit was recovered by sending them through the heat exchangers (HE3 and HE4). The cold lean flue gas was finally released into the atmosphere, while the low-temperature concentrated CO_2 gas was directly utilized or stored after compression.

3.1.1.4 Double calcium looping integrated biomass fired power plant (BFPP3)

The proposed configuration for the novel BFPP3 system, which is composed of a double calcium loop, biomass combustion and ORC systems (Fig. 3.6). Unlike direct heat transfer as a way to promote endothermic reactions in the calciner, this calcium looping integrated biomass fired power plant model utilizes indirect heat transfer method via a double calcium configuration. This not only avoids the need for oxygen separation plant but also ensures high CO_2 capture efficiency. In the first calcium loop, the solid CaO stream that circulates between the combustor and calciner acts as a simple heat carrier. In the second calcium loop, the CO_2 was captured by the solid CaO sorbent in the carbonator reactor, where the exothermic reaction takes place at 650 ^{0}C. The resulting carbonated solids that act as a CO_2 carrier were then transported to calciner, where concentrated CO_2 was released and CaO sorbent was regenerated at around 904 ^{0}C.

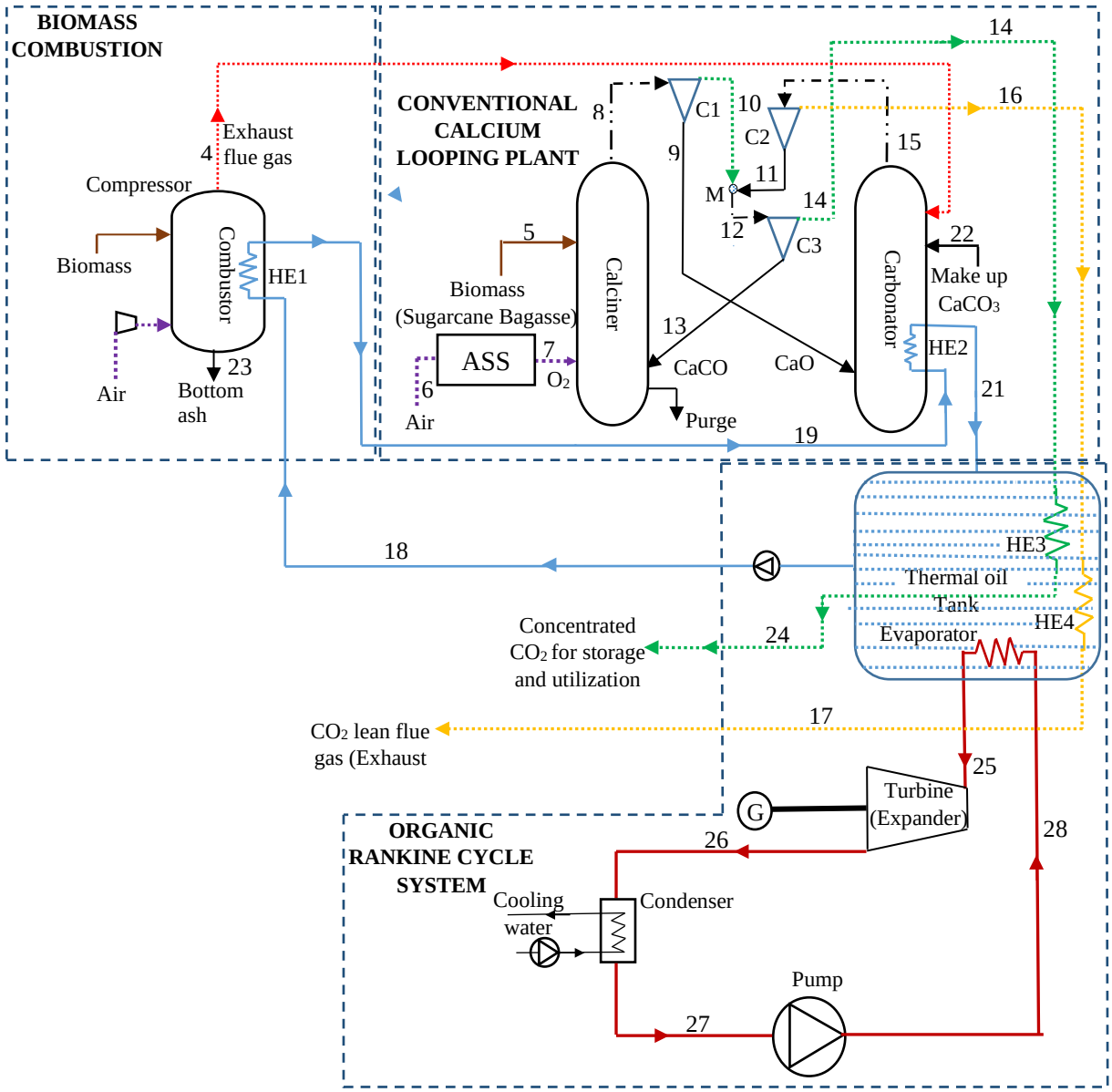

Legend

	Biomass Fuel		Working fluid (R-245fa)
	Sorbent/ Bottom ash		Solid gas separator
	Sorbent + Gas		Mixer
	Clean / lean CO_2 gas		Thermal Oil
	Flue gas stream		Heat exchanger
	CO_2 stream		Pump
	Air / O_2 stream	G	Generator

Fig. 3.5 Schematic layout of BFPP2

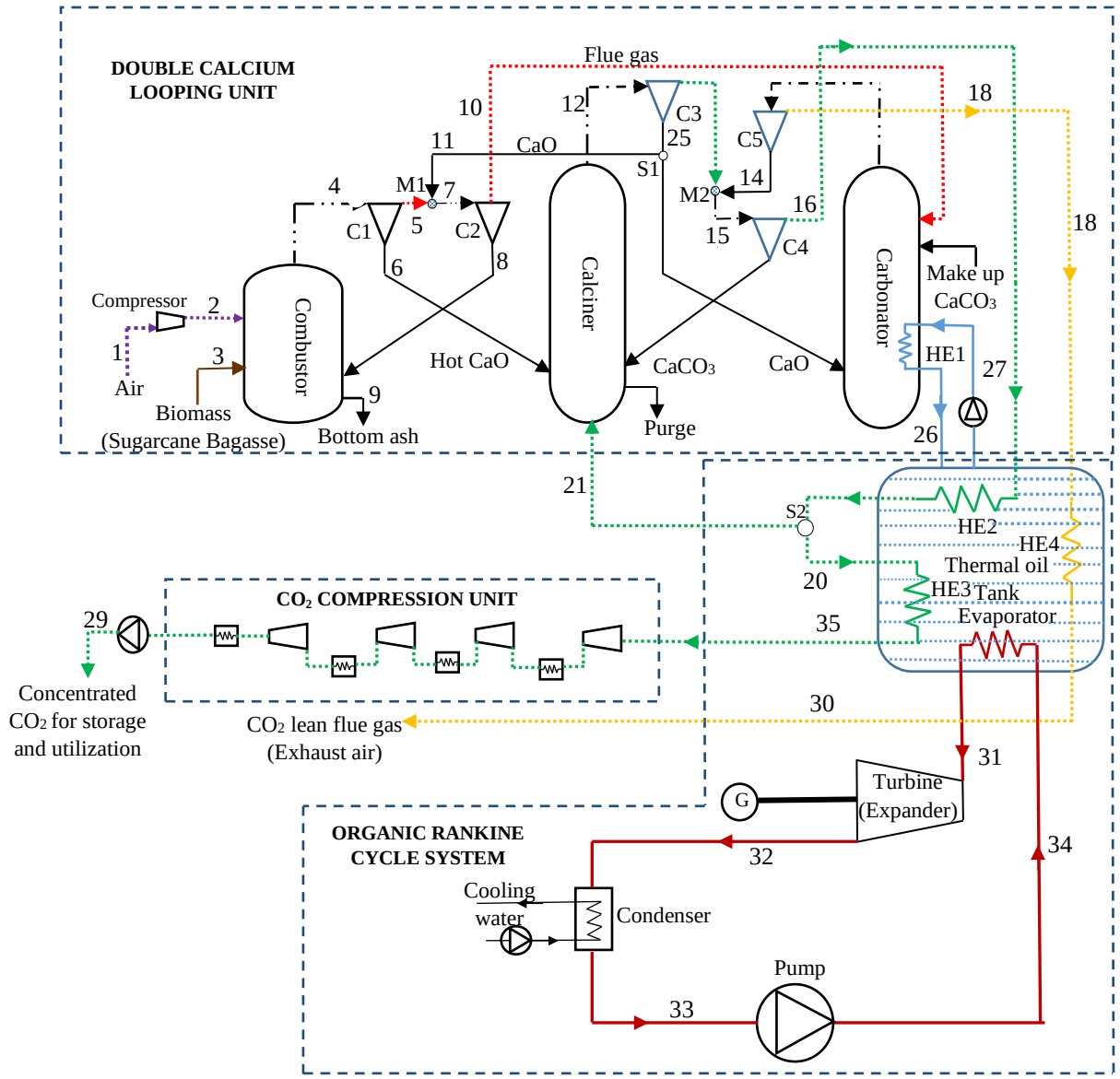

Legend

	Biomass Fuel		Working fluid (R-245fa)
	Sorbent	▽	Solid gas separator
	Sorbent + Gas	⊗	Mixer
	Clean / lean CO_2 gas	○	Splitter
	Flue gas stream		Heat exchanger
	CO_2 stream		Thermal oil
	Air stream	G	Generator

Fig. 3.6 Schematic layout of BFPP3

Preheating the $CaCO_3$ sorbents entering the calciner from the second calcium loop minimizes the heat transfer from the combustor to the calciner. This reduces the sensible energy requirement from combustor to the calciner. Although the CO_2 released during calcination enables a self-fluidization behavior in the calciner, a part of the high-concentrated CO_2 stream leaving the calcium looping system was recirculated back for effective fluidization. Finally, the concentrated CO_2 stream was sent to compression unit (CU) to increase the pressure up to 110 bar. Deactivated and inert compounds (mainly $CaSO_4$ and ash) were removed in the form of purge from calciner. To compensate for this loss, fresh limestone is fed to the carbonator as a makeup.

The high-grade available energy in the carbonator was utilized to heat the high-pressure working fluid leaving the evaporator of ORC system by using a thermal oil that acts as an intermediate stream between the combustor and ORC unit. The operation and characteristics of this ORC were the same as that of BFPP1. To enhance the thermal efficiency of the overall plant, the concentrated CO_2 and lean flue gas leaving the calcium looping system were also passed through the heat exchangers (HE2, HE3, and HE4) to preheat the thermal oil. The low temperature lean flue gas leaving the thermal oil tank was released into the atmosphere, while the low temperature concentrated CO_2 gas was sent through CU to compress and store.

3.1.2 Category 2: Calcium looping for CO_2 capture in coal fired power plants

The process followed for configuring the two coal fired power plants is explained in this section. At first a supercritical coal fired power plant was simulated and validated against the published results. This validated coal fired power plant configuration was further integrated with single and double calcium looping for CO_2 capture. At the end, the fuel and operating conditions were replaced as per the Indian climatic conditions. The validated results of the coal fired power plant and the description of the two proposed configurations are presented in the sub sections given below.

3.1.2.1 Model validation

The coal fired power plant as shown in Fig. 3.7 was adopted from Espatolero et al., 2010 and referred in this work as CFPP1. This super critical power plant mainly consists of a power boiler, a condenser with centrifugal pump, a set of high-pressure feed pumps and a section of high, low and intermediate pressure turbines (HPT, IPT and LPT) to generate power. In addition, a de-

aerator, a number of high pressure and low-pressure feed water heaters were also provided along with other accessories to enhance the performance of power plant. This power plant configuration is simulated using aspenONE software. The two thermodynamic methods that were used in modelling the boiler heat exchange sections are Peng-Robinson-Boston-Mathias (PR-BM) equation of state for coal, air and flue gas streams and steam table (STEAM-NBS) for H_2O streams. The results represented in Table 3.3 show that the streams of the simulated model in aspenONE with the relative error in between -1.37% and 3.44% is in very good agreement with Espatolero et al., (2010) model.

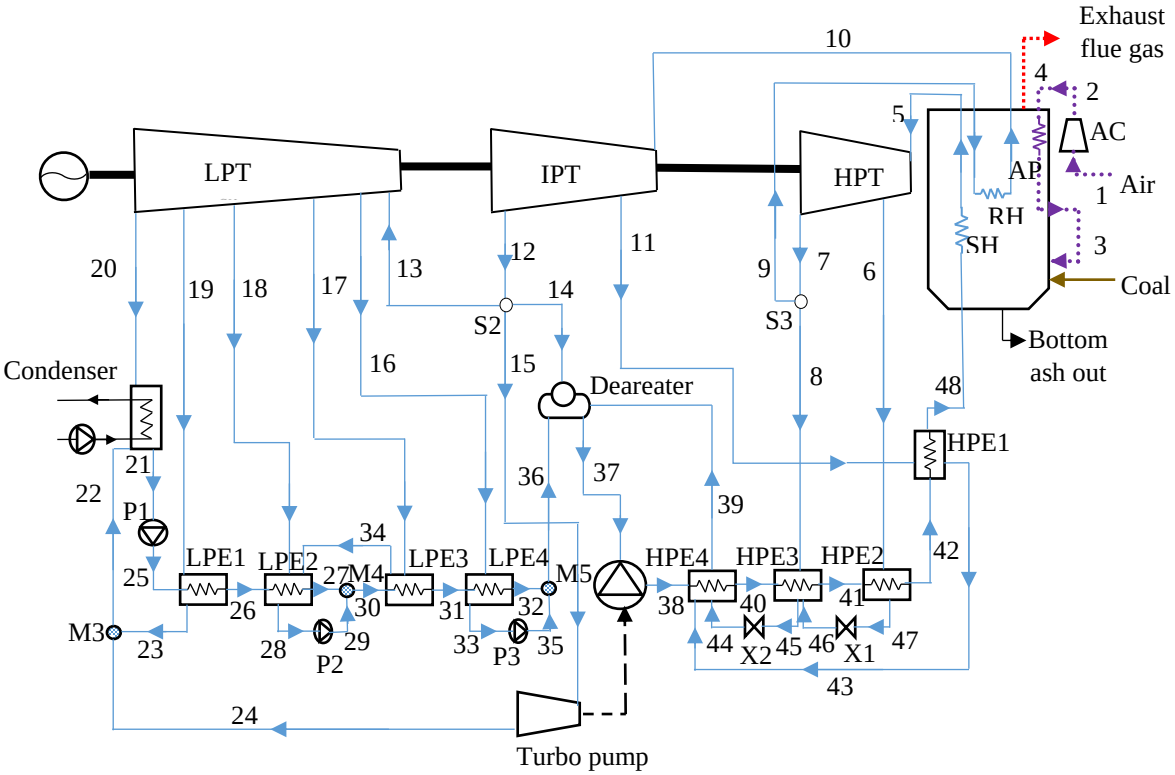

Legend

	Fuel		Mixer		Bottom ash
	Air stream		Splitter		
	Flue gas		Heat exchanger		
	H_2O stream		Pump		

Fig. 3.7 Schematic layout of CFPP1 (Source: Espatolero et al., 2010)

A detailed explanation of the simulation and validated results of conventional and double calcium looping processes considered in the study has already been provided in subsection 3.1.1.1. Considering the validated supercritical coal fired power plant and calcium looping configurations, two new coal fired power plant configurations are derived. In the proposed configurations, the Indian (high ash) coal is used as a fuel and operating conditions were modified based on Indian climatic conditions. Since the ambient conditions affect the thermal performance of power plant, these operating conditions were based on the worst-case scenario approach (Suresh et al., 2010). The following subsections detailed the operation principle and characteristics of the proposed configurations.

Table 3.3. Validation of supercritical coal fired power plant based on main stream parameters

	Source model	ASPEN model		Source model	ASPEN model		Source model	ASPEN model	
Stream ID	Mass flowrate (kg/s)	Mass flowrate (kg/s)	Error %	Temperature (^oC)	Temperature (^oC)	Error %	Pressure (bar)	Pressure (bar)	Error %
5	450	450	0.00	590	589.9	0.02	300	300	0.00
6	28.23	28.23	0.00	371.2	359.43	3.17	76.8	76.8	0.00
8	33.37	33.36	0.03	334.2	322.99	3.35	58.37	58.37	0.00
9	388.4	388.4	0.00	334.2	322.99	3.35	58.37	58.37	0.00
10	388.4	388.4	0.00	610	609.9	0.02	57.2	57.2	0.00
11	21.91	21.91	0.00	496.4	491.44	1.00	28.1	28.1	0.00
12	47.87	47.87	0.00	366.1	361.66	1.21	11.04	11.04	0.00
13	318.62	318.62	0.00	330.98	326.24	1.43	8.34	8.34	0.00
16	17.71	17.71	0.00	256.9	252.62	1.67	4.42	4.42	0.00
17	17.72	17.72	0.00	148.8	145.2	2.42	1.48	1.48	0.00
18	11.11	11.11	0.00	79.4	79.3	0.13	0.46	0.46	0.00
19	13.89	13.89	0.00	57.8	57.8	0.00	0.18	0.18	0.00
20	258.19	258.19	0.00	32.9	32.9	0.00	0.05	0.05	0.00
21	296.48	296.48	0.00	32.4	32.3	0.31	0.05	0.05	0.00
25	296.48	296.48	0.00	33	32.9	0.30	22	22	0.00
26	296.48	296.48	0.00	58	56.8	2.07	22	22	0.00
30	325.31	325.31	0.00	80	78.75	1.56	22	22	0.00
31	325.31	325.31	0.00	110	108.7	1.18	22	22	0.00
36	343.02	343.02	0.00	140.5	139.3	0.85	22	22	0.00
37	450	450	0.00	183	182.9	0.05	10.82	10.82	0.00
38	450	450	0.00	189.5	188.51	0.52	344	344	0.00

40	450	450	0.00	216.05	214.89	0.54	344	344	0.00
41	450	450	0.00	251.92	251.77	0.06	344	344	0.00
42	450	450	0.00	277.54	277.31	0.08	344	344	0.00
48	450	450	0.00	281.85	281.69	0.06	344	344	0.00
43	21.91	21.91	0.00	303.8	303.7	0.03	28.1	28.1	0.00
47	28.23	28.23	0.00	258.8	258.7	0.04	75.26	75.26	0.00
46	28.23	28.23	0.00	258.8	258.61	0.07	58.37	58.37	0.00
45	61.59	61.59	0.00	222.5	214.84	3.44	57.2	57.2	0.00
44	61.59	61.6	-0.02	222.66	215.04	3.42	28.1	28.1	0.00
39	83.5	83.51	-0.01	202.1	201.95	0.07	27.54	27.54	0.00
14	23.47	23.47	0.00	366.1	361.66	1.21	11.04	11.04	0.00
15	24.4	24.4	0.00	366.1	361.66	1.21	11.04	11.04	0.00
24	24.4	24.4	0.00	36.16	36.16	0.00	0.06	0.06	0.00
23	13.89	13.89	0.00	57	57.8	-1.4	0.18	0.18	0.00
28	28.82	28.83	-0.03	78.6	78.5	0.13	0.46	0.46	0.00
29	28.82	28.83	-0.03	79	78.8	0.25	22	22	0.00
33	17.71	17.71	0.00	139.8	138.99	0.58	4.42	4.42	0.00
35	17.71	17.71	0.00	140.14	139.39	0.54	22	22	0.00
34	17.72	17.72	0.00	108	107.9	0.09	1.46	1.48	-1.3

3.1.2.2 Conventional (single) calcium looping integrated coal fired power plant (CFPP2)

The validated calcium looping process was modified and integrated with supercritical CFPP1 model. Fig. 3.8 shows the CO_2 capture process of calcium looping integrated to CFPP1. This conventional calcium looping unit (CCaLU) consists of a calciner and carbonator reactor along with an ASS. The configuration helps to capture the CO_2 emitted after the combustion of coal in the power plant. Lime was used as an adsorbent to capture CO_2. The CCaLU separates the CO_2 from the flue gases via carbonation and calcination reaction cycle as explained in Chapter 1. In general, the CO_2 capture using CaO is a reversible reaction. At the operating temperature of 665 ^{0}C in carbonator, the rate of decomposition of $CaCO_3$ is very low. Similarly, by maintaining the calciner at 904 ^{0}C the rate of carbonation is restricted.

Indian coal was combusted in the calciner to supply required heat to operate them at isothermal condition. An ASS supplies oxygen to calciner which is essential to get pure CO_2 from calciner by means of coal combustion and $CaCO_3$ decomposition. Cyclone separators were used to separate sorbent from CO_2 stream and lean flue gases. The hot concentrated CO_2 gas and lean flue gases leaving the calciner and carbonator contains a significant amount of heat energy, which

was recovered using multiple heat exchangers (HPE5, HPE4, HPE2 and LPE4) as shown in Fig. 3.8. A certain amount of calcium sorbent gets deactivated during the cyclic operation and it was removed in the form of purge from the calciner. This sorbent loss was compensated by using fresh material in the form of makeup stream. Apart from the combustor, the high-grade energy available in the carbonator was also utilized to generate the live steam in the supercritical steam cycle by using the reheater (RH2). The cooled concentrated CO_2 gas can be compressed and sequestrated accordingly.

3.1.2.3 Double calcium looping integrated coal fired power plant (CFPP3)

The synthesized double calcium looping integrated coal fired power plant is shown in Fig. 3.9. The process of double calcium looping has already been described previously. In the power plant configuration, the operating temperature of combustor was maintained by continuous supply of required amount of coal and 20% excess air. Excess air was supplied to ensure complete combustion of fuel. The configuration helps to avoid the need of oxygen separation plant for calcium looping system and ensures high CO_2 capture efficiency.

The high-grade available energy in the carbonator was utilized to generate the live steam using superheater (SH) and reheater (RH) which was used in the supercritical steam cycle. The live steam enters the HPT at 573 ^{0}C and 300 bar and was expanded to 58.37 bar. It was then reheated again by the hot lean flue gases present in the carbonator, before sending it to the IPT and LPT. To enhance the thermal efficiency of steam cycle, the hot concentrated CO_2 gas was used to preheat air entering into the combustor. At the same time, multiple heat exchangers i.e., HPE5, HPE4, HPE2 and LPE4 were used to recover the maximum possible heat energy from the lean flue gas. The cooled concentrated CO_2 can be stored and utilized by CO_2 capture and compression unit (CU) accordingly.

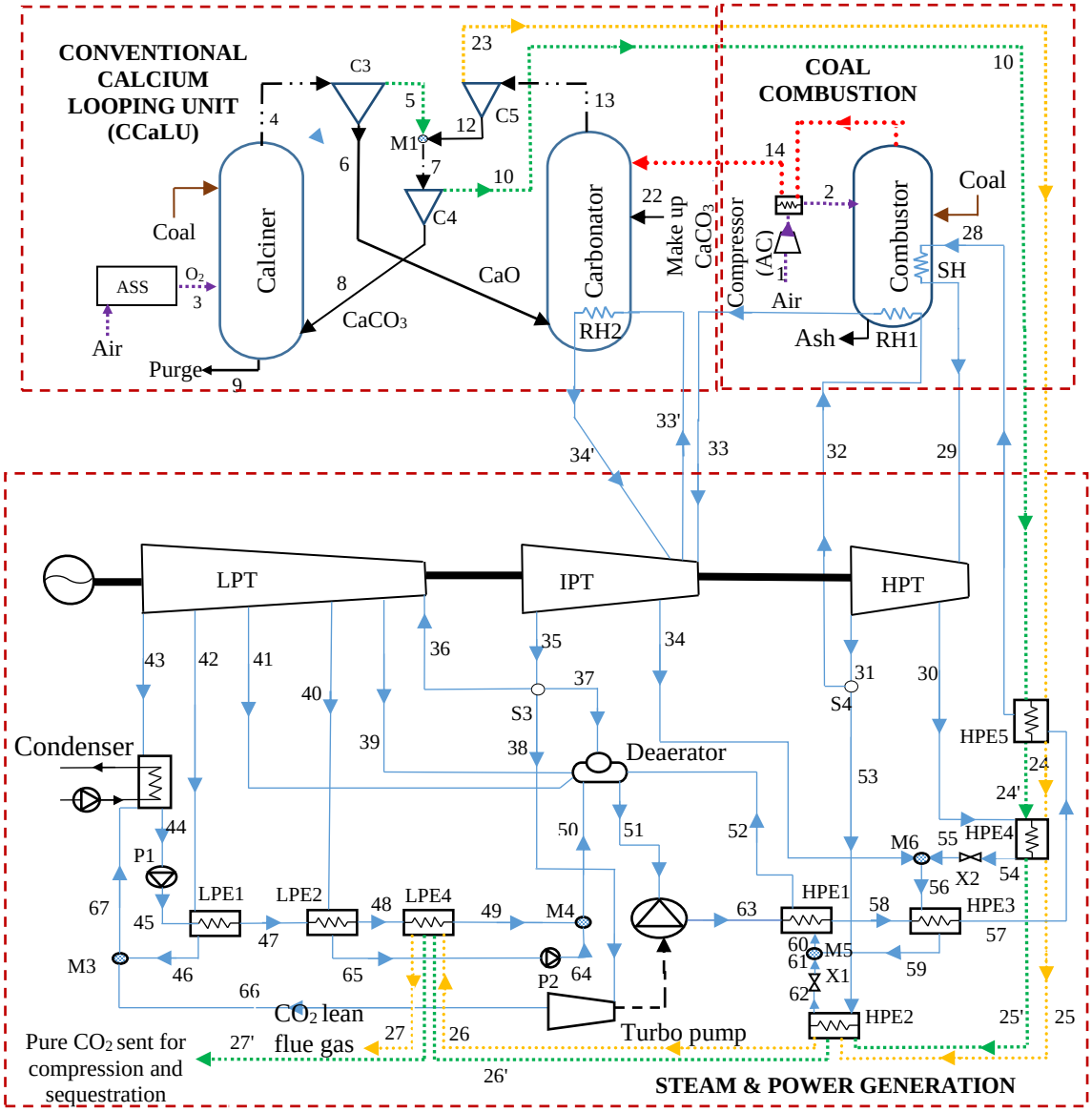

Legend

Fuel		Mixer
Air stream		Splitter
Flue gas		Heat exchanger
H_2O stream		Pump
Lean CO_2 gas		Sorbent / Ash
Sorbent + Gas		Generator

Fig. 3.8 Schematic layout of CFPP2

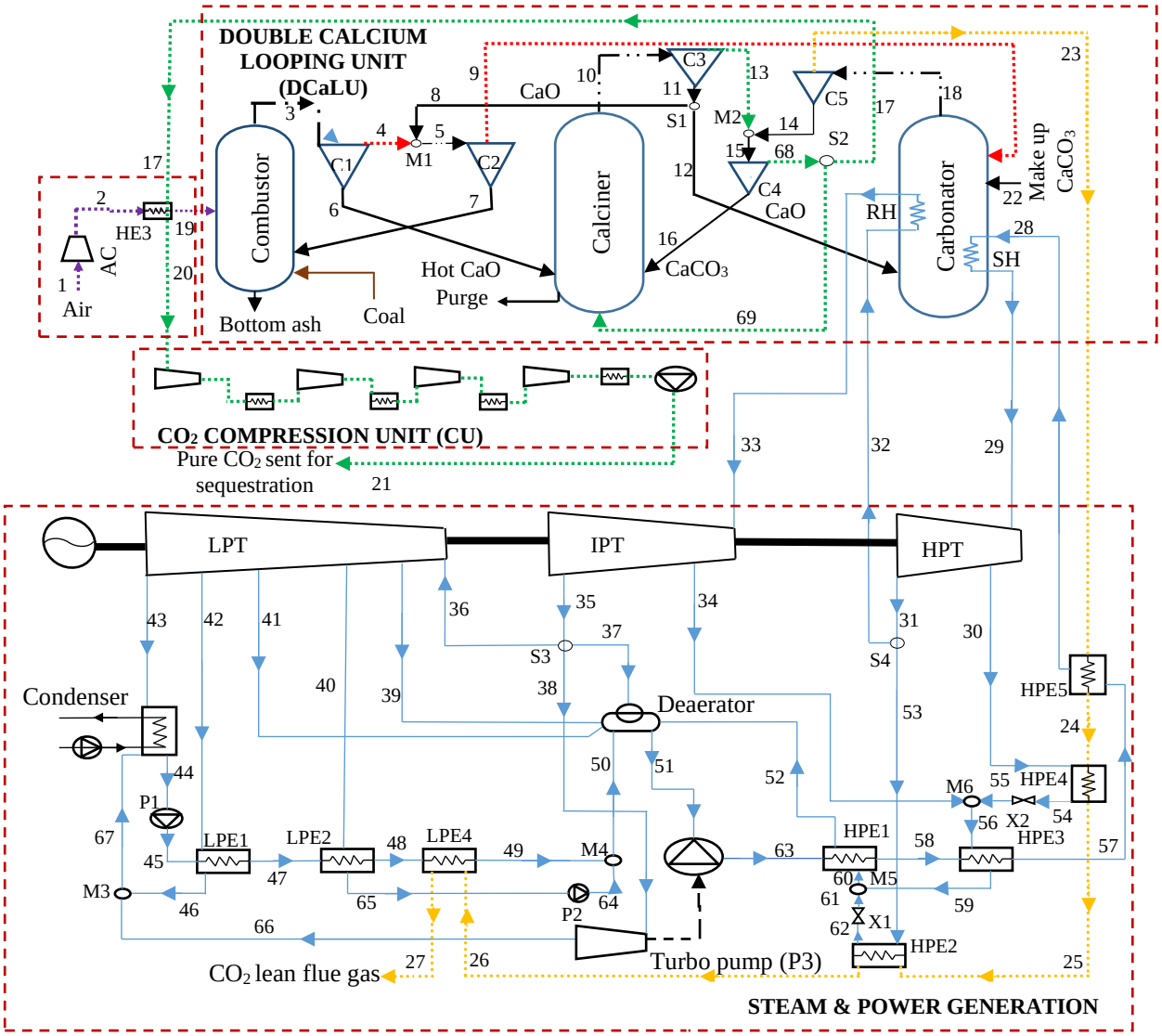

Legend

——→	Fuel	⊛	Mixer
·····→	Air stream	○	Splitter
·····→	Flue gas	⏦	Heat exchanger
——→	H_2O stream	⊳	Pump
·····→	Lean CO_2 gas	——→	Sorbent / Bottom ash
-·-·-·→	Sorbent + Gas	·····→	Pure CO_2 stream

Fig. 3.9 Schematic layout of CFPP3

3.1.3 Category 3: Calcium looping for CO_2 capture in natural gas fired combined cycle power plants

The methodology to synthesize novel calcium looping integrated natural gas fired combined cycle power plant configurations is presented in this study. A reference natural gas fired combined cycle power plant is adopted from the literature and successfully validated. The conventional and double calcium looping based CO_2 capture processes were further integrated with this natural gas fired combined cycle power plant to capture CO_2. A detailed description of model validation, novel flowsheet synthesis and process integration for power generation and CO_2 capture are presented in the below subsections:

3.1.3.1 Model validation

The conventional natural gas fired combined cycle power plant (considered as NGFCPP1) was simulated by considering indigenous feed and environmental conditions. Fig. 3.10 shows the flowsheet of the configuration that was adopted from Reddy et al., 2012. The fuel, i.e., natural gas, was burned in the combustors C1 and C2 at high pressure of 9.6 bar in this system. A 300% excess air was supplied to the C1 and C2 using air compressors AC1 and AC2 to regulate the temperature of flue gases (Bolland and Saether., 1992). This is done, to bring the inlet temperature of gas turbine to the permissible limits that it can sustain (Lugo-Leyte et al., 2010). The hot flue gases from the C1 and C2 were sent through the gas turbine and then through the Heat Recovery Steam Generators (HRSG1 and HRSG2) to recover the maximum possible energy.

The gas power generation unit (GPGU) was used as a topping cycle and works on the principle of Brayton cycle, while the Steam Power Generation Unit (SPGU) works on the principle of Rankine cycle which was used as a bottoming cycle. The exhaust flue gases leaving the HRSG1 and HRSG2 units were finally released into the atmosphere. The natural gas was supplied at 6.05 kg/sec to each GPGU. This scheme produces a total gross power of 330.34 MW via gas turbines and 115.82 MW via high and low pressure steam turbines. This NGFCPP1 generates a total amount of 31.92 kg/sec of CO_2 during its operation. The simulated results tabulated in Table 3.4 are validated results of the power plant adopted from Reddy et al., 2012. The reproduced model was able to match most of the stream data with a relative error percentage of less than 0.02 % when compared to the original model.

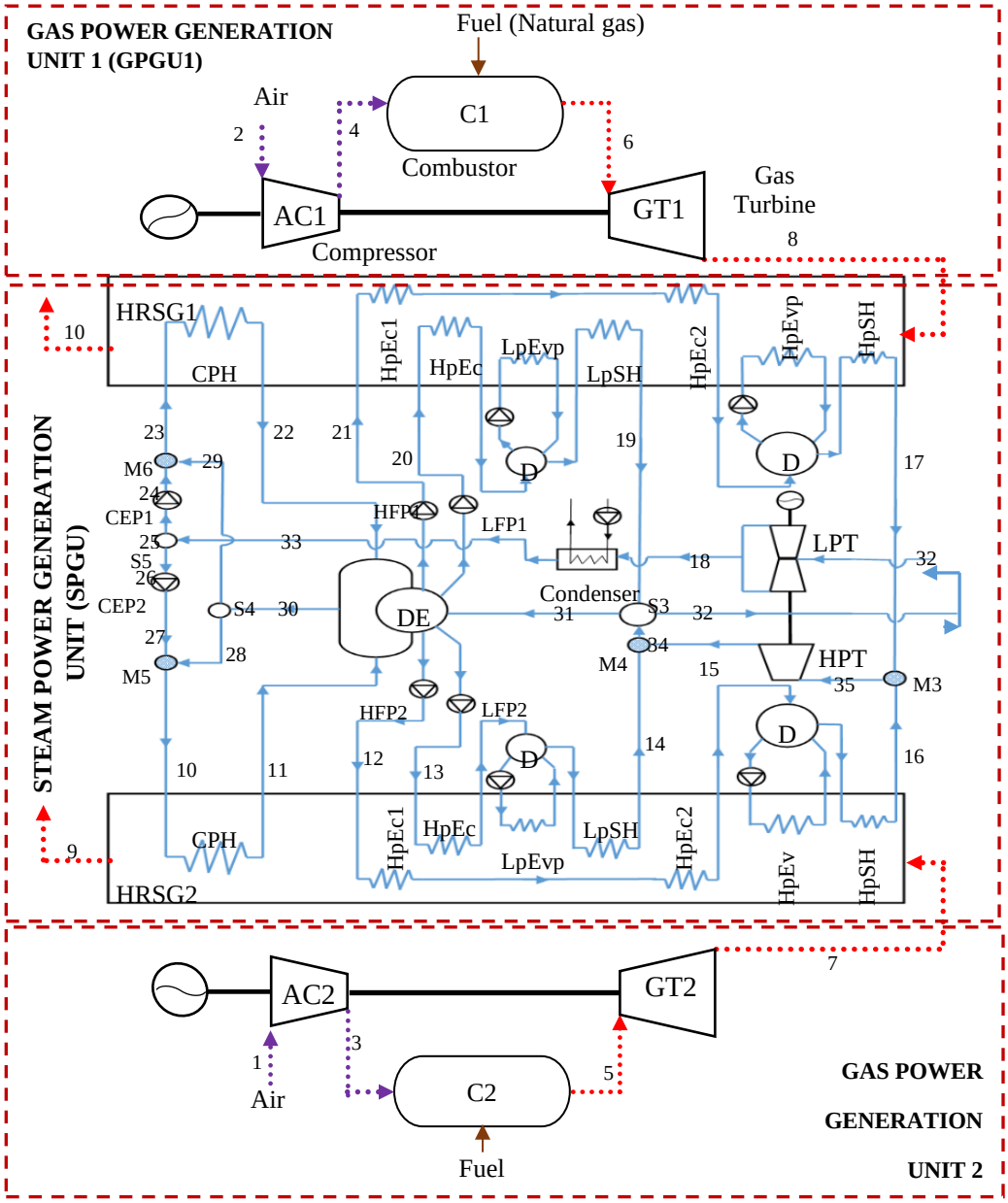

Legend

——→	Fuel	⊗	Mixer
·····→	Air stream	○	Splitter
·····→	Flue gas	⏦	Heat exchanger
——→	H_2O stream	⊳	Pump

Fig. 3.10 Schematic layout of NGFCPP1

Table 3.4. Validation of natural gas fired combined cycle power plant based on main stream parameters

Stream ID	Mass flowrate (kg/sec)		Relative error (%)	Temperature (K)		Relative error (%)	Pressure (bar)		Relative error (%)
	Source model	Aspen model		Source model	Aspen model		Source model	Aspen model	
1	360	360	0.00	302	302	0.00	1.013	1.013	0
2	360	360	0.00	302	302	0.00	1.013	1.013	0
4	360	360	0.00	637	635.81	0.19	10.2	10.2	0
3	360	360	0.00	637	635.81	0.19	10.2	10.2	0
6	366	366	0.00	1345	1231.72	8.42	9.6	9.6	0
5	366	366	0.00	1345	1231.72	8.42	9.6	9.6	0
8	366	366	0.00	824	823.71	0.04	1.1	1.1	0
7	366	366	0.00	824	823.71	0.04	1.1	1.1	0
24	51.73	51.74	-0.01	321.10	321.10	0.00	3.64	3.64	0
27	51.73	51.74	-0.01	321.10	321.10	0.00	3.64	3.64	0
23	79.57	79.58	-0.01	345.24	345.24	0.00	3.64	3.64	0
22	79.57	79.58	-0.01	409.42	409.42	0.00	3.64	3.64	0
11	79.57	79.58	-0.01	409.42	409.42	0.00	3.64	3.64	0
21	43.97	43.98	-0.01	410.4	410.40	0.00	72.6	72.6	0
12	43.97	43.98	-0.01	410.4	410.40	0.00	72.6	72.6	0
16	87.95	87.95	0.00	791.23	791.23	0.00	55.25	55.25	0
15	87.95	87.95	0.00	479.68	479.86	-0.04	5.6	5.6	0
20	10.34	10.34	0.00	409.7	409.7	0.00	21.3	21.3	0
13	10.34	10.34	0.00	409.7	409.7	0.00	21.3	21.3	0
19	10.34	10.34	0.00	474.32	473.80	0.11	5.6	5.6	0
32	103.47	103.47	0.00	474.32	474.32	0.00	5.6	5.6	0
18	103.47	103.47	0.00	323	323.16	-0.05	0.123	0.123	0
33	103.47	103.47	0.00	321	321	0.00	0.112	0.112	0
10	366	366	0.00	383	383	0.00	1.013	1.013	0
9	366	366	0.00	383	383	0.00	1.013	1.013	0

3.1.3.2 Conventional calcium looping integrated natural gas fired combined cycle power plant (NGFCPP2)

In this section, a detailed description of the proposed NGFCPP2 is presented. A schematic view of the proposed configuration is shown in Fig. 3.11. In this configuration, a CCaLU was integrated with natural gas fired combined cycle power plant configuration for CO_2 capture by replacing GPGU1. This CCaLU mainly consists of a calciner, carbonator and an ASS unit. The

configuration helps to capture the emitted CO_2 from the natural gas fired combined cycle power plant. Lime was used as an adsorbent to capture CO_2. The CCaLU separates the CO_2 from the flue gases via carbonation and calcination reactions. Natural gas was combusted in both the reactors to supply the required heat to operate them at isothermal conditions. An ASS provides oxygen to the calciner, which is essential to get pure CO_2 from the calciner by means of natural gas combustion and $CaCO_3$ decomposition.

On the other hand, natural gas entering the carbonator utilizes the oxygen present in the input flue gas, coming from HRSG2. This adjustment in the configuration ultimately reduces the net electrical energy requirement for ASS. The hot concentrated CO_2 gas leaving the calciner contains a significant amount of heat energy, which was recovered using multiple heat exchangers as shown in Fig. 3.11. Cyclone separators were used to separate sorbent from CO_2 stream and lean flue gases. At the end, the captured CO_2 gas was sent for compression to enable sequestration. A certain amount of calcium sorbent gets deactivated during the cyclic operation, and it was removed in the form of purge from the calciner. This sorbent loss was compensated using fresh material in the form of makeup stream.

3.1.3.3 Double calcium looping integrated natural gas fired combined cycle fired power plant (NGFCPP3)

In this section, a detailed description of the proposed novel NGFCPP3 configuration is presented. A schematic view of the proposed configuration is shown in Fig. 3.12. In this configuration, a double calcium looping unit (DCaLU) for CO_2 capture was integrated by replacing GPGU1. Contrary to the scheme of NGFCPP1 where the high grade energy was directly transferred from GPGU1 to SPGU for steam generation, an indirect mode of heat transfer process is adopted in the NGFCPP3 configuration to meet the energy requirements of calciner. Part of the stream leaving from the high-pressure turbine was routed to carbonator to extract the released energy during the carbonation process. The heat integration network was also enforced between the exit and intermediate streams to extract the low-grade energy from exit streams. The energy from the hot lean flue gases leaving the carbonator was recovered via HRSG1 for steam generation and the hot concentrated CO_2 gases was allowed to pass through air preheater (AP) that utilizes its thermal energy to heat the air entering the combustor. Thus, the DCaLU enables the utilization of

the high and low-grade energy produced during the CO_2 capture for power generation without much modification in the overall plant configuration.

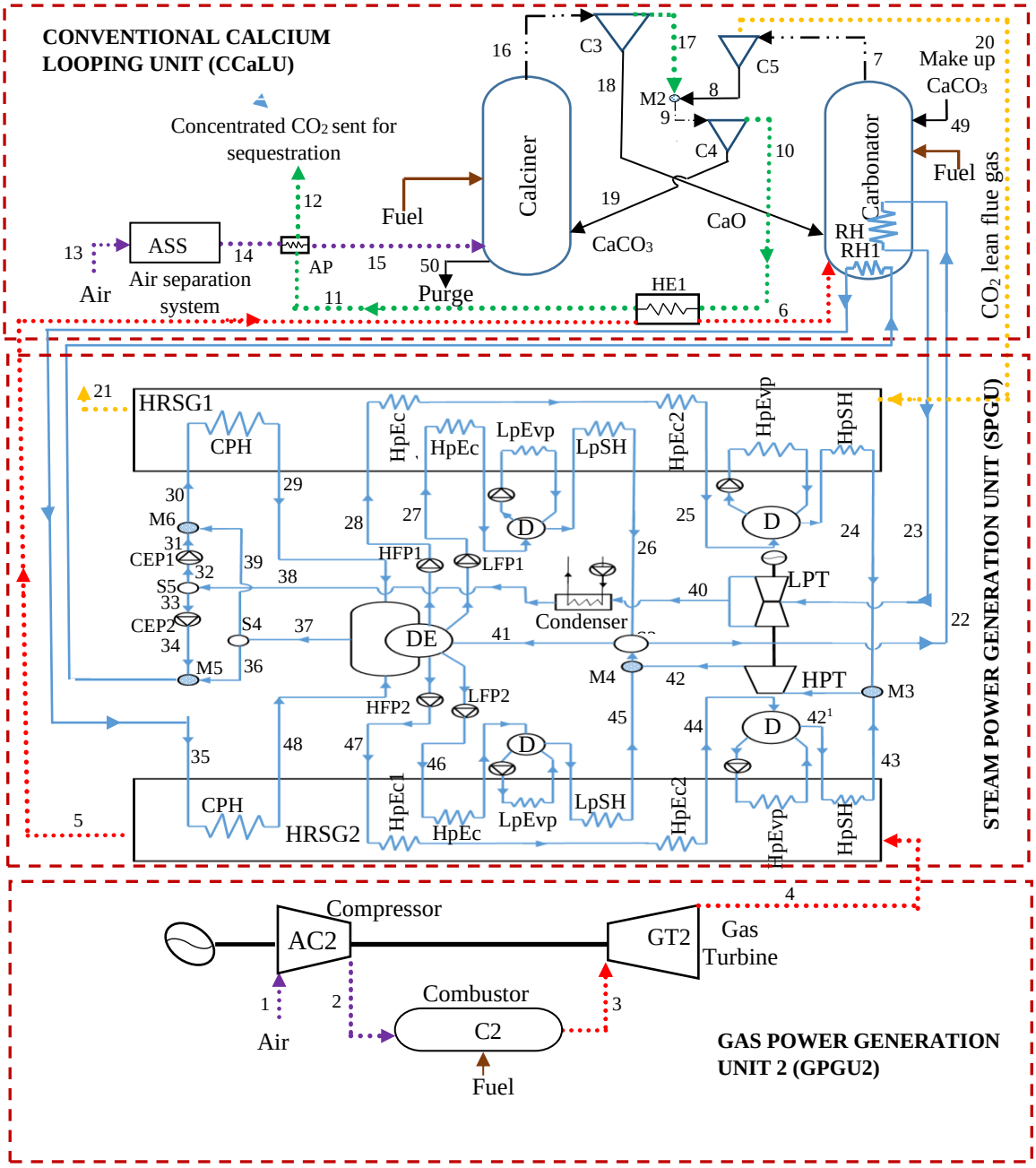

Legend

——→	Fuel	○	Splitter	——→	Sorbent
·····→	Air	⊸	Heat exchanger	–··–··–→	Sorbent + Gas
·····→	Flue gas	◑	Pump	·····→	Lean CO_2 gas
——→	H_2O stream	⊗	Mixer	·····→	CO_2 gas stream

Fig. 3.11 Schematic layout of NGFCPP2

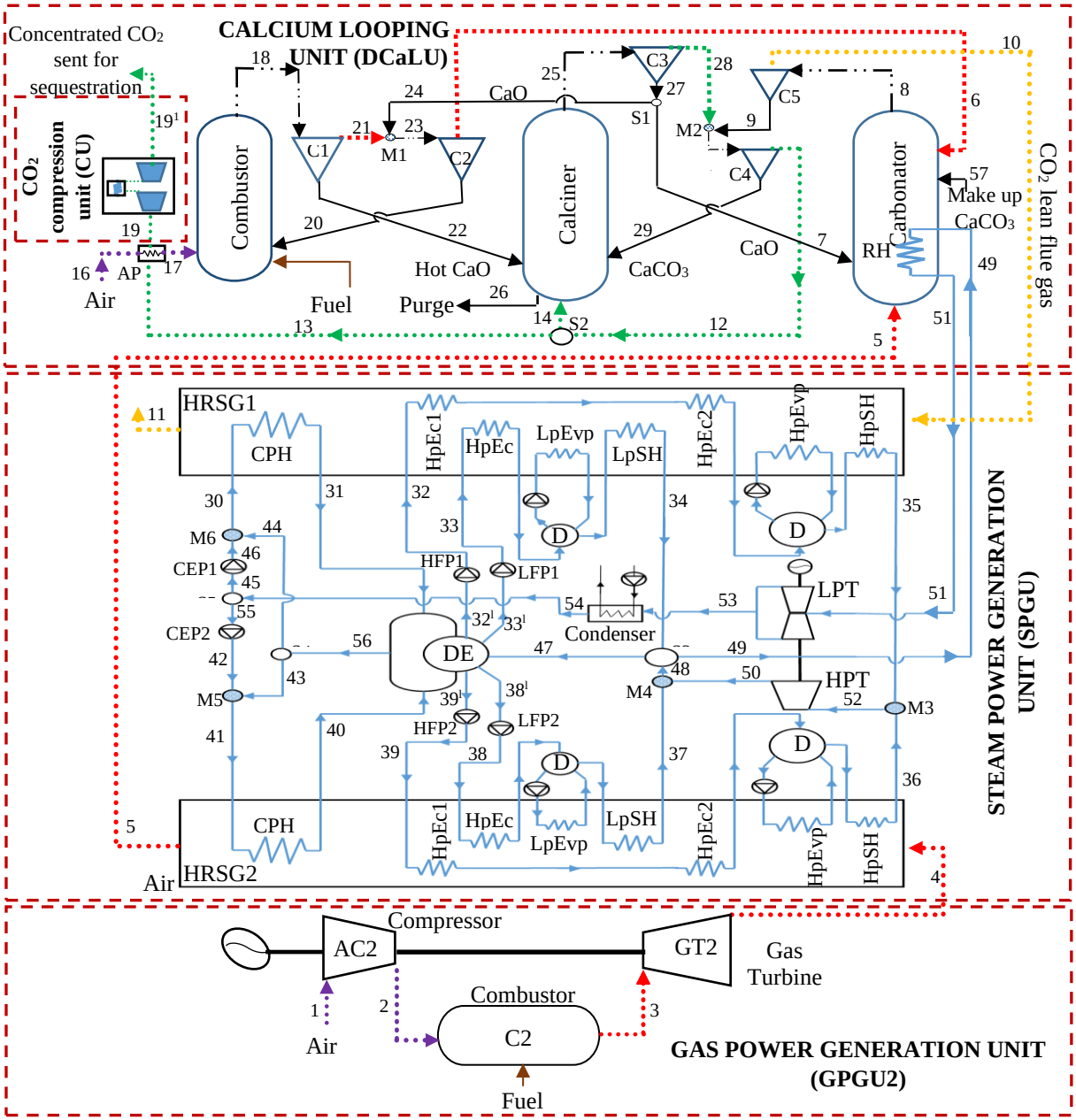

Legend

→	Fuel	○	Splitter	→	Sorbent
⋯→	Air	⊸	Heat exchanger	–·–·→	Sorbent + Gas
⋯→	Flue gas	⊳	Pump	⋯→	Lean CO_2 gas
→	H_2O stream	⊗	Mixer	⋯→	CO_2 gas stream

Fig. 3.12 Schematic layout of NGFCPP3

Likewise, the mechanism to transfer heat for the carbonation and calcination reactions to separate CO_2 from flue gas in DCaLU is different from that of CCaLU where the fuel is directly combusted in the calciner for calcination. In the DCaLU, a secondary calcium sorbent loop was introduced between the calciner and the newly added combustor. The sorbent running in this loop acts as an energy carrier and provides heat energy for the calcination (endothermic) reaction occurring at 900 ^{0}C. The high concentrated CO_2 gas and CaO sorbent from the calciner was separated using a cyclone separator. The separated CaO sorbent stream was divided into two streams. One stream was sent back to the combustor as an energy carrier, and the other stream was used in the carbonator for CO_2 capture from flue gas.

Thus, unlike the CCaLU this configuration does not require ASS and reduces the electrical power consumption significantly as compared to the NGFCPP2 configuration. In NGFCPP3, the carbonator operates at 600 ^{0}C, and this isothermal condition was maintained by adjusting the steam flowrate. Although the calcination reaction enables the self-fluidization behaviour inside the reactor by releasing CO_2 gas, a portion of CO_2 gas leaving the DCaLU was recycled back to support the fluidization activity. The captured CO_2 was compressed to sequestration ready pressure using a CU.

3.1.4 Category 4: Calcium looping for CO_2 capture, H_2 and electricity coproduction in coal fired power plants

In this section, a detailed description of the conventional and double calcium looping integrated Indian coal fired power plants for CO_2 capture, electricity and H_2 coproduction (HCFPP1 and HCFPP2) is presented. The CFPP2 and CFPP3 configurations, presented in Section 3.1.2, were further extended for H_2 production by integrating the calcium looping gasification based H_2 production scheme. Fig. 3.13 and Fig. 3.14 shows the detailed layouts of the HCFPP1 and HCFPP2. A sensitivity analysis has been carried out to identify the optimal operating conditions for gasifier and riser process units. The maximum H_2 production was observed at the gasifier and riser operating temperatures of 570 ^{0}C and 326 ^{0}C. As the coal, steam and calcium sorbent (mainly CaO) were fed into the gasifier, the gasification shown in Equation 3.1, water gas shift reaction shown in Equation 3.2 and CO_2 adsorption shown in Equation 3.3 takes place simultaneously.

$$C + H_2O \rightarrow CO + H_2 \qquad \Delta H_{25^0{}_C} = +131.3\,\frac{kJ}{mol} \tag{3.1}$$

$$CO + H_2O \leftrightarrow CO_2 + H_2 \qquad \Delta H_{25^0{}_C} = -50.1\,\frac{kJ}{mol} \tag{3.2}$$

$$CaO + CO_2 \rightarrow CaCO_3 \qquad \Delta H_{25^0{}_C} = -178.9\,\frac{kJ}{mol} \tag{3.3}$$

The gasification process between the coal and steam is endothermic. But the carbonation reaction between the CO_2 (generated during gasification process) and calcium sorbent is exothermic. Thus, it compensates the heat needed for gasification. A substantial amount of the CO_2 generated during this process was captured by the CaO sorbent while the remaining CO_2 gas along with other products (mainly H_2 and H_2O) was sent to the riser reactor for complete capture of CO_2. The leaving stream from the gasifier contains sorbent is separated by using cyclone separator (C5). The sorbent was then sent to the CCaLU in case of HCFPP1 configuration and DCaLU in case of HCFPP2 configuration for regeneration. The gaseous mixture mainly consists of H_2 and H_2O was further processed by using a series of heat exchangers, compressors and flash columns where most of the H_2O in vapour form was condensed into liquid and separated. At the end, the concentrated H_2 gas (with around 93% pure) was sent for storage.

A considerable amount of heat was released due to the exothermic carbonation reaction in the riser and during the compression and cooling of H_2 and H_2O mixture. A part of this heat energy was utilized to generate the necessary amount of steam required in the gasifier, while the remaining high-grade heat energy was used to generate low pressure steam which was used in SPGU for electrical power generation. The integrated scheme of HCFPP1 captures CO_2 and produces highly concentrated H_2. This technique of calcium looping gasification used in HCFPP1 improves the overall performance of the plant by enhancing the water gas shift reaction involved in the H_2 production process (Perejón et al., 2016). The HCFPP2 scheme further improves the CO_2 capture, H_2 and electricity cogeneration process by eliminating the need of ASS and simplifying the energy integration process for steam generation when compared with HCFPP1 configuration.

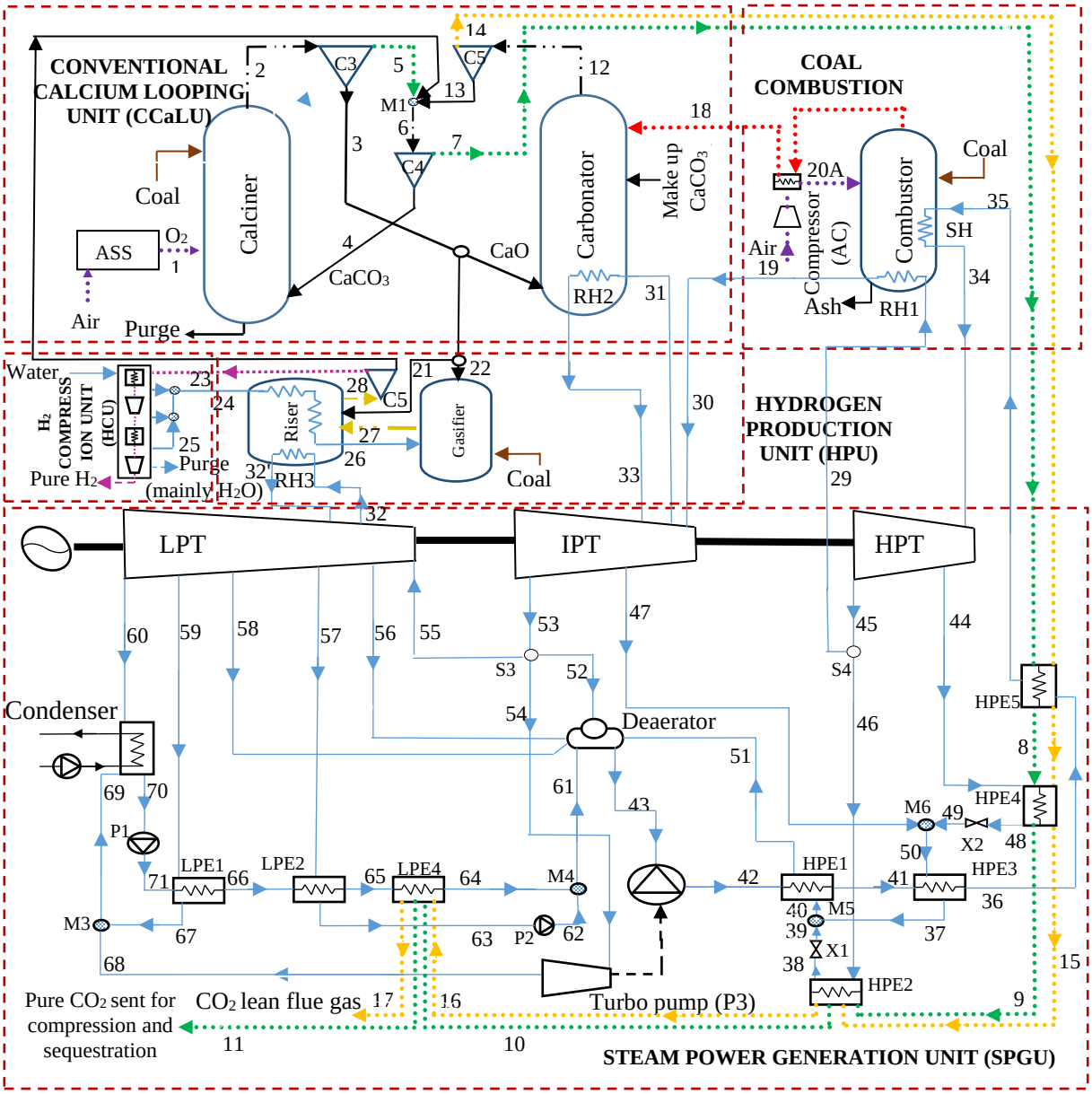

Legend

——→	Fuel	○	Splitter	——→	Sorbent / Ash
·····→	Air/O_2	-W-	Heat exchanger	—·—·—→	Sorbent + Gas
·····→	Flue gas	⊖	Pump	·····→	Lean CO_2 gas
——→	H_2O	⊗	Mixer	·····→	Pure CO_2 gas
·····→	H_2 and H_2O	▽	Solid gas separator	—·—·—→	Solid gas mixture of CO_2, $CaCO_3$, H_2, H_2O etc.

Fig. 3.13 Schematic layout of HCFPP1

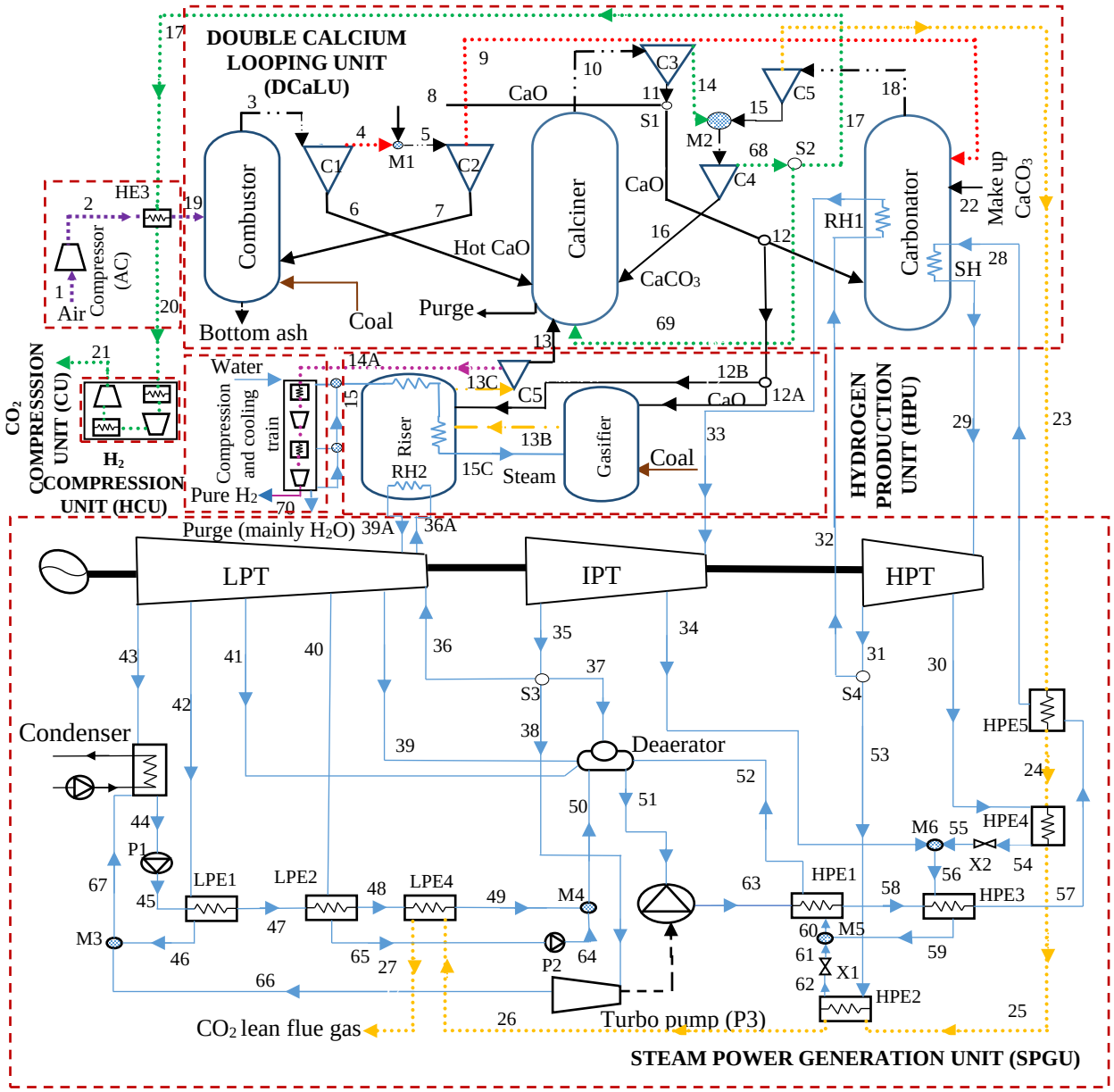

Legend

——→	Fuel	○	Splitter	——→	Sorbent / Ash
·····→	Air/O_2	⁓⁓	Heat exchanger	–·–·–→	Sorbent + Gas
·····→	Flue gas	⊖	Pump	·····→	Lean CO_2 gas
——→	H_2O	⊗	Mixer	·····→	Pure CO_2 gas
·····→	H_2 and H_2O	▽	Solid gas separator	–·–·–→	Solid gas mixture of CO_2, $CaCO_3$, H_2, H_2O etc.

Fig. 3.14 Schematic layout of HCFPP2

3.1.5 Category 5: CO_2 utilization in double calcium looping integrated natural gas fired combined cycle power plants

The synthesis and operational characteristics of the developed CO_2 capture and utilization strategies integrated with reference NGFCPP3 are discussed in detail in this section. The integration of different cogeneration modules to the NGFCPP3 is systematically elaborated. In order to effectively utilize the captured CO_2 from the proposed NGFCPP3 configuration in section 3.1.3.3 it was integrated with DME production and vapor absorption refrigeration (VAR) process models and the resulting configuration is referred as DNGFCPP1. The performance of DNGFCPP1 configuration was further enhanced by utilizing renewable energy. The environmental conditions such as ambient temperature and pressure etc. were updated in the proposed configurations in accordance with the climatic conditions of India.

3.1.5.1 Model validation

The DME process flowsheet from Schakel et al., 2016 and VAR process flowsheet from Mishra and Singh., 2018 were considered as reference models and as shown in Fig. 3.15 and Fig. 3.16 respectively. These process configurations were reproduced using aspenONE v10.0 software. The simulated results are compared with the literature data in Table 3.5 and Table 3.6. From the comparison it is observed that the reproduced models were very well converged with the data obtained from the literature with the relative error of less than 2%.

3.1.5.2 Description of the DNGFCPP1 configuration

The schematic operational flowsheet of DNGFCPP1 is shown in Fig. 3.17. The captured CO_2 using NGFCPP3 configuration was utilized to produce DME. The CO_2 captured from the DCaLU was preheated and sent to the Dry Reforming Reactor (DRR) for syngas production. In DRR, the natural gas reacts with the CO_2 and forms syngas as shown in Equations 3.4-3.7. Since this reaction is endothermic in nature, a continuous supply of heat energy was ensured from the combustor. This hot syngas was further cooled and compressed using a compression train and then transferred to the DME Synthesis Reactor (DMESR). The series of exothermic equilibrium reactions presented in Equations 3.8-3.11 occur in DMESR.

$$CH_4 + CO_2 \rightarrow 2CO + 2H_2 \qquad \Delta H_{25^0 c} = +247 \frac{kJ}{mol} \tag{3.4}$$

$$C_2H_6 + 2CO_2 \rightarrow 4CO + 3H_2 \qquad \Delta H_{25^0c} = +430\frac{kJ}{mol} \tag{3.5}$$

$$C_3H_8 + 3CO_2 \rightarrow 6CO + 4H_2 \qquad \Delta H_{25^0c} = +622\frac{kJ}{mol} \tag{3.6}$$

$$C_4H_{10} + 4CO_2 \rightarrow 8CO + 5H_2 \qquad \Delta H_{25^0c} = +817.1\frac{kJ}{mol} \tag{3.7}$$

$$CO + 2H_2 \leftrightarrow CH_3OH \qquad \Delta H_{25^0c} = -90.9\frac{kJ}{mol} \tag{3.8}$$

$$CO_2 + 3H_2 \leftrightarrow CH_3OH + H_2O \qquad \Delta H_{25^0c} = -41.1\frac{kJ}{mol} \tag{3.9}$$

$$CO + H_2O \leftrightarrow CO_2 + H_2 \qquad \Delta H_{25^0c} = -50.1\frac{kJ}{mol} \tag{3.10}$$

$$2CH_3OH \leftrightarrow CH_3OCH_3 + H_2O \qquad \Delta H_{25^0c} = -23.4\frac{kJ}{mol} \tag{3.11}$$

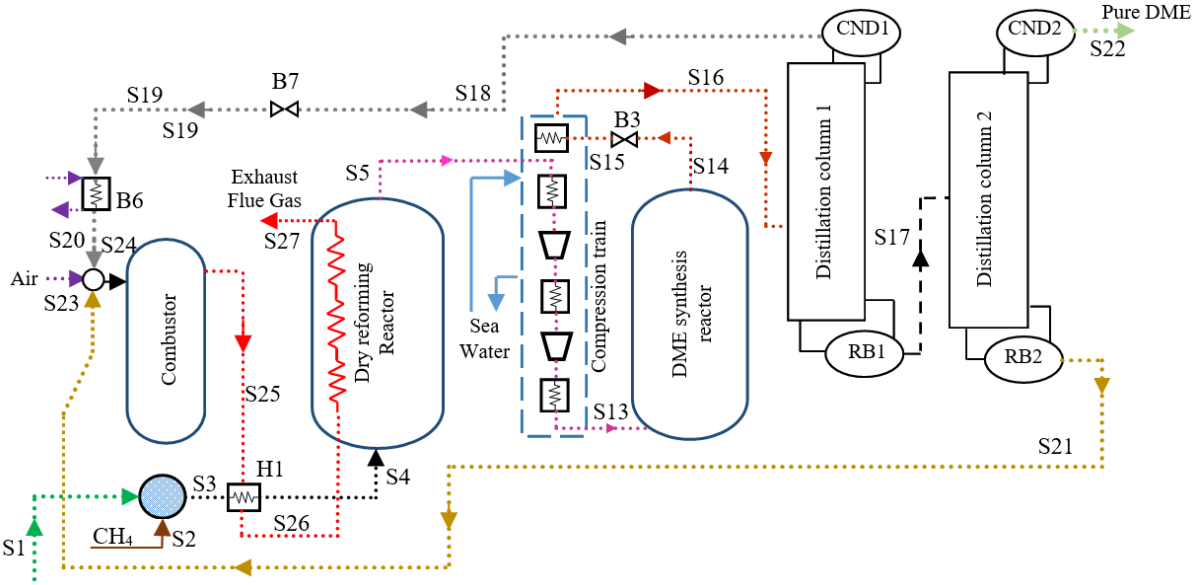

Legend

→	CH_4	⊛	Mixer	⇢	Pure CO_2 gas
⇢	Air stream	○	Splitter	⇢	Syngas + Methanol + CO_2 + H_2O
⇢	DME + Impurities (Syngas, Methanol, CO_2 ,H_2O)	⏦	Heat exchanger	⇢	Syngas
→	H_2O stream	⋈	Expansion valve	⇢	Pure DME
⇢	Flue gas				

Fig. 3.15 Schematic layout of dry reforming based DME production plant (Source: Schakel et al., 2016)

Table 3.5 Validation of dry reforming based DME production plant on main stream parameters

Stream ID	Temperature (^{0}C)		Relative error (%)	Pressure (bar)		Relative error (%)	Mass flowrate (kg/hr)		Relative error (%)
	Source model	Aspen model		Source model	Aspen model		Source model	Aspen model	
S1	41	41	0	2	2	0	41856.93	41856.93	0
S2	400	400	0	20	20	0	15257.2	15257.2	0
S3	237	238.76	0.02	2	2	0	57114	57114	0
S4	800	800	0	2	2	0	57114	57114	0
S5	800	800	0	1	1	0	57114	57114	0
S13	250.7	250.7	0	79	79	0	56505	56505	0
S14	250	250	0	79	79	0	56505	56505	0
S15	229.6	229.6	0	10	10	0	56505	56505	0
S16	31.48	31.48	0	10	10	0	56505	56505	0
S17	44.85	44.85	0	10	10	0	24556	24556	0
S18	-48.3	-48.2	0	10	10	0	31949	31949	0
S19	-60.3	-60.2	0.16	1	1	0	31949	31949	0
S20	0	0	0	1	1	0	31949	31949	0
S21	70.03	70	0.04	10	10	0	722.7	722.7	0
S22	44.31	44.3	0.02	10	10	0	23833.2	23833.2	0
S23	15	15	0	1	1	0	51000	51000	0
S24	2.10	2.11	-0.47	1	1	0	83671	83671	0
S25	1536	1536.3	-0.02	1	1	0	83671	83671	0
S26	1014	1013.5	0.05	1	1	0	83671	83671	0
S27	80	80	0	1	1	0	83671	83671	0

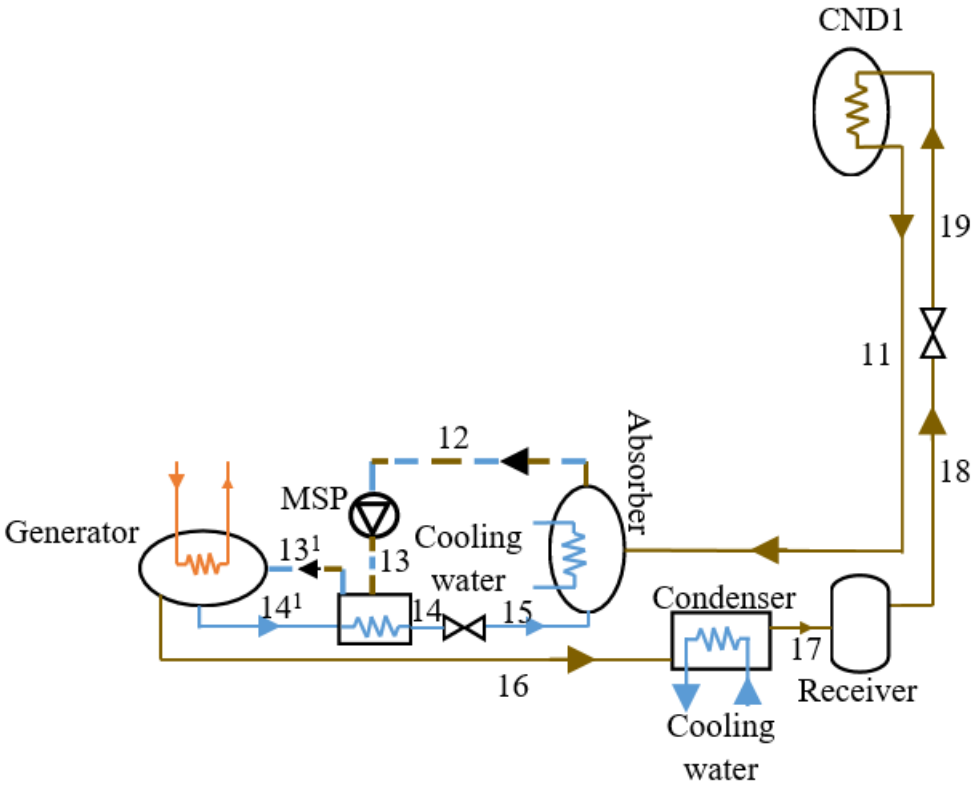

Legend

→	H_2O stream	-WW-	Heat exchanger
→	Ammonia (NH_3)	▷	Pump
⋈	Expansion valve		

Fig. 3.16 Schematic layout of VAR cycle configuration (Source: Mishra and Singh., 2018)

The products from the DMESR were sent to the DME Separation Unit (DSU). The DSU consists of a distillation column (DIS1) and an ammonia-water based VAR system. The DSU separates the unconverted gases (CH_4, CO_2, H_2) and by-products (CH_3OH, CO, H_2O) from the DME. These separated gases and by-products were redirected to the combustor where they were used as a subsidiary fuel for combustion along with natural gas. The excess heat energy released during the DME synthesis reaction was used to meet the distillation column's reboiler duty and the energy required in the VAR system. The VAR system supplies the NH_3 refrigerant to the DIS1 column condenser which was operating at 235 K (-38 ^{0}C). This VAR system consists of an absorber (A1), multistage pump (MSP1), generator (GEN1), expansion valves (X1 and X2) and a heat exchanger (H1). It utilizes the low-grade heat energy, available from the DMESR for refrigeration. This CO_2 capture and utilization scheme does not convert the entire captured CO_2

into DME. Therefore, the unconverted CO_2 along with CO_2 generated in combustor was released into the atmosphere.

Table 3.6 Validation of VAR cycle configuration based on main stream parameters

Stream ID	Fluid	Mass flow rate (kg/sec)		Relative error (%)	Temperature (K)		Relative error (%)	Pressure (bar)		Relative error (%)
		Source model	Aspen model		Source model	Aspen model		Source model	Aspen model	
11	NH_3	0.246	0.246	0	274.28	274.28	0	1.4	1.4	0
12	NH_3-H_2O	2	2	0	303.12	303.12	0	1.4	1.4	0
13	NH_3-H_2O	2	2	0	303.19	303.19	0	10.8	10.8	0
13^l	NH_3-H_2O	2	2	0	358.1	368.98	-3.04	10.8	10.8	0
14	NH_3-H_2O	1.754	1.754	0	321.9	318.38	1.09	10.8	10.8	0
14^l	NH_3-H_2O	1.754	1.754	0	389.8	389.9	-0.02	10.8	10.8	0
15	NH_3-H_2O	1.754	1.754	0	321.98	318.57	1.05	1.4	1.4	0
16	NH_3	0.246	0.246	0	389.8	389.8	0	10.8	10.8	0
18	NH_3	0.246	0.246	0	303.12	303.12	0	10.8	10.8	0
19	NH_3	0.246	0.246	0	254.83	249.4	2.13	1.4	1.4	0

3.1.5.3 Description of the solar energy aided DME production unit coupled with double calcium looping integrated natural gas fired combined cycle power plant configuration (DNGFCPP2)

The total utilization of CO_2 cannot be achieved with the developed DNGFCPP1 configuration. As the conversion of CO_2 increases, the amount of thermal energy required by the DRR and distillation column reboiler increases. To meet this thermal energy demand, more natural gas needs to be used as fuel in the DPU which further increases the CO_2 emissions proportionally. Therefore, the proposed configuration of DNGFCPP1 was unable to handle complete utilization of CO_2. Integration of renewable energy with DNGFCPP1 configuration is one of the potential

options that can be explored for complete utilization of captured CO_2. In this section a novel renewable energy supported configuration was investigated for complete utilization of CO_2. The schematic view of the proposed configuration is shown in Fig. 3.18 and referred as DNGFCPP2. The combustor of DPU used in DNGFCPP1 configuration (shown in Fig. 3.17) was replaced with the CSP system. This enables the configuration to supply heat energy to the DRR via heat transfer fluids (e.g., molten salts) for syngas production without combusting any additional fuel. It also eliminates the release of CO_2 gas into the atmosphere contrary to the case of DNGFCPP1 configuration where partial CO_2 emission from DPU was unavoidable.

The conceptual design of the CSP is taken in accordance with Zhai et al., 2016. In this system, solar energy received in the form of sunlight on a large area is reflected and concentrated on a central receiver (heat exchanger) by using mirrors (heliostats). The energy integration strategy applied for dry reforming based DPU in the DNGFCPP1 configuration mainly focused on effective utilization of energy from combustor. However, less attention was given to utilization of high and low grade heat energy from other unit operations. For instance, in the compression train, during the intermediate cooling stage, a significant amount of energy was released and it was not effectively utilized.

The proposed DNGFCPP2 configuration explored the energy efficient integration strategy for CO_2 utilization scheme (DPU and DSU) along with the possible options for enhancing the CO_2 utilization capacity. The heat energy released during the intermediate cooling in the compression train was used for the generation of superheated steam. The steam turbines represented as T1 and T2 were used for the generation of electricity respectively. The proposed CO_2 utilization scheme without combustor eliminates the additional fuel combustion and ensures complete utilization of CO_2. Therefore, the CO_2 captured and sent by the DCaLU was completely utilized to produce DME in the proposed DNGFCPP2 configuration. A set of two distillation columns (DIS1 & DIS2) were required in this DSU to recycle unreacted gases and by products to the DPU. This resulted in an increase in total condenser load and energy required for vapor absorption cycle.

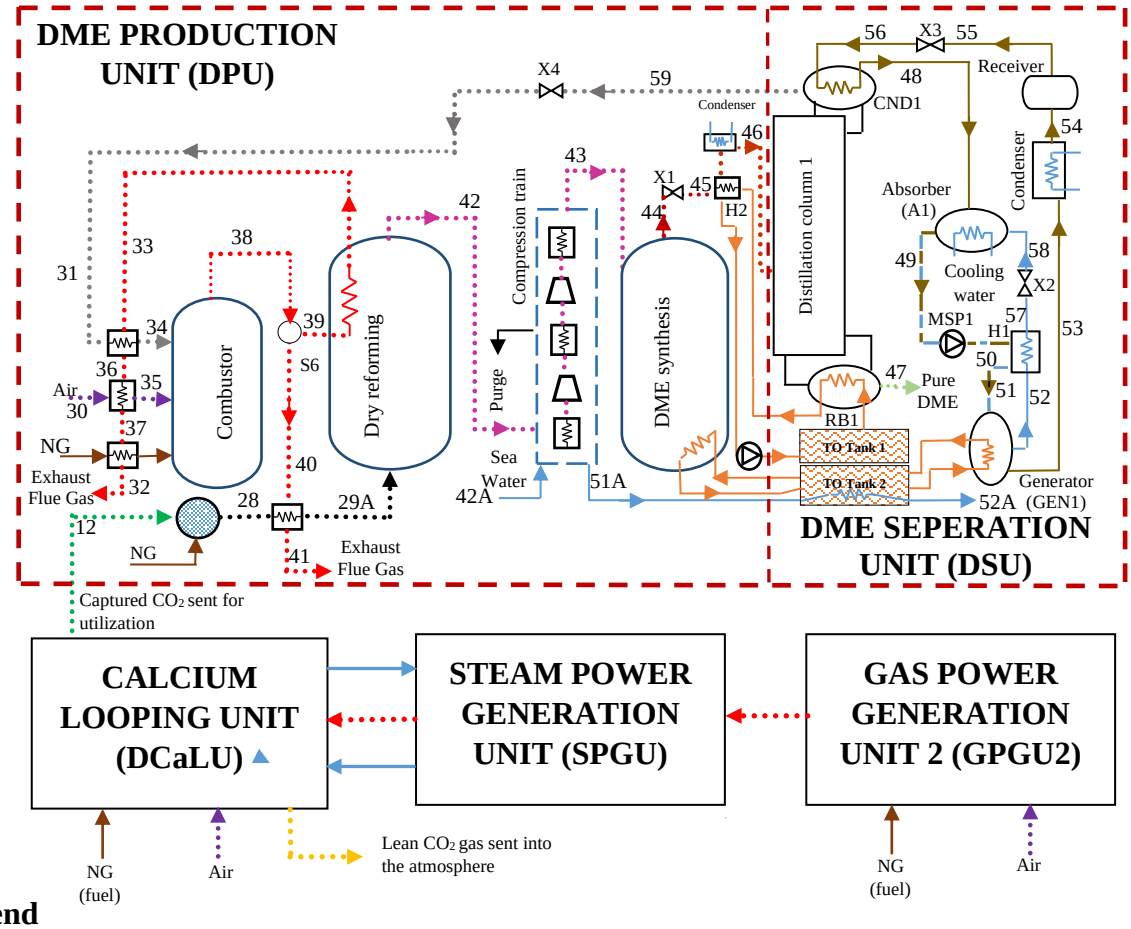

Legend

→	Fuel	⊗	Mixer	⇢	Lean CO_2 gas
⇢	Air stream	○	Splitter	⇢	Pure CO_2 gas
⇢	DME + Impurities (Syngas, Methanol, CO_2 ,H_2O)	⏦	Heat exchanger	⇢	Syngas + Methanol + CO_2 + H_2O
→	H_2O stream	⊳	Pump	⇢	Syngas
⇢	Flue gas	⋈	Expansion valve	⇢	Pure DME
→	Ammonia (NH_3)				

Fig. 3.17 Schematic layout of DNGFCPP1

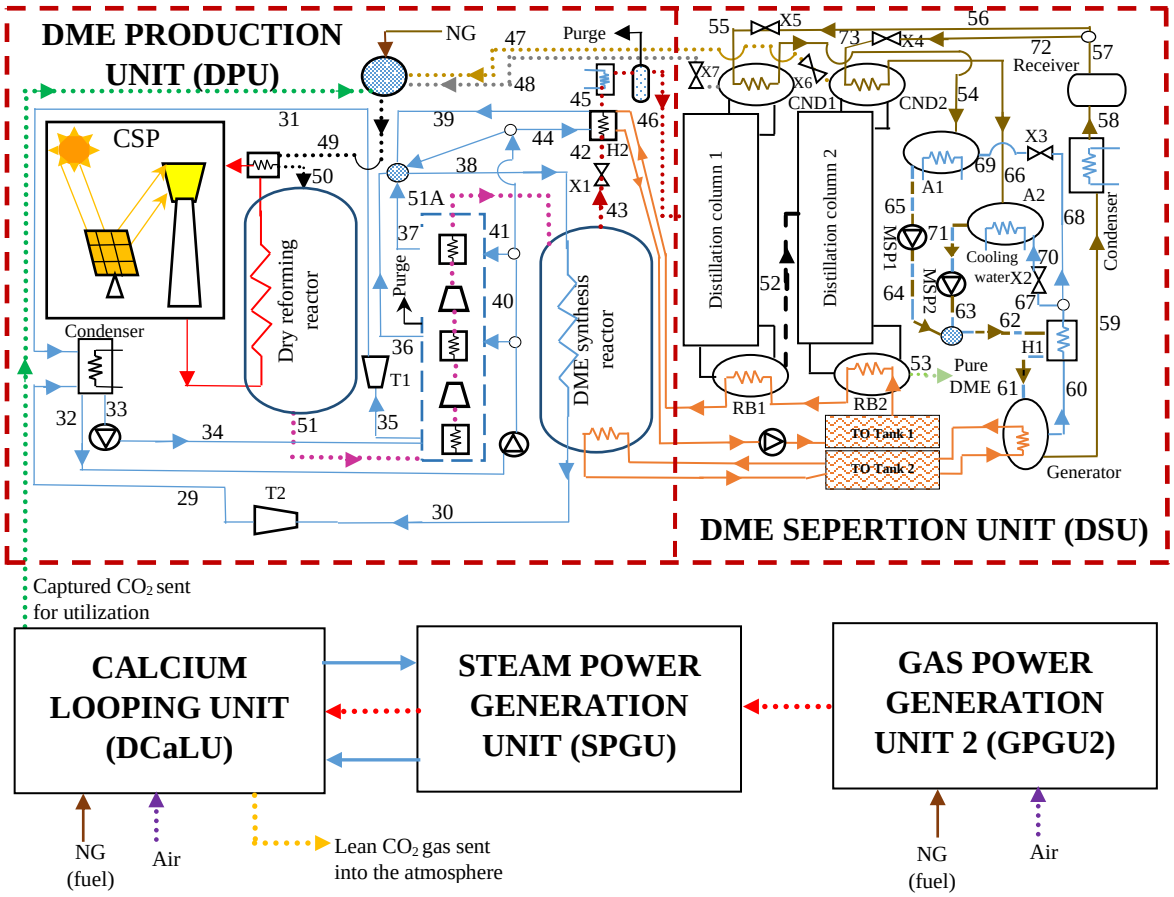

Legend

→	Fuel	⊛	Mixer	⋯→	Lean CO_2 gas
⋯→	Air stream	○	Splitter	⋯→	Pure CO_2 gas
⋯→	DME + Impurities (Syngas, Methanol, CO_2 ,H_2O)	-WW-	Heat exchanger	⋯→	Syngas + CO_2
→	H_2O stream	▷	Pump	⋯→	Syngas
⋯→	Flue gas	⋈	Expansion valve	⋯→	Pure DME
→	Ammonia (NH_3)	⋯→	H_2O + Methanol	- - - →	DME + Methanol + H_2O

Fig. 3.18 Schematic layout of DNGFCPP2

3.2 Analysis and modelling

The performance of different power plant configurations proposed in the systems description section was investigated based on energy, exergy, cost and environmental analysis. The composition of fuels used in the respective power plants are shown in Table 3.7-3.9. Using the validated process models, the configurations were synthesized by exploring different processes

and heat integration possibilities. A detailed analysis was carried out to identify the best possible configuration in terms of energy, exergy, environmental, cost and exergoeconomic parameters. Further, a parametric analysis was also presented for CCS based configurations to assess the system's performance. These simulation studies were carried out using the aspenONE software. In this work, MIXCINC is selected as the stream class to define the conventional and non-conventional forms of various solid and fluid components. Peng Robinson and Boston Mathias (PR-BM) was used for the estimation of properties of various components involved in the calcium looping, ORC, DME generation, gas based power generation and VAR processes and International Association for the Properties of Water and Steam 95 (IAPWS-95) and STEAMNBS were used for the steam and water used in steam based power generation processes (Hanak et al., 2014; Hagi et al., 2013).

The initial design conditions and main operating parameters of all process models based on Indian climatic conditions shown in Table 3.10-3.13. Since the ambient conditions affect the thermal performance of the process units, these operating conditions were based on the worst-case scenario approach (Suresh et al., 2010). The assumptions, methods and specifications used for the development and analysis of the proposed configurations (Wang et al., 2009; Suresh et al., 2010a; Wang et al., 2013; Jenkins and Bhatnagar., 1991; Khushi food products., 2021; Uday limestone., 2021; Zhu et al., 2020; Hanak and Manovic., 2017a; CIL., 2018; Suresh et al., 2010b; Motwani et al., 2013; ET markets., 2020) were listed as:

1. The process was operating under a steady state condition.
2. Pressure drop and thermal loss in the pipes (streams) were neglected.
3. Energy loss in the combustor (mainly convection and radiation losses) is approximated as 1.5% of input fuel energy.
4. Energy loss in the calciner and carbonator (mainly convection and radiation losses) is approximated as 0.5% of input fuel energy.
5. The power plant operates 7008 hours annually for a period (N) of 20 years for biomass fired power plants.
6. The auxiliary power consumption ($\dot{W}_{aux}$) in pumps, plant control systems, heating, ventilation and air conditioning (HVAC), generator, lighting and transformer losses, etc. were assumed to be 5% of gross power output for biomass fired power plants.

7. Cost of raw limestone used as a sorbent was taken as 6.88 €/ton (570 Rs/ton).
8. Cost of sugarcane bagasse used as fuel was taken as 36.23 €/ton (3000 Rs/ton).
9. Cost of thermal oil and working fluid were assumed to be 2% of the total investment of ORC.
10. The auxiliary power consumption (W_{aux}) was assumed to be 9% of the gross power output of the power plant that includes lighting and control systems, transformer losses, heating, ventilation and air conditioning systems etc. for coal and natural gas fired power plants.
11. The expected lifetime of all coal and natural gas fired power plant configurations was assumed to be 25 years with capacity factor (CF) of 80% i.e., 7008 annual operation hours.
12. Cost of the Indian coal input as fuel in terms of specific fuel cost (SFC) was taken as 203.992 Rs/MWh or 2.463 €/MWh.
13. The project interest rate (i) was assumed to be 12%.
14. Cost of the natural gas used as a fuel in terms of specific fuel cost (SFC) was taken as 464.39 Rs/MWh or 5.6086 €/MWh.

Table 3.7 Composition of biomass (Xie et al., 2018)

Ultimate analysis (wt%: as fired)	
Carbon	44.48
Hydrogen	6.057
Oxygen	40.69
Sulfur	0.047
Nitrogen	0.19
Moisture	6.44
Ash	2.09
LHV_b (MJ/kg)	14.91
HHV_b (MJ/kg)	16.45
$SCEx_b$ (MJ/kg)	16.96

Table 3.8 Composition of Indian coal (Suresh et al., 2010a)

Ultimate analysis (wt%: as fired)	
Carbon	39.16
Ash	48.87
Oxygen	7.92
Hydrogen	2.76
Sulfur	0.51
Nitrogen	0.78
HHV_c (MJ/kg)	15.83
$SCEx_c$ (MJ/kg)	17.3

Table 3.9 Composition of natural gas (GAIL., 2009)

Components	Composition (% mole)
Methane	90.84
Ethane	5.02
Propane	0.68
Isobutane	0.05
Carbon dioxide	3.3
Nitrogen	0.11
LHV_{ng} (MJ/kg)	45.61
$SCEx_{ng}$ (MJ/kg)	48.35

Table 3.10 Commonly adopted design conditions and system parameters used in all the configurations (Suresh et al., 2010a; Duan et al., 2016)

Conventional solid, liquid and gaseous components	Defined with molecular structure
Simulation strategy	Sequential modular approach
Property estimation method used	PR-BM, STEAM-NBS, IAPWS-95

Unit models	
Combustor, calciner and carbonator	RYield, RGibbs
Mixers/splitters	Mixer/Fsplit
Separators	Sep/SSplit
Pressure changers	Pump/Compr/MCompr
Heat exchangers	Heater/HeatX/MHeatX
Ambient conditions, air composition and CU specifications	
Ambient temperature	33 ^{0}C
Chemical composition of air (mole percent)	75.62% N_2, 20.3% O_2, 3.12% H_2O, 0.03% SO_2, 0.92% others.
Ambient pressure	1.013 bar
CU	Stage number 4, outlet condition 40.5 ^{0}C, 110 bar

Table 3.11 Operating conditions and specifications used in all biomass fired power plant based configurations (Ozdil et al., 2015; Forristall., 2003; Therminol., 2022)

Excess air	20%
Properties of Therminol VP-1 used in the process	Recommended temperature range: 12 – 400 ^{0}C. Heat of vaporization at maximum use temperature: 206 kJ/kg
Chemical Composition of working fluid (R-245fa)	$C_3H_3F_5$
Biomass feed rate in combustor of BFPP1 and BFPP3	0.139 kg/s (500 kg/h)
Biomass feed rate in combustor of BFPP2	0.093 kg/s (338 kg/h)
Biomass feed rate in combustor of BFPP2	0.045 kg/s (162 kg/h)
Operating conditions of calciner	904 ^{0}C, 1.013 bar

Operating conditions of carbonator in BFPP2	666 ^{0}C, 1.013 bar
Operating conditions of carbonator in BFPP3	650 ^{0}C, 1.013 bar
Flowrate of $CaCO_3$ in BFPP2	0.30 kg/s
Flowrate of $CaCO_3$ in BFPP3	0.47 kg/s
ASS's energy consumption	0.22 kWh/kg O_2
Isentropic efficiency of turbine	90%
Operating pressure of turbine	2.4 bar
Operating conditions of combustor in BFPP3	1610 ^{0}C, 1.013 bar
Flowrate of working fluid in BFPP3	10.43 kg/s
Refrigerant cycle load	100%
Centrifugal pump	11.4 bar

Table 3.12 Operating conditions and specifications used in all Indian coal fired power plant based configurations (Suresh et al., 2010a; Espatolero et al., 2010; Diego et al., 2016)

Excess air	20%
Main steam conditions	573.38 ^{0}C, 300 bar
Reheat steam conditions	617.26 ^{0}C, 57.2 bar
Bottom to fly ash ratio	20:80
Operating conditions of combustor in CFPP1	1878 ^{0}C, 1.013 bar
Operating conditions of combustor in CFPP2	1855 ^{0}C, 1.013 bar
Operating conditions of combustor in CFPP3	1832 ^{0}C, 1.013 bar
Coal feed rate in the combustor of CFPP1 and CFPP3	90.48 kg/sec
Coal feed rate in the combustor of CFPP2	62.23 kg/sec
Coal feed rate in the calciner of CFPP2	28.25 kg/sec
Flowrate of $CaCO_3$ in CFPP2	178.44 kg/s
Flowrate of $CaCO_3$ in CFPP3	270.82 kg/s

Carbonator temperature in CFPP2	665 ^{0}C
Carbonator temperature in CFPP3	650 ^{0}C
Calciner temperature	904 ^{0}C
Condenser pressure	0.103 bar
Isentropic efficiency of HPT, IPT and LPT	89%
Carbonator temperature in HCFPP1	669 ^{0}C
Carbonator temperature in HCFPP2	652 ^{0}C
Gasifier temperature	570 ^{0}C
Riser temperature	326 ^{0}C

Table 3.13. Operating conditions and specifications used in natural gas fired combined cycle power plant based configurations (Reddy et al., 2012; Berstad et al., 2014; Schakel et al., 2016; Zhai et al., 2016)

Excess air for GPGU	300%
Carbonator temperature	600 ^{0}C
Calciner temperature	900 ^{0}C
Condenser pressure	0.103 bar
Isentropic efficiency of gas turbine	81%
Isentropic efficiency of HPT and LPT	96%
Combustion temperature in GPGU	1102 ^{0}C
Mass flowrate of air supplied to the GPGU	290 kg/s
Mass flowrate of $CaCO_3$ in NGFCPP2	41.97 kg/s
Flowrate of $CaCO_3$ in NGFCPP3	66.27 kg/s
Operating parameters and specifications used in the CO_2 utilization schemes	
Lower calorific value of DME	29 MJ/kg
Specific exergy of DME	32.29 MJ/kg
Direct normal irradiance (solar radiation)	700 W/m^2
Heliostat's reflectivity, clean factor, field efficiency, interception factor	93%, 95%, 76%, 99% and 87%

and absorber efficiency	
Flowrate of natural gas supplied to the DPU in DNGFCPP1	16.5 kg/s
Flowrate of natural gas supplied to the DPU in DNGFCPP2	34.3 kg/s
DME produced from DNGFCPP1	18 kg/s
DME produced from DNGFCPP2	58 kg/s
DRR	800 ^{0}C, 1.013 bar
DMESR	250 ^{0}C, 79 bar

3.2.1 Thermodynamic, environmental and cost assessment

Different model equations have been formulated by considering conservation of mass and energy, exergy, cost and ecological aspects. The thermodynamic, environmental and cost analysis of calcium looping combustion processes has been carried by considering key performance indicators such as energy efficiency, exergy efficiency, CO_2 capture efficiency, levelized cost of electricity (LCOE) and Levelized product cost of H_2 and DME (LPCH & LPCD) etc.

3.2.1.1 Energy analysis

For steady flow processes, the mass and energy balances are shown in Equation 3.12 and 3.13 (Kanoğlu et al., 2012):

$$(\sum \dot{m}_n)_{in} = (\sum \dot{m}_n)_{out} \tag{3.12}$$

$$\left(\sum \dot{E}_n\right)_{in} = \left(\sum \dot{E}_n\right)_{out} \tag{3.13}$$

The plant net power ($\dot{W}_{net}$) was calculated by using Equation 3.14, where, $\dot{W}_{gross}$ is the gross power output of turbine, $\dot{W}_{comp}$ is the energy consumption by air compressor, $\dot{W}_{pump}$ is the energy consumption by centrifugal pump, $\dot{W}_{ASS}$ is the energy consumption by ASS and $\dot{W}_{aux}$ is the sum of all auxiliary power consumptions.

$$\dot{W}_{net} = \dot{W}_{gross} - \dot{W}_{comp} - \dot{W}_{pump} - \dot{W}_{ASS} - \dot{W}_{aux} \tag{3.14}$$

The net energy efficiency (η_{bp}) of biomass fired power plants were determined by using Equation 3.15. The chemical energy of biomass ($\dot{E}_b$) was calculated by using Equation 3.16 and the Higher Heating Value of biomass (HHV_b) in kJ/kg was calculated empirically by using Equation 3.17 which was based on Dulong's and Petit law (Sahoo et al., 2016). In the HHV_b calculation the carbon, H_2, oxygen and sulphur components weight percent are represented as C, H_2, O_2 and S, whereas m_b denotes the mass flow rate (kg/sec) of biomass in biomass fired power plants.

$$\eta_{bp} = \frac{(\dot{W}_{net.bp})}{(\dot{E}_b)} \tag{3.15}$$

$$\dot{E}_b = \dot{m}_b \times HHV_b \tag{3.16}$$

$$HHV_b = 338.3 \times C + 1443 \times \left(H_2 - \frac{O_2}{8}\right) - 94.2 \times S \tag{3.17}$$

The net energy efficiency of the Indian coal fired power plant (η_{cp}) configurations was estimated using Equation 3.18 which represents the ratio between net work output ($\dot{W}_{net.cp}$) and total energy input ($\dot{m}_c \times HHV_c$). The $\dot{W}_{net}$ was determined in terms of MW by using Equation 3.14. $\dot{m}_c$ represents the input mass flowrate of Indian coal in kg/sec in CFPP and HHV_c is the higher heating value of Indian coal taken from the data provided in literature (Suresh et al., 2010a).

$$\eta_{cp} = \frac{\dot{W}_{net.cp}}{\dot{m}_c \times HHV_c} \tag{3.18}$$

The net energy efficiency of the natural gas fired combined cycle power plant (η_{ngp}) configurations was determined by using Equation 3.19. The $\dot{W}_{net.ngp}$ is net work output determined in terms of MW by using Equation 3.14. The variable $\dot{m}_{ng}$ represents the input mass flowrate of natural gas in kg/s and LHV_{ng} is the lower heating value of natural gas provided in the literature (GAIL., 2009).

$$\eta_{ngp} = \frac{(\dot{W}_{net.ngp})}{(\dot{m}_{ng} \times LHV_{ng})} \tag{3.19}$$

The net electrical energy output ($\dot{W}_{net.hcp}$) and the net electrical energy efficiency of HCFPP1 and HCFPP2 configurations (η_{hcp}) was determined by using the Equation 3.14 and

Equation 3.20 respectively. The overall plant energy efficiency of HCFPP1 and HCFPP2 configurations ($\eta_{o.hcp}$) is defined in Equation 3.21. The $\dot{m}_{H_2}$ and $\dot{m}_c$ represented in Equation 3.21 are the mass flowrate of produced H_2 in kg/s and input coal in HCFPP1 and HCFPP2 configurations. LHV_{H_2} represents the lower heating value in terms of MJ/kg considered as 119.90 MJ/kg (Shaikh et al., 2022).

$$\eta_{hcp} = \frac{\dot{W}_{net.hcp}}{\dot{m}_c \times HHV_c} \tag{3.20}$$

$$\eta_{o.hcp} = \frac{\dot{W}_{net.hcp} + (\dot{m}_{H_2} \times LHV_{H_2})}{\dot{m}_c \times HHV_c} \tag{3.21}$$

To assess the performance of the DNGFCPP1 and DNGFCCPP2 configurations from the electrical energy generation perspective, the net electrical energy efficiency (η_{dnp}) was calculated by considering only the net electrical energy output and total energy input as shown in Equation 3.22. The overall plant efficiency of the DNGFCPP1 and DNGFCPP2 configurations is presented in Equation 3.23 as ratio between the total energy output (vis-a-vis overall net electrical energy output of the plant and energy of DME product) and total energy input (vis-a-vis input energy supplied to the calcium looping and GPGUs ($\dot{E}_{ng}$) and input energy supplied to the DPU in the form of natural gas ($\dot{E}_{dpu}$) and solar energy ($\dot{E}_s$)). The DME energy is calculated by multiplying the mass flowrate of produced DME ($\dot{m}_{dme}$) in kg/s and its lower calorific value (LHV_{dme} in MJ/kg).

$$\eta_{dnp} = \left(\frac{\dot{W}_{net.dnp}}{\dot{E}_{dpu} + \dot{E}_{ng} + \dot{E}_s}\right) \tag{3.22}$$

$$\eta_{o.dnp} = \left\{\frac{\dot{W}_{net.dnp} + (\dot{m}_{dme} \cdot LHV_{dme})}{\dot{E}_{dpu} + \dot{E}_{ng} + \dot{E}_s}\right\} \tag{3.23}$$

3.2.1.2 Exergy analysis

Exergy is defined as the maximum possible work obtained from a system as it undergoes a reversible process to attain a complete equilibrium state with the reference environment (usually surrounding environment). The exergy estimation for material/energy streams is done by using EXERGYMS property set provided by aspenONE (Olaleye et al., 2015). This property set estimate the exergy at a particular temperature and pressure considering the user defined ambient

conditions. A detailed calculation path that has been embedded in aspenONE to determine exergy of streams is described in the literature (Hinderink et al., 1996). These exergy data of streams were further used to carry out the exergy analysis of overall system as well as for all individual units.

The overall exergy balance equation for a steady state process can be written as shown in Equation 3.24. Where $\left(\sum \dot{E}x_n\right)_{in}$, $\left(\sum \dot{E}x_n\right)_{out}$ and $\left(\sum \dot{E}x\right)_{dest}$ are the exergy rates associated with input, output and destruction respectively.

$$\left(\sum \dot{E}x_n\right)_{in} = \left(\sum \dot{E}x_n\right)_{out} + \left(\sum \dot{E}x\right)_{dest} \tag{3.24}$$

The exergy efficiency (ψ_n) and exergy destruction ratio (λ_n) of any individual unit or component n is determined by using Equation 3.25 and 3.26. In this $\left(\dot{E}x_{in}\right)_n$, $\left(\dot{E}x_{out}\right)_n$ and $\left(\dot{E}x_{dest}\right)_n$ are the exergy input, output and destruction flow rates for any individual unit or component n, respectively and $\sum \dot{E}x_{\text{dest}}$ is the overall destruction rate of the system.

$$\psi_n = \frac{(\dot{E}x_{out})_n}{(\dot{E}x_{in})_n} = 1 - \frac{(\dot{E}x_{dest})_n}{(\dot{E}x_{in})_n} \tag{3.25}$$

$$\lambda_{\text{n}} = \frac{(\dot{E}x_{dest})_n}{\sum \dot{E}x_{dest}} \tag{3.26}$$

Exergetic improvement potential of various components and units $(\dot{IP})_n$ was determined to analyze the exergetic efficiency that can be attainable in rate form and is calculated as shown in Equation 3.27 (Uysal et al., 2017).

$$(\dot{IP})_n = (1 - \psi_n)\left[\left(\dot{E}x_{in}\right)_n - \left(\dot{E}x_{out}\right)_n\right] \tag{3.27}$$

The net exergy efficiency of the biomass fired power plants (ψ_{bp}), coal fired power plants (ψ_{cp}) and natural gas fired combined cycle power plants (ψ_{ngp}) was calculated by using Equation 3.28, 3.32 and 3.33 respectively. The specific exergy of the fuel ($SCEx_b$) for biomass fired power plants was calculated by using Equation 3.29, 3.30 and 3.31 (Sahoo et al., 2016; Kotas., 1985). In these equations the LHV_b and $SCEx_b$ represent lower heating value and standard specific exergy of biomass. The w denotes the mass fraction of moisture present in the biomass whereas h represents latent heat of vaporization of H_2O at ambient temperature (T_0) i.e., 33 ^{0}C. The specific

exergy of Indian coal ($SCEx_c$) and natural gas ($SCEx_{ng}$) considered for calculating ψ_{cp}, ψ_{hcp} and ψ_{ngp} is shown in Table 3.8 and Table 3.9.

$$\psi_{bp} = \frac{\dot{W}_{net.bp}}{\dot{m}_b \times SCEx_b} \tag{3.28}$$

$$SCEx_b = (LHV_b + w \times h).\varphi + 9417 \times S \tag{3.29}$$

$$\varphi = 0.1882\frac{H_2}{C} + 0.061\frac{O_2}{C} + 0.0404\frac{N_2}{C} + 1.0437 \tag{3.30}$$

$$LHV_b = HHV_b - (226.04 \times H_2) - 25.82 \times w \tag{3.31}$$

$$\psi_{cp} = \frac{\dot{W}_{net.cp}}{\dot{m}_c \times SCEx_c} \tag{3.32}$$

$$\psi_{ngp} = \frac{\dot{W}_{net.ngp}}{\dot{m}_{ng} \times SCEx_{ng}} \tag{3.33}$$

The net electrical exergy efficiency of HCFPP1 and HCFPP2 was determined by using Equation 3.34. The overall plant efficiency of these configurations in terms of exergy was determined by using the Equation 3.35. $\dot{m}_c$ shown in Equation 3.34 and 3.35 is the mass flowrate of coal used in the respective HCFPP1 and HCFPP2 configurations. The term $SCEx_{H2}$ indicates the specific exergy of H_2 considered as 118.30 MJ/kg (Ozcan and Dincer., 2016) and ($\dot{W}_{netex}$) represents the plant net exergy output.

$$\psi_{hcp} = \frac{\dot{W}_{net.hcp}}{\dot{m}_c \times SCEx_c} \tag{3.34}$$

$$\psi_{o.hcp} = \frac{\dot{W}_{net.hcp} + (\dot{m}_{H_2} \times SCEx_{H2})}{\dot{m}_c \times SCEx_c} \tag{3.35}$$

The exergetic efficiency ($\psi_{o.dnp}$) of the DNGFCPP1 and DNGFCPP2 was determined by using Equation 3.36. The $SCEx_{dme}$ in Equation 3.36 represents the specific exergy of the generated DME (Ibrahim et al., 2018; Taghavifar et al., 2019). The solar exergy input is calculated by using the variables $\dot{E}_{solar}$ and T which represents the solar energy input and temperature of the absorber

in CSP system respectively. $\dot{E}x_{ng}$ indicates the exergetic input supplied to the calcium looping and GPGUs and ($\dot{E}x_{dpu}$) shows the input exergy supplied to the DPU in the form of natural gas.

$$\psi_{o.dnp} = \frac{\dot{W}_{net.dnp} + (\dot{m}_{dme} \times SCEx_{dme})}{\dot{E}x_{dpu} + \dot{E}x_{ng} + \dot{E}_{solar}.(1-\frac{T_o}{T})} \tag{3.36}$$

3.2.1.3 Environmental assessment

Specific CO_2 emission for all biomass fired power plants (SCE_{bp}), coal fired power plants (SCE_{cp}) and natural gas fired combined cycle power plants (SCE_{ngp}) configurations was assessed by using Equation 3.37. Equations 3.38 and 3.39 respectively. The variable $\dot{m}_{CO_2e}$, in these equations represents the mass flow rate of CO_2 emission to the atmosphere.

$$SCE_{bp} = \left(\frac{\dot{m}_{CO_2e}}{\dot{W}_{net}}\right)_{(bp/cp/ngp)} \tag{3.37}$$

$$SCE_{o.hcp} = \frac{\dot{m}_{CO_2e.hcp}}{\dot{W}_{net.hcp} + (\dot{m}_{H_2} \times LHV_{H_2})} \tag{3.38}$$

$$SCE_{o.dnp} = \frac{\dot{m}_{CO_2e.dnp}}{\dot{W}_{net.dnp} + (\dot{m}_{dme}\,.\,LHV_{dme})} \tag{3.39}$$

CO_2 capture efficiency (CCE) is defined as the percentage of CO_2 captured from a power plant's total CO_2 emissions and was calculated by using Equation 3.40. Purity of captured CO_2 used in the environmental analysis refers to the percentage of CO_2 present in the concentrated CO_2 stream, obtained at the end of CO_2 separation process. CO_2 utilization efficiency (CUE) for the CCU schemes proposed in this research work was calculated by using Equation 3.41. In these corresponding equations, the parameters $\dot{m}_{capCO_2}$ and $\dot{m}_{CO_2ut}$ denotes the amount of CO_2 captured by the calcium looping system and the amount of DME utilized by DPU respectively. The term $\dot{m}_{genCO_2}$ represents the total amount CO_2 generated by the overall power plant (kg/s).

$$CCE = \left(\frac{\dot{m}_{capCO_2}}{\dot{m}_{genCO_2}}\right)_{(bp/cp/ngp/hcp/dnp)} \tag{3.40}$$

$$CUE = \left(\frac{\dot{m}_{CO_2ut}}{\dot{m}_{genCO_2}}\right)_{dnp} \tag{3.41}$$

3.2.1.4 Cost analysis

A cost analysis was done to compare the financial viability of all the configurations. The LCOE and CO_2 avoided cost (CA) were chosen as the main parameters to evaluate the performance of all the configurations. The LCOE is defined as the cost associated per unit of electricity generation over the lifetime of the plant and was calculated by using Equation 3.42 for all biomass fired power plant configurations and by using Equation 3.43 for all other configurations. The CA represents the cost incurred to capture the unit amount of CO_2 as shown in Equation 3.44. The parameters TCR, MC and FC in these equations are the total capital requirement, maintenance cost and fuel (biomass) cost respectively. The parameters FCF, CF, FOM and VOM are the fixed charge factor, capacity factor, fixed and variable (operation and maintenance) costs respectively.

The TCR, MC, FOM and VOM were computed by first estimating the capital cost of each unit/subsystem and then using the correlation provided in the literature (Whitesides., 2005; Zhu et al., 2020; Hanak and Manovic., 2017a; Manzolini et al., 2013). Further, the necessary data required to calculate each unit/subsystem cost and raw sorbent cost were obtained from the literature (Hanak and Manovic., 2017a; Manzolini et al., 2013; Uday limestone., 2021; Castillo., 2007; Mustafa et al., 2012; Whitesides.,2005; Chauvel et al., 2003). In Equation 3.44, the suffix C1 represents the base case configuration, and Ci represents the other proposed configurations that were demonstrated with respect to the base case. The FCF was calculated by using Equation 3.45 where i represents the yearly project interest rate and N is the economical plant lifetime in years.

$$LCOE = \left(\frac{TCR \times FCF + MC + FC}{\dot{W}_{net} \times CF \times 8760}\right)_{bp} \tag{3.42}$$

$$LCOE = \left(\frac{TCR \times FCF + FOM}{\dot{W}_{net} \times CF \times 8760} + VOM + \frac{SFC}{\eta}\right)_{(cp/ngp/hcp/dnp)} \tag{3.43}$$

$$CA = \frac{LCOE_{Ci} - LCOE_{C1}}{E_{CO_2 C1} - E_{CO_2 Ci}} \tag{3.44}$$

$$FCF = i\,\frac{(1+i)^N}{(1+i)^N - 1} \tag{3.45}$$

The levelized product cost is defined as the average cost per kg of product produced by the plant. The H_2 and DME can be sold as a feedstock for manufacturing different chemicals. Keeping

this in view, the LPCH and LPCD were determined by using Equation 3.46. The APP in Equation 3.46 is the annual product production that represents the amount of product generated in terms of kg/year using the developed configurations.

$$LPCH\ or\ LPCD = \left(\frac{TCR \times FCF + FOM + VOM}{APP}\right)_{(hcp/dnp)} \tag{3.46}$$

3.2.1.5 Exergoeconomic analysis

The exergoeconomic analysis is a method to study the exergy of the system along with the consideration of economic principles. It helps to provide an integrated approach by an established relationship between the cost and thermodynamic inefficiencies of the system. The exergoeconomic factor was chosen as an indicator to evaluate the performance of all the units or components of the configurations and to improve the performance of the system cost effectively.

The exergoeconomic factor (f) for any component or unit (n) was calculated by using Equation 3.47. The cost rate associated with capital investment $(\dot{Z})$ and cost rate of exergy destruction $(\dot{CD})$ were calculated by using Equation 3.48 and Equation 3.49. The variable CC denotes the overall cost that includes FOM, VOM and capital cost of the corresponding unit or component n and c_F represents the cost of exergy associated with the fuel.

$$f_n = \frac{\dot{Z}_n}{\dot{Z}_n + \dot{CD}_n} \tag{3.47}$$

$$\dot{Z}_n = \frac{FCF}{CF \times 8760} \times CC_n \tag{3.48}$$

$$\dot{CD}_n = c_{F.n} \times \dot{Ex}_{dest.n} \tag{3.49}$$

CHAPTER 4

RESULTS AND DISCUSSION

Chapter 4

Results and Discussion

This section presents a detailed discussion of the results obtained from the simulation of proposed configurations, parametric analyses, and comparison studies. This is done by carrying out a comparative assessment of all the developed configuration on the basis of energy, exergy, environmental, cost and exergoeconomic parameters. These discussions were made corresponding to the objectives described in this thesis. The results help to demonstrate the effectiveness of the proposed biomass, coal and natural gas fired power plant configurations integrated with CO_2 capture, utilization and cogeneration schemes. The different configurations proposed for a given fuel input such as coal/biomass/natural gas are analyzed independently and compared their performances. At the end, the resulted effective biomass fired power plant, coal fired power plant and natural gas fired combined cycle configurations are considered to study the effect of fuel on performance of the power plant.

4.1 Performance assessment of calcium looping integrated biomass fired power plants

The performance of the proposed calcium looping integrated BFPP plants (BFPP2 and BFPP3) were evaluated on the basis of energy exergy, environmental, cost and exergoeconomic parameters. Various sensitive analyses to study the effect of carbonator temperature and mass flow rate of organic fluid on the performance of BFPP3 were also presented in this sub section. The performance of the proposed configurations are compared against the conventional BFPP (BFPP1) to assess the merits and demerits. The key outcome of this study is to come up with an efficient calcium looping integrated biomass fired power plant for CO_2 capture and electricity generation. This feasibility study opens the avenues for construction of low capacity and grid-independent power plants operates with the indigenous fuel and meets the electricity demands with carbon negative technology in rural areas.

4.1.1 Plant performance

The energy and exergy analyses of the BFPP2 and BFPP3 configurations were carried out and compared with the BFPP1 configuration to assess the thermodynamic performance. In this

study the reference state for exergy analysis is considered as T_0 = 33 ^{0}C and p_0 = 1.013 bar. The results revealed that net energy and exergy efficiencies of the BFPP2 configuration were 9.20% and 8.92%, while in the case of BFPP3 without CU the energy and exergy efficiency were found to be 11.09% and 10.75% respectively. The results were shown in Table 4.1.

Table. 4.1 Plant performance indicators on thermodynamic basis for BFPP1, BFPP2 and BFPP3

Parameters	Energy basis				Exergy basis			
	BFPP1	BFPP2	BFPP3		BFPP1	BFPP2	BFPP3	
			Without CU	With CU			Without CU	With CU
Heat input from biomass combustion (kW)	2284.7	2284.7	2284.7	2284.7	2356.5	2356.5	2356.5	2356.5
ASS work (kW)		45.4				45.4		
CO_2 compression work (kW)				91				91
Gross power output (kW)	286	286	284.6	284.6	286	286	284.6	284.6
Net power output (kW)	254.7	210.3	253.4	162.4	254.7	210.3	253.4	162.4
Gross efficiency (%)	12.52	12.52	12.46	12.46	12.14	12.14	12.08	12.08
Net efficiency (%)	11.15	9.2	11.09	7.11	10.81	8.92	10.75	6.89
Efficiency penalty (%)		1.94	0.1	4.04		1.89	0.1	3.92

It indicates that for the same energy input from biomass combustion, the energy and exergy penalty of a BFPP2 configuration was 1.94% and 1.89% while the BFPP3 without CU was only 0.1% as compared with BFPP1. This is mainly due to the energy saving configuration of the double calcium

looping that enables the elimination of ASS and thus contributes in improving the thermal efficiency of the overall plant. The proposed BFPP3 not only minimizes net auxiliary power requirement but also leads to better utilization of energy with effective heat integration as compared with conventional calcium looping system. Subsequently an additional power of 91 kW was required to compress and store the concentrated CO_2 streams leaving the calcium looping system.

The thermodynamic performance of BFPP3 with CU resulted in an efficiency penalty of 4.04% and 3.92% on energy and exergy basis respectively. Therefore, for further improvement of the proposed configuration, more emphasis needs to be given to identify different heat integration strategies for the reduction of CU's power requirement. Though, the primary role of integrating calcium looping process with the biomass fired power plants is to reduce overall CO_2 emissions into the atmosphere, the thermodynamic parameters cannot be the only criteria for assessment. Therefore, an ecological assessment was also carried out to assess the performance of BFPP3 based on environmental parameters as shown in Table 4.2.

Table. 4.2 Results of the environmental assessment for BFPP1, BFPP2 and BFPP3

Environmental performance indicators	BFPP1	BFPP2	BFPP3	
			Without CU	With CU
Instantaneous flow of emitted CO_2 (kg/s)	0.23	0.022	0.022	0.022
CO_2 capture efficiency (%)		90.43	90.43	90.43
Specific CO_2 emission (g/kWh)	3250.63	376.62	312.56	487.83
Lifetime CO_2 emission of the power plant (kg x 10^3)	116052.48	11100.67	11100.67	11100.67

It was assumed that both standalone and calcium looping integrated biomass fired power plants operate for 7008 hours annually for an overall plant life period of 20 years. On this basis, an overall lifetime CO_2 emission associated with BFPP1 was found to be 116052.48×10^3 kg while the BFPP2 and BFPP3 capturing 90.43% of CO_2 generated from combustion and have lower lifetime CO_2 emission of 11100.67×10^3 kg only. Also, the So emissions were found to be negligible because of the formation of $CaSO_4$ in the carbonator.

4.1.2 Exergy analysis of major units and components

As the BFPP3 configuration was energetically, exergetically and environmentally efficient than other configuration, it was further analyzed in detail. An exergy analysis for major units of BFPP3 was carried out to identify the scope for further performance enhancement. Fig. 4.1 shows that the turbine and centrifugal pump have the highest exergy efficiencies of 93.97% and 98.23%. This indicates that a large part of energy entering into the turbine and centrifugal pump has been converted into useful work and thus exergy destruction is minimal in these two units. On the contrary, it is evident from Fig. 4.2A that the highest amount of exergy destruction was found to be in the DCaLU. It accounts for 47.83% of exergy destruction of the overall system. In this 41.23% of exergy destruction occurs in the combustor while 6.6% of exergy destruction occurs in the calcium looping system. Followed by this is the evaporator that accounts for around 37.57% of exergy destruction. A major reason for the exergy losses in the evaporator is due to the large temperature difference between hot and cold fluid streams, (Yang et al., 2013) while the exergy destruction in DCaLU is due to the irreversibilities associated with the chemical reactions (Wang et al., 2013; Som et al., 2008).

The study also helps to locate the energy savings opportunities associated with the proposed BFPP3 as shown in Fig. 4.2B. The results clearly demonstrate that there is a huge scope of improvement potential (around 44.96%) within the evaporator present in the ORC section. Incorporating regeneration and turbine bleeding techniques in the ORC are some of the options that can be explored to improve the performance of the evaporator (Safarian and Aramoun., 2015). The DCaLU that comprises mainly of the combustor, carbonator, and calciner also holds together a good amount of improvement potential of exergy saving of around 40.68%.

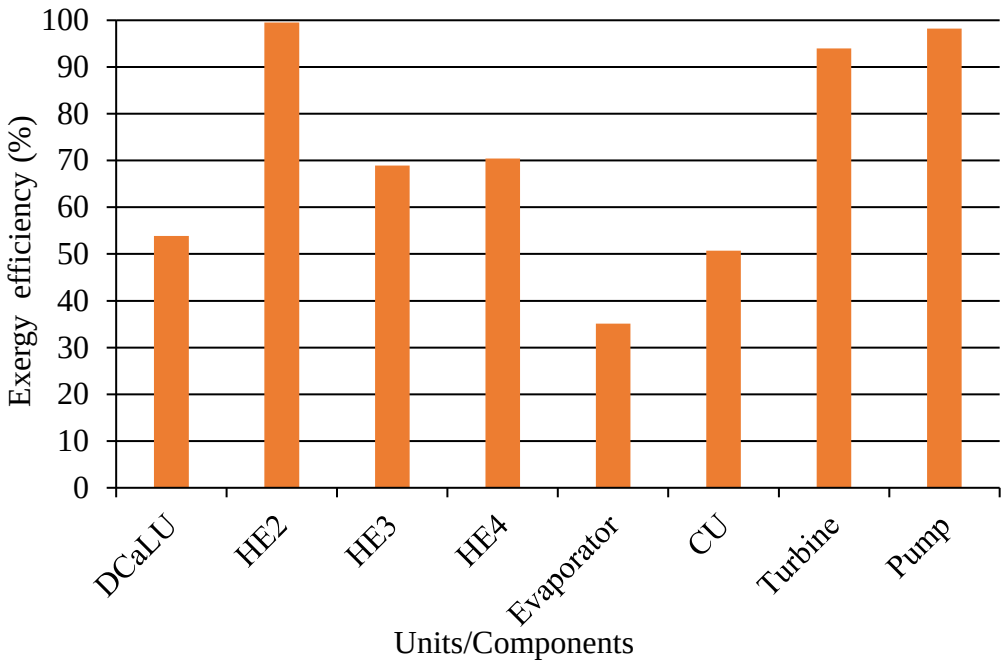

Fig. 4.1 Exergy efficiency of all the units and components of BFPP3

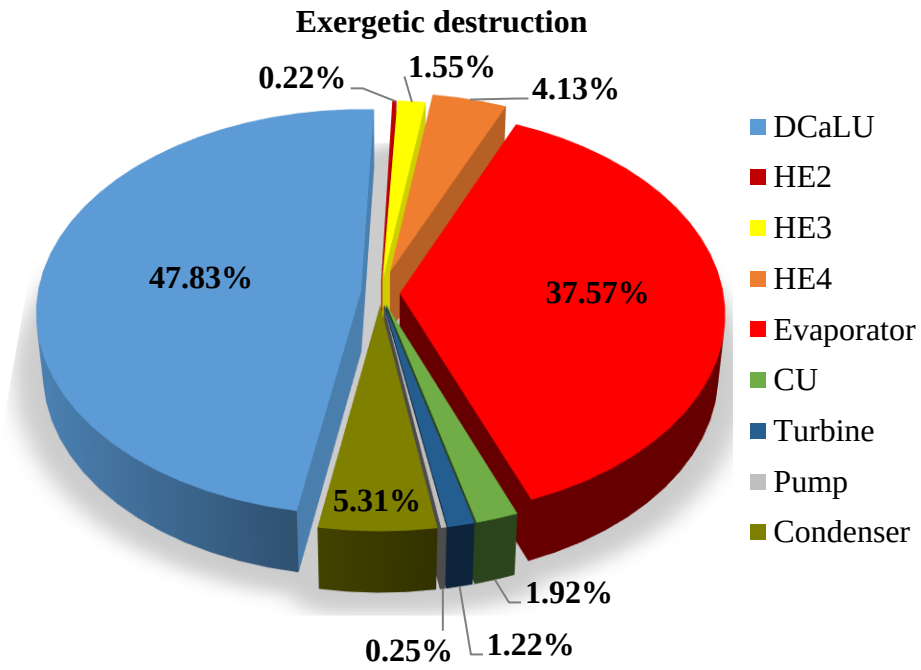

(A)

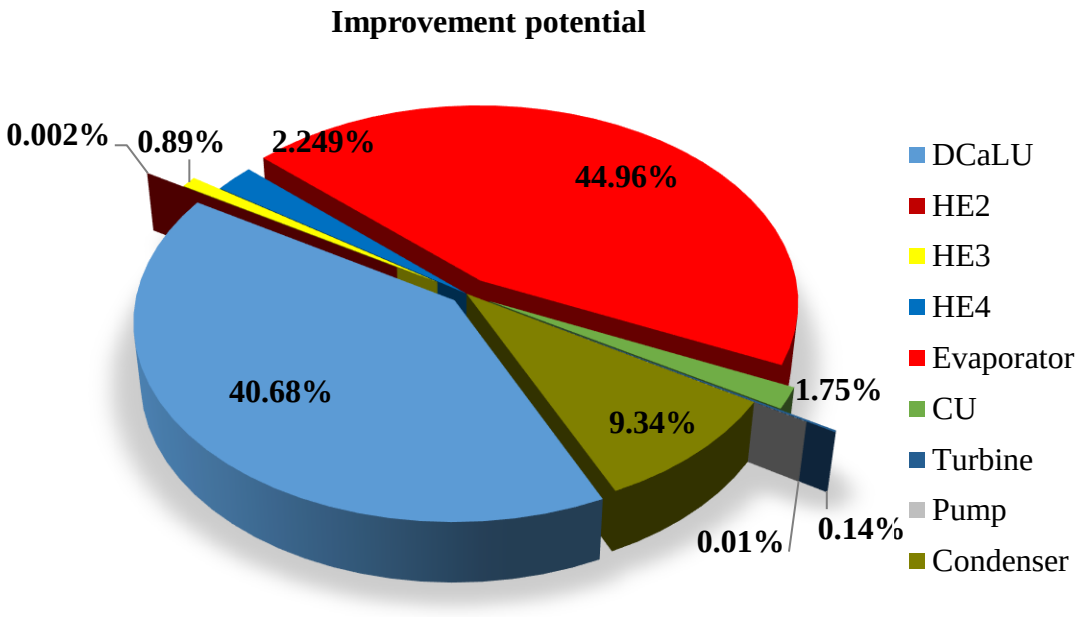

(B)

Fig. 4.2 (A) – Distribution of exergy destruction (B) – Improvement potential of BFPP3

4.1.3 Cost and exergoeconomic analysis

Cost analysis provides valuable information in predicting the commercial feasibility of new technologies. In this section, the results of cost analysis of BFPP1, BFPP2 and BFPP3 are explained in detail. The results from Table 4.3 indicate that the TCR of the BFPP3 and BFPP2 were 7.57 M€ and 10.19 M€ as compared to BFPP1 having a TCR of 3.01 M€. The higher TCR of both the calcium looping integrated biomass fired power plants are because of the additional cost of calcium looping units that were used to capture the CO_2 generated by the power plant. It was also found out the TCR of BFPP2 is higher than the BFPP3. This is because of the additional cost imposed by the ASS that was used to supply pure O_2 in the BFPP2. Elimination of ASS in BFPP3 configuration leads to 0.71 €/kWh of LCOE which is significantly less than the BFPP2 configuration LCOE of 1.13 €/kWh.

It was also found out that the LCOE of these organic rankine cycle based BFPP1, BFPP2 and BFPP3 were quite higher as compared to rankine cycle based biomass fired cogeneration

power plants and ASS coupled calcium looping integrated biomass fired cogeneration power plants having the LCOE of approximately 0.06 €/kWh – 0.41 €/kWh (Neto et al., 2021). This is because of the plant which is integrated with organic rankine cycle that has low power production efficiency than the steam rankine cycle. However, the power plant configurations with biomass as fuel were designed with an intention to build low-capacity systems and for rural areas of India. For such small scale power production configurations, the organic rankine cycle is more effective than the steam cycle (Vankeirsbilck et al., 2011; Dai et al., 2009). Hence, this proposed BFPP3 configuration is certainly unique than other types of biomass fired power plants. The CA determined from the cost analysis indicates that BFPP3 configuration require 0.13 € to avoid kg of CO_2 emission into atmosphere which is very minimum as compared BFPP2 having 0.28 €/kg of CO_2. The overall results clearly indicate that the BFPP3 is economically and environmentally better suitable as compared to BFPP2.

The exergoeconomic factor determined under this analysis for all the units/components provides an insight of the relative importance of the exergy destruction, capital investment and operation and maintenance costs. The results from Fig. 4.3 reveal that the highest exergoeconomic factor in the BFPP3 was found to be in DCaLU with 93.79% and turbine with 94.28%. This is due to the high cost associated with their capital, operating and maintenance. The relatively higher cost of exergy destruction as compared to the capital cost has led to a low exergoeconomic factor of 15.84%, 5.67%, 8.36% and 16.09% in evaporator, HE3, HE4 and condenser respectively. Therefore, in this case efforts must be made in the corresponding components to further reduce the irreversibility or increase the overall investment with an aim to attain an exergoeconomic factor of around 50%.

Table 4.3 Cost performance indicators of the BFPP1, BFPP2 and BFPP3

Parameter	BFPP1	BFPP2	BFPP3
TCR (M€)	3.01	10.19	7.57
LCOE (€/kWh)	0.33	1.13	0.71
CA (€/kg)	--	0.28	0.13

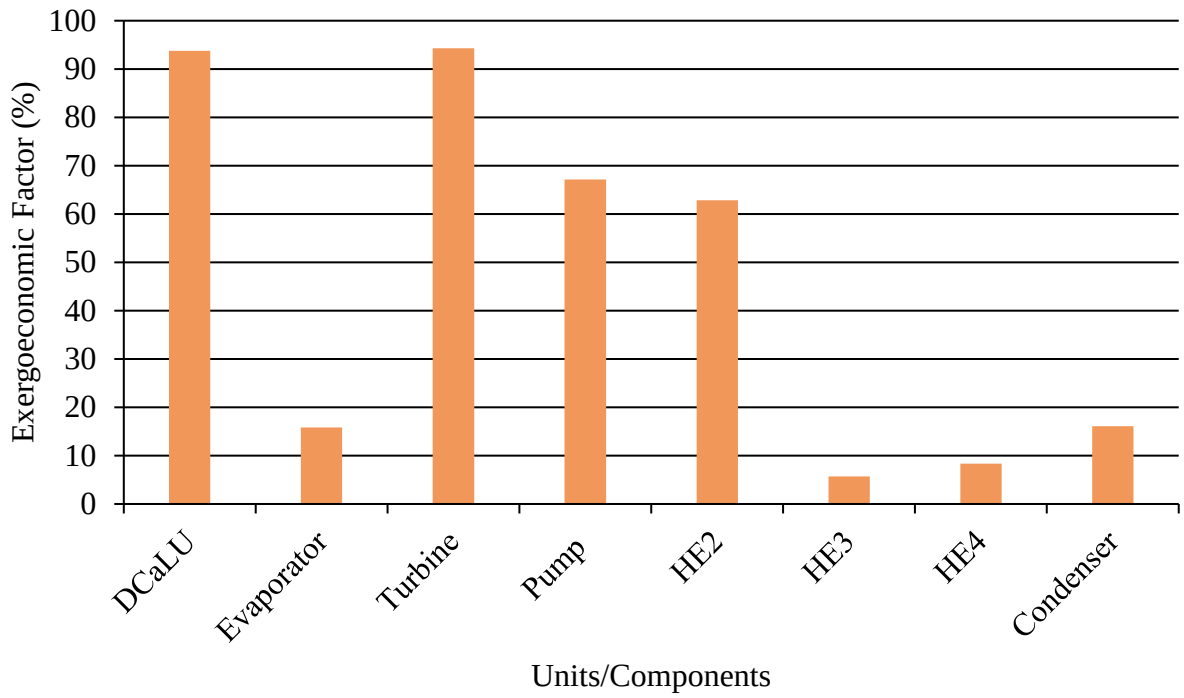

Fig. 4.3 Exergoeconomic factor of all the units and components of BFPP3

4.1.4 Sensitivity analysis

Sensitivity analysis is a key tool to assess the effect of key design and operating parameters on the performance of the overall system. In this section, the carbonator temperature and mass flow of organic fluid were varied with an aim to study their influence on CO_2 capture, sorbent content and net efficiency of BFPP3.

4.1.4.1 Effect of carbonator temperature on the performance of BFPP3

Fig. 4.4A illustrates the noticeable effect of carbonator temperature on specific CO_2 emissions and CO_2 capture efficiency at steady state. It has been observed that the CO_2 capture efficiency decreases significantly with the increase in carbonator temperature. The highest carbon capture efficiency of 94.28% was observed at 630 ^{0}C while the lowest (74.8%) was achieved was at 690 ^{0}C. This huge variation of carbon capture was due to the inhibition of carbonation reaction at higher temperatures (Yin et al., 2015; Charitos et al., 2010). The specific CO_2 emissions increase with an increase in carbonator temperature, as shown in Fig. 4.4A. However, it can be observed

from Fig. 4.4B that the net energy efficiency of 11.09% is independent of carbonator temperature at optimal sorbent circulation rate.

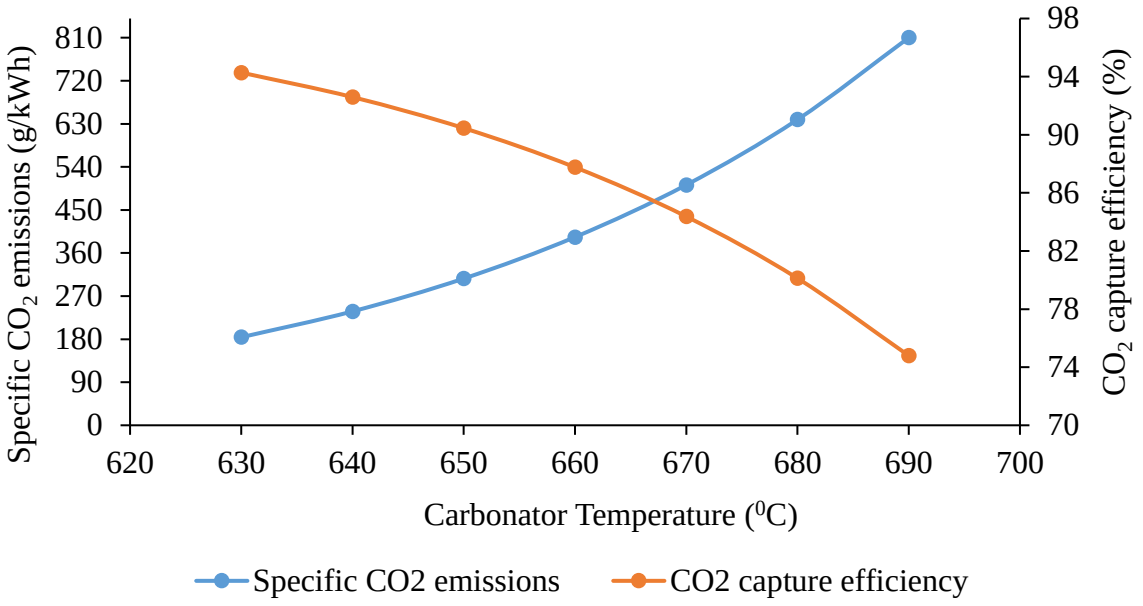

(A)

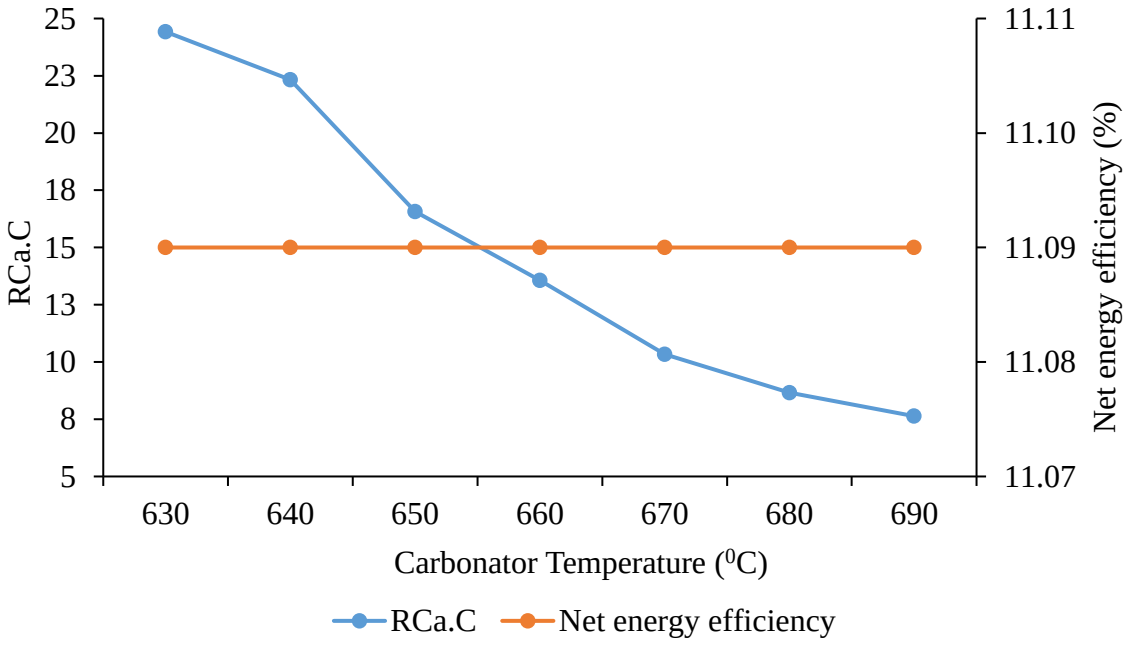

(B)

Fig. 4.4 Effect of carbonator temperature on (A) specific CO_2 emissions and CO_2 capture efficiency (B) net energy efficiency and CaO circulation rate per unit of CO_2 in flue gas

In addition, Fig. 4.4B also shows the optimal CaO circulation rate per unit of CO_2 in flue gas (RCa.C) at different carbonator temperatures. At the carbonator reactor temperature of 630 ^{0}C, the RCa.C value was found to be very high which indicates more CO_2 is being adsorbed at this temperature. As the carbonator reactor temperature increases the sorption rate decreases hence low amount of CaO is needed in the loop which resulted in decreasing of RCa.C ratio.

4.1.4.2 Effect of mass flow rate of organic fluid on the performance of BFPP3

Since the exergy analysis reveals that the highest exergy destruction was in the evaporator of the ORC section, a parametric study in ORC was carried out to investigate the scope for possible improvements in system design. The key parameters that affect the system performance include the mass flow rate of the organic fluid, outlet temperature, and the power consumption by the centrifugal pump. Based on the results of Fig. 4.5A and 4.5B, the optimal parameters can be deduced at constant pressure drop across the turbine. Fig. 4.5A indicates that the energy and exergy efficiency of the BFPP3 increase with increase in mass flow rate of the organic fluid (R-245fa). This is due to the lower turbine outlet temperature that results in lower enthalpy loss and higher work output at higher mass flow rates of organic fluid. In the following analysis, it has been found out that an energy and exergy efficiency of 11.26% and 10.92% can be achieved at the lowest turbine outlet temperature of 48.58 ^{0}C.

The characteristics of organic fluid also play a critical role in the performance of the system. The thermal capacity (UA), i.e., the product of overall heat transfer coefficient (assumed as constant) of the organic fluid and evaporator area was calculated as a function of mass flow rate of the organic fluid. Fig. 4.5B represents the gradual decline of the UA as the mass flow rate of organic fluid increases. The highest UA of 11.56 kW/K was observed at an organic fluid mass flow rate of 7 kg/s while the lowest (10.39 kW/K) was found to be at 11 kg/s. This analysis reveals that for a given heat input of hot fluid (thermal oil), evaporator surface area is decreasing with the increase in mass flow rate of organic fluid. The energy consumption of the centrifugal pump was also calculated to determine its influence on the performance of the overall system.

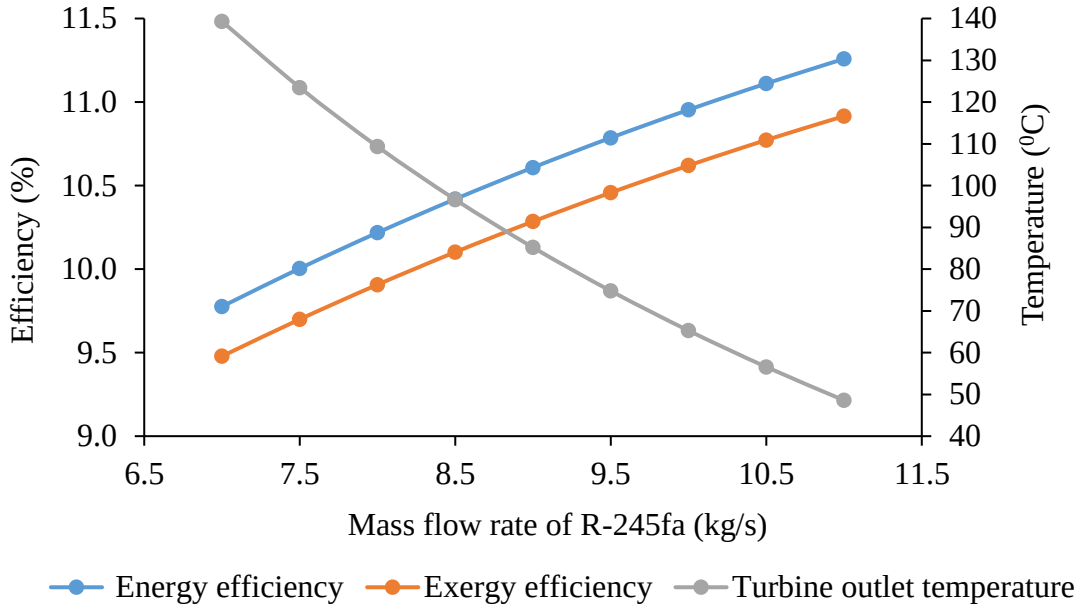

(A)

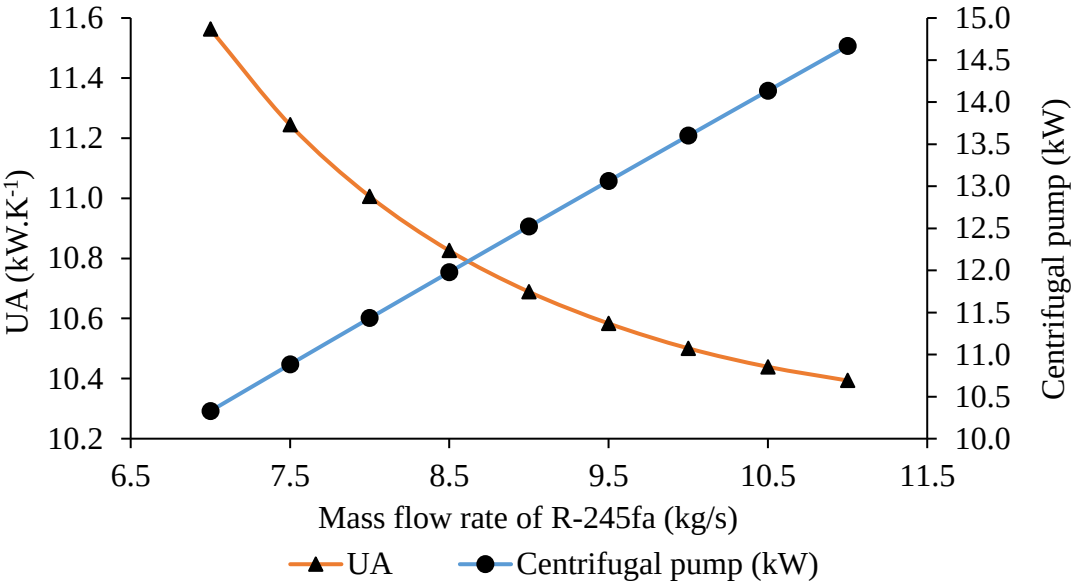

(B)

Fig. 4.5 Effect of organic fluid (R-245fa) mass flow rate on turbine outlet parameters
(A) temperature and system efficiency, (B) pump energy consumption and thermal capacity

The results indicate that the energy requirement of the pump steadily increases from 10.33 kW to 14.67 kW as the mass flow of organic fluid increases. However, this result when

compared with Fig. 4.5A clearly indicates that the rate of increase in power consumption by the centrifugal pump is much lower than the rate of increase in turbine power output resulting in the higher efficiency of the overall system with increase in mass flow rate of the organic fluid. The thermodynamic analysis favors high organic fluid circulation rate for better efficiency of the cycle; however, this will lead to the requirement of larger pump and turbine units and thus can increase the capital and operating cost of the system. This leads to a tradeoff assessment between the desired power generation and organic fluid circulation for an economical process development.

4.2 Performance assessment of calcium looping integrated coal fired power plants

In this sub-section, the performance assessment was carried out for the proposed Calcium looping integrated Coal Fired Power Plants (CFPP2 & CFPP3). The merits of the proposed configurations were evaluated by comparing them with conventional CFPP (CFPP1). The overall assessment of all the developed configurations were carried out on the basis of energy, exergy, environmental and cost parameters. The key outcome of this study is to propose an efficient calcium looping integrated coal fired power plant configuration for CO_2 capture and electricity.

4.2.1 Plant performance

In this section, Table 4.4 and Table 4.5 presents the overall comparative evaluation of CFPP1, CFPP2 and CFPP3 power plant configurations on energy and exergy basis while Table 4.6 represents the same on environmental basis. The environmental reference state taken for the study is 1.013 bar and 33 ^{0}C. All the three power plant configurations were analyzed at same amount of energy and exergy input of 1432.30 MW and 1565.30 MW respectively. The net energy and exergy efficiency of CFPP3 (without CU) was found to be 35.46% and 32.44%. This is higher than CFPP2, which has an overall energy and exergy efficiency of 32.46% and 29.70%. The net energy penalty of CFPP3 was found to be 0.52% only against the energy efficiency of CFPP1. Likewise, the exergy penalty of CFPP3 was also found to very low i.e., 0.48%. The results revealed that the proposed integration strategy in CFPP3 possess a higher degree of energy utilization as compared to the CFPP2 in which the energy and exergy penalty was found to be 3.52% and 3.22% when compared against the CCFP1. Since CO_2 compression is an essential process for carbon sequestration, the energy and exergy efficiency were also calculated for the CFPP3 by integrating

a CU. The results revealed that the energy and exergy penalty of CFPP3 with CU were 4.20% and 3.85%.

Table 4.4 Plant performance of CCFP1, CFPP2 and CFPP3 on energy basis

Parameters	CFPP1	CFPP2	CCFP3	
			Without CU	With CU
Energy input from coal combustion (MW)	1432.30	1432.30	1432.30	1432.30
Gross power output (MW)	590.56	592.07	591.70	591.70
Total electricity consumption (MW)	75.25	127.11	83.85	83.85
Electricity consumption by CU (MW)				52.75
Net power output (MW)	515.31	464.96	507.85	455.10
Net energy efficiency (%)	35.98	32.46	35.46	31.77
Energy efficiency penalty (%)		3.52	0.52	4.20

Table 4.5 Plant performance of CCFP1, CFPP2 and CFPP3 on exergy basis

Parameters	CFPP1	CFPP2	CCFP3	
			Without CU	With CU
Exergy input from coal combustion (MW)	1565.3	1565.3	1565.3	1565.3
Gross power output (MW)	590.56	592.07	591.70	591.70
Total electricity consumption (MW)	75.25	127.11	83.85	83.85
Electricity consumption by CU (MW)				52.75
Net power output (MW)	515.31	464.96	507.85	455.10
Net exergy efficiency (%)	32.92	29.70	32.44	29.07
Exergy efficiency penalty (%)		3.22	0.48	3.85

Since the foremost objective of any CO_2 capture system is to lower the CO_2 emissions significantly, an analysis as shown in Table 4.5 was also carried out to assess the performance of the proposed configuration on environmental basis. It was assumed that all the three power plant configurations have an overall plant life period of 25 years and operate 7008 hours annually. The results revealed that as compared to the CCFP1 that produces the lifetime CO_2 emissions of around 7,99,16,195 Mg, the lifetime CO_2 emissions in CFPP2 and CFPP3 (without CU) were found to be the lowest with around 73,79,424 Mg and a CO_2 capture efficiency of approximately 91%. The results also revealed that with the addition of CU, the specific CO_2 emission of CFPP3 was higher i.e., 92.55 kg/MWh as compared to CFPP3 (without CU) that was having a specific CO_2 emission of 82.94 kg/MWh.

Table 4.6 Plant performance of CFPP1, CFPP2 and CFPP3 based on environmental analysis

Environmental performance indicators	CFPP1	CFPP2	CFPP3	
			Without CU	With CU
Instantaneous flow of emitted CO_2 (kg/s)	126.71	11.7	11.7	11.7
CO_2 capture efficiency (%)		91.05	91.05	91.05
Specific CO_2 emission (kg/MWh)	885.17	90.59	82.94	92.55
Annual CO_2 emission (kg x 10^3)	31,96,648	2,95,177	2,95,177	2,95,177
Lifetime CO_2 emission of the power plant (kg x 10^3)	7,99,16,195	73,79,424	73,79,424	73,79,424

4.2.2 Exergy analysis of major units and components

The exergy analysis was performed to investigate the thermal losses due to irreversibilites of the major units in the CFPP3, which is the most efficient configuration among the three CFPP configurations. The analysis not only identifies the location of losses but also helps to determine the maximum scope of improvement possible in the system. It was observed from Fig. 4.6 that the HPT and IPT have the highest exergetic efficiency of 98.39% and 98.24%. This was followed by the LPT and the air compressor (AC) having an exergy efficiency of 92.97% and 72.26%

respectively, and thus these corresponding units hold very less exergy destruction. On the contrary, the highest exergetic destruction was found to be in the DCaLU with an exergetic destruction of 88.86% as shown in Fig. 4.7A. In this, the combustor and calcium looping system holds 68.43% and 20.43% respectively. A major reason for this exergy destruction was because of the irreversibilities of the chemical reactions that occur in the combustor and the reactors of calcium looping unit (Wang et al., 2013; Som et al., 2008).

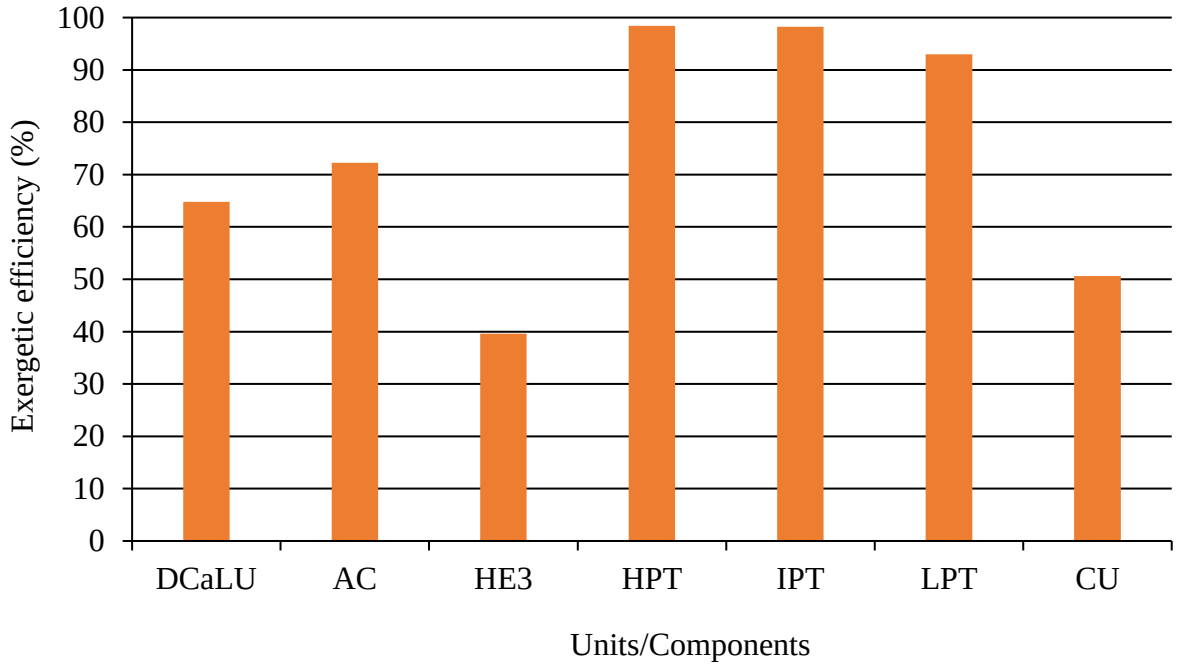

Fig. 4.6 Exergy efficiency of units and components in CFPP3

The results also indicate that the air preheater (HE3) and the CU although holds significantly lower exergetic destruction as compared to DCaLU but was the second and third largest exergetic destruction, i.e., 3.49% and 2.94% as compared to all other units. This exergy destruction was mainly due to the large difference in temperature between its cold and hot fluids (Zhao et al., 2017). As mentioned above, the exergy analysis also helps to evaluate the margin for potential improvement of the CFPP3 configuration. This is illustrated in Fig. 4.7B.

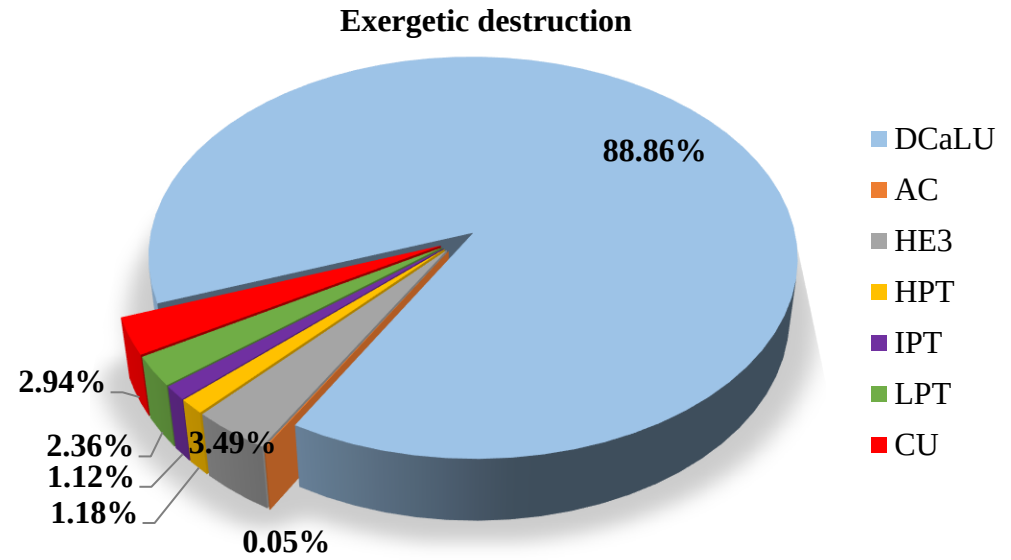

(A)

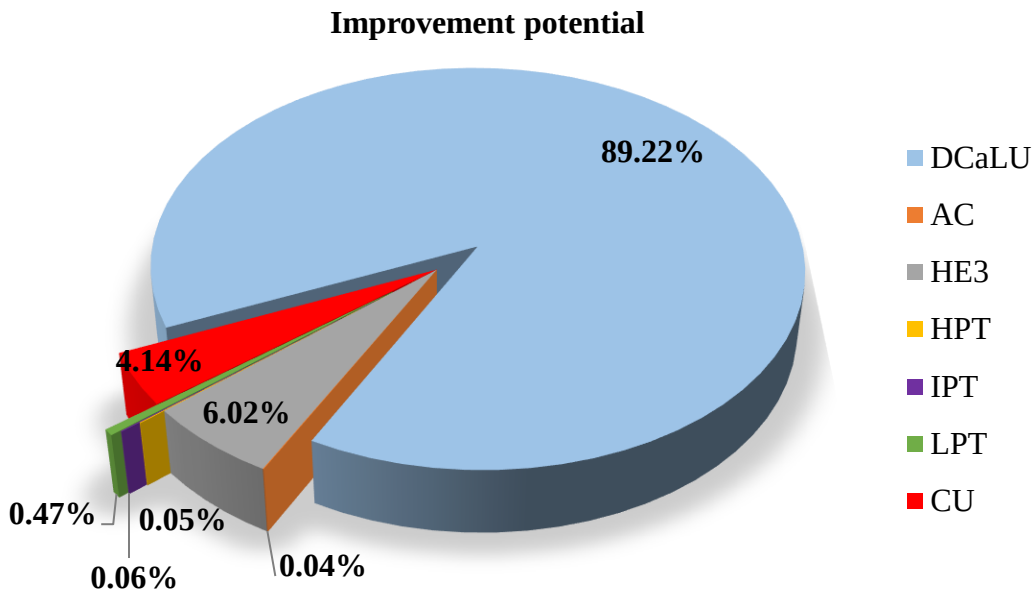

(B)

Fig. 4.7 (A) – Distribution of exergy destruction, (B) – Improvement potential in CFPP3

The results indicate that the highest scope of improvement potential was in the DCaLU that holds an exergetic improvement potential of around 89.22% (284.62 MW). One way to explore this exergetic improvement potential is to increase the combustion temperature (Anheden and Svedberg., 1998). This can be done by reducing the excess air ratio. However, more research is needed to identify materials that can endure such higher temperatures. The HE3 and CU also hold a reasonable amount of exergetic improvement potential of 6.02% (19.2 MW) and 4.14% (13.2 MW) respectively.

4.2.3 Cost and exergoeconomic analysis

In this section, the comparative cost analysis of CFPP1, CFPP2 and CFPP3 was carried out to demonstrate the competitiveness of the proposed CFPP3 in terms of economics. The main assumptions considered in this study were reported in Chapter 3. The results of all the three configurations are presented in Table 4.7. The comparative assessment of CFPP1, CFPP2 and CFPP3 reveals that the TCR of CFPP2 and CFPP3 were 1107.78 M€ and 998.52 M€ as compared to the TCR of CFPP1 i.e., 696.26 M€. This is due to the additional installation of calcium looping unit that captures the CO_2 produced from the power plant. A higher TCR of CFPP2 as compared to the CFPP3 was primarily because of the ASS in CFPP2 which was needed to produce O_2 for combustion. The CFPP3 configuration has a better LCOE of 51.14 €/MWh and CA of 17.36 €/t of CO_2 when compared against the CFPP2 that has a LCOE of 61.13 €/MWh and CA of 30.11 €/t of CO_2.

Table 4.7 Cost performance indicators of the CFPP1, CFPP2 and CFPP3

Cost parameters	CFPP1	CFPP2	CFPP3
TCR (M€)	696.26	1107.78	998.52
LCOE (€/MWh)	37.21	61.13	51.14
CA (€/t)	-	30.11	17.36

The results from exergoeconomic analysis of CFPP3 shown in Fig. 4.8 reveals that the cooling water system and BOP unit has the lowest exergoeconomic factor of 26.74%. This implies that the cost of exergy destruction is dominant than its associated investment cost. Therefore, more investment can be made in the cooling water and BOP unit to further reduce the exergy destruction.

The calcium looping plant and steam turbine, generator and auxiliaries possess an exergoeconomic factor of 93.04% and 94.81% respectively. For these units, it is beneficial to identify a more cost-effective way that can lead to an improvement in the overall process.

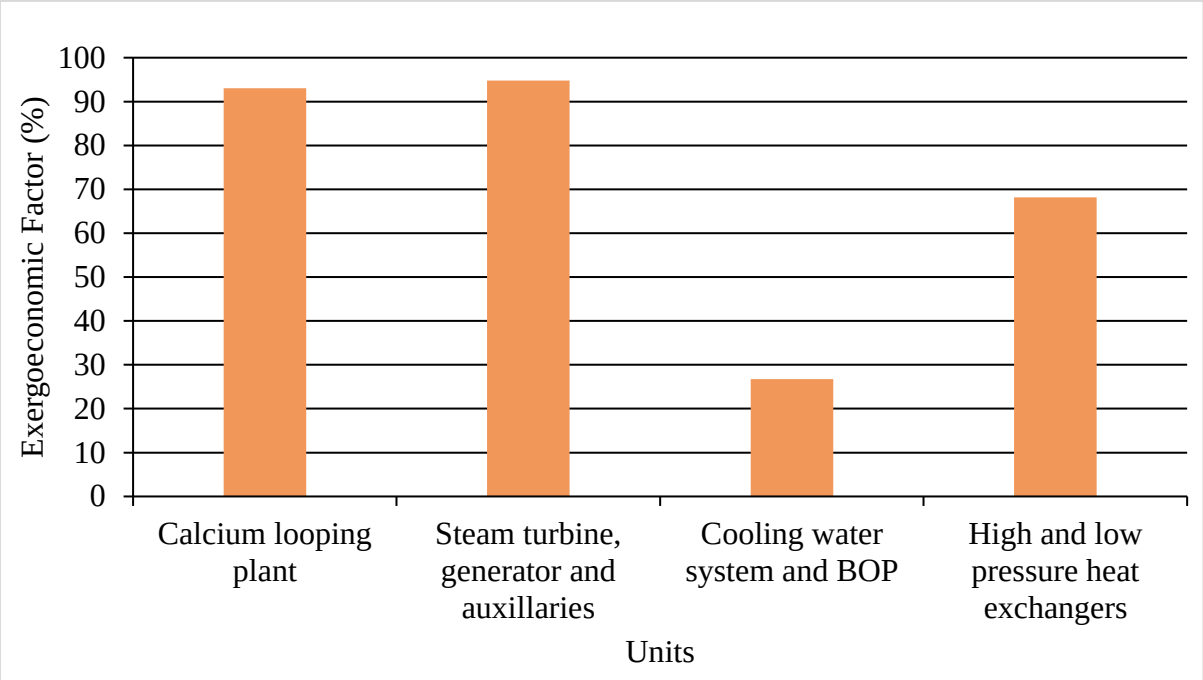

Fig. 4.8 Exergoeconomic factor of different units in CFPP3

4.2.4 Sensitivity analysis

A sensitivity analysis was carried out for CFPP3 configuration and presented the effect of carbonator temperature, condenser pressure and isentropic efficiency of the turbines on plant performance. The results obtained from these sensitivity analyses were discussed in this section.

4.2.4.1 Effect of carbonator reactor temperature on the performance of CFPP3

The carbonator reactor temperature was varied and its outcome on the performance of CFPP3 was analyzed by observing its effect on specific CO_2 emissions, CO_2 capture efficiency, RCa.C and net energy efficiency. Fig. 4.9A shows the variation of specific CO_2 emission and CO_2 capture efficiency with respect to the carbonator reactor temperature. The results indicate that as the carbonator reactor temperature was increased from 630 ^{0}C to 690 ^{0}C, the CO_2 capture efficiency was reduced from 94.64% to 76.37%. On the other hand, the specific CO_2 emission

increased considerably from 49.76 kg/MWh to 219.14 kg/MWh. This behavior in carbonator temperature was due to the inhibition of carbonation reaction with the increase in temperature (Charitos et al., 2010; Yin et al., 2015).

Fig. 4.9B illustrates the variation of RCa.C and net energy efficiency with respect to the carbonator rector temperature. The net energy efficiency was found to be nearly constant i.e., 35.46% with the variation of carbonator reactor temperature. This reveals that net energy efficiency of CCFP3 (without CU) is an independent parameter with respect to the change in carbonator temperature. For the carbonator temperature of about 690 ^{0}C, the RCa.C value was found to be around 4.16 while at the temperature of 630 ^{0}C, it was 6.36. The decreasing trend of RCa.C clearly shows the lower sorption rates at higher carbonator temperatures.

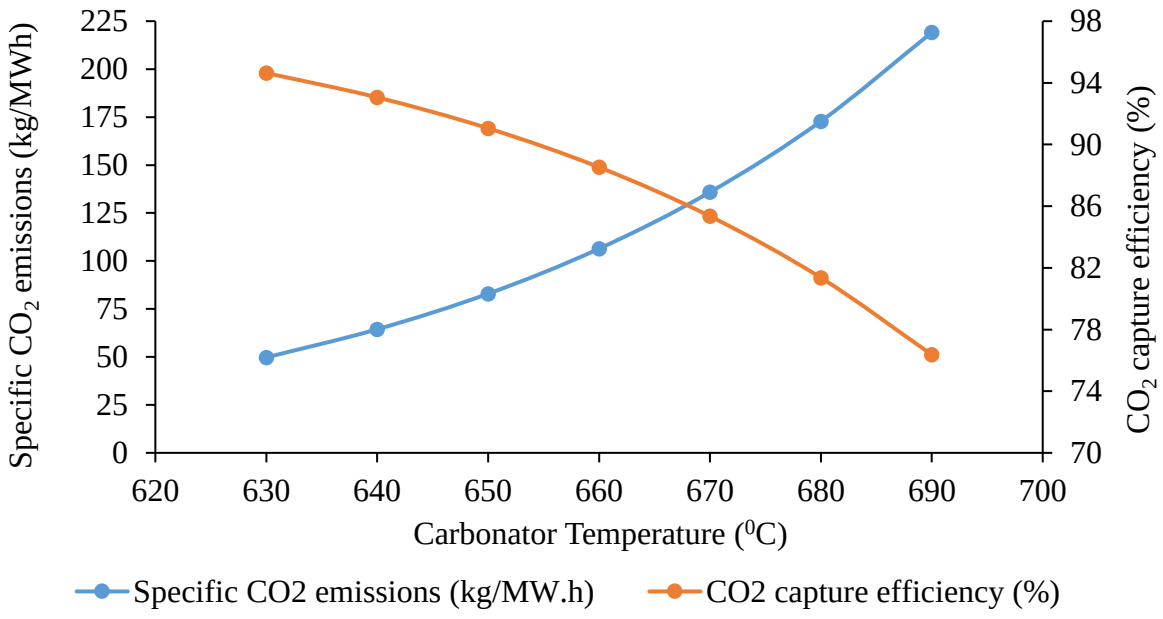

(A)

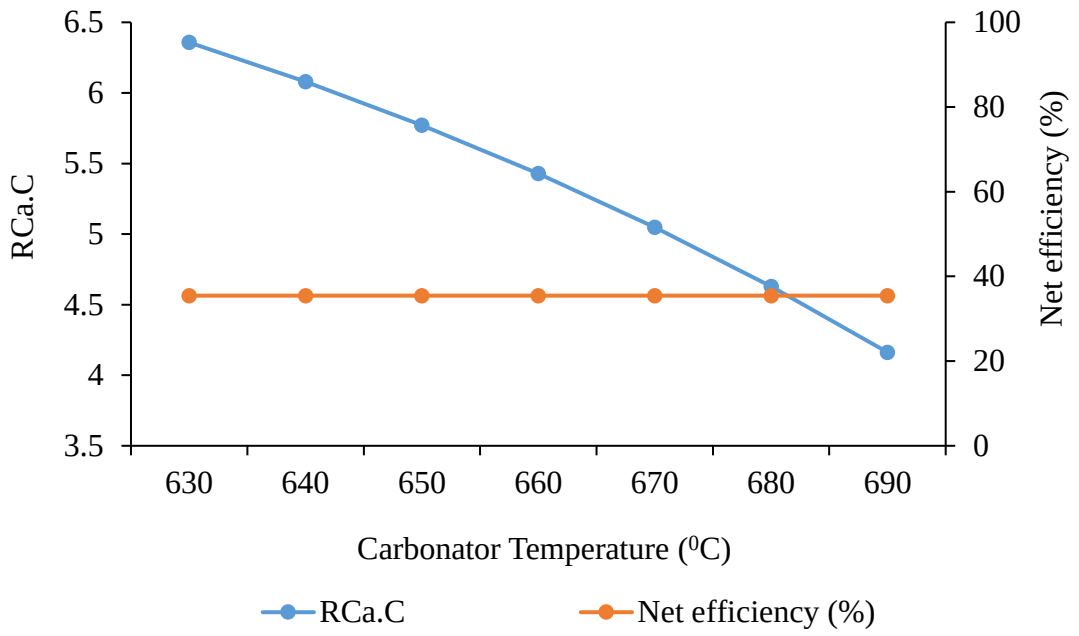

(B)

Fig. 4.9 Effect of carbonator temperature on (A) specific CO_2 emissions and CO_2 capture efficiency (B) net energy efficiency and CaO circulation rate per unit of CO_2 in flue gas

4.2.4.2 Effect of isentropic efficiency of steam turbines on the performance of CFPP3

The relationship between the net energy efficiency, net exergy efficiency and specific CO_2 emission for different values of isentropic steam turbine efficiencies is presented in Fig. 4.10. The results indicate that the net energy efficiency and net exergy efficiency increases in a linear proportion with respect to the isentropic efficiency of steam turbines. The highest energy and exergy efficiency were found to be 36.73% and 33.61% at an isentropic steam turbines efficiency of 94% while lowest energy and exergy efficiency were found to be 31.41% and 28.74% at an isentropic steam turbine efficiency of 74%. It also shows that with the increase in work output, the specific CO_2 emissions also decrease steadily.

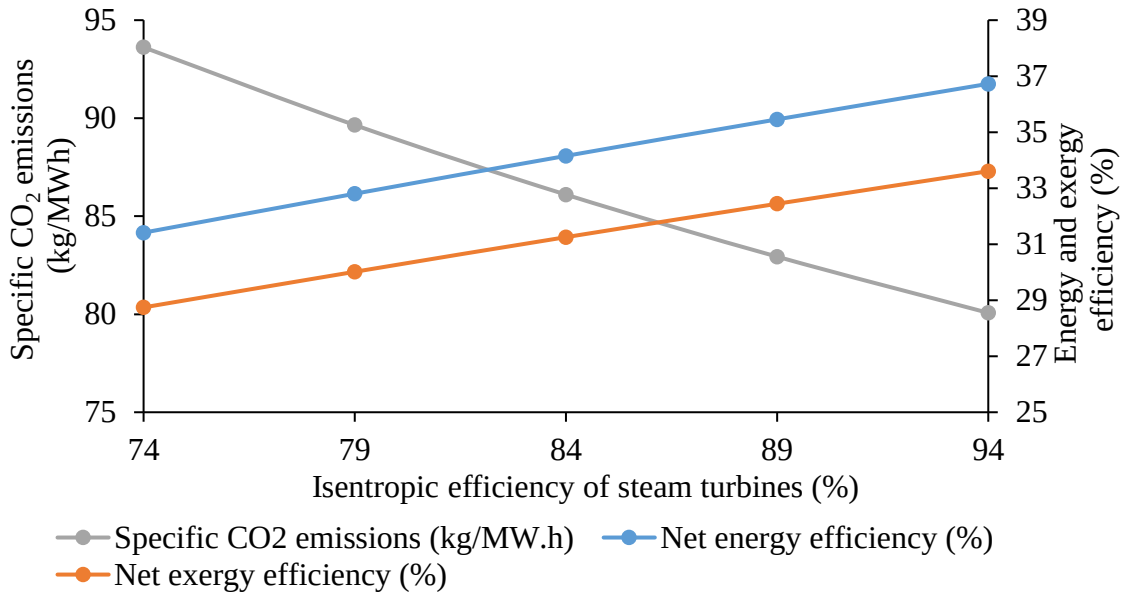

Fig. 4.10 Effect of isentropic efficiency of steam turbines on specific CO_2 emission, net energy and exergy efficiency

The specific CO_2 emission ranges between 80.07 kg/MWh and 93.32 kg/MWh indicates the possible amount of CO_2 emission reduction per unit of electricity generation that can be attained between a range of 74% and 94% of isentropic steam turbine efficiency. Thus, the results reveal that with the increase in isentropic efficiency of steam turbines, the thermal losses of the steam turbines were reduced and hence lead to higher efficiency (Rahman et al., 2011) and lower specific CO_2 emissions. Implementation of certain modifications in steam turbines as reported in the literature (Bhatt., 2011; Lee et al., 2017) can provide an option to enhance this isentropic efficiency of steam turbines and to improve the overall performance of CFPP3.

4.2.4.3 Effect of condenser pressure on the performance of CFPP3

The variation in the performance of CFPP3 with respect to the change in condenser pressure is illustrated in Fig. 4.11. Net energy efficiency, net exergy efficiency, specific CO_2 emission and the net electrical energy consumption of the power plant were taken as main parameters for this analysis. It should be noted that when the condenser pressure was changed, the total heat input and mass flowrate of water/steam remains constant.

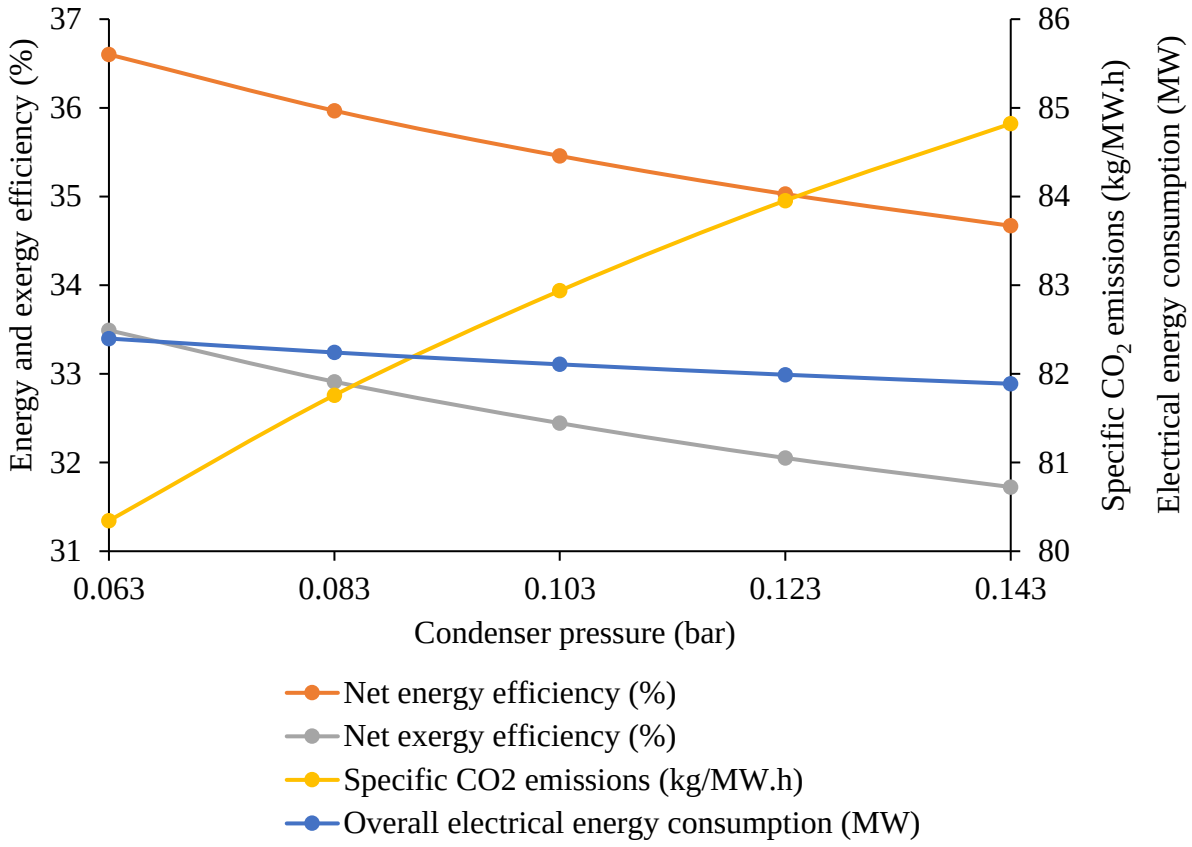

Fig. 4.11 Effect of condenser pressure on specific CO_2 emission, net energy efficiency, net exergy efficiency and electrical energy consumption

The observation from Fig. 4.11 indicates that the electrical energy consumption increases from 81.89 MW to 82.40 MW with the reduction in condenser pressure. This was due to the higher energy consumption of the pumps to maintain the constant pressure required. However, the result also reveals the simultaneous increase in net energy efficiency from 34.67% to 36.60% and net exergy efficiency from 31.72% to 33.49% with the decrease of condenser pressure. The main reason for this was because of the higher steam expansion in turbines that ultimately leads to higher net work output. The specific CO_2 emission was also calculated at various values of condenser pressure considered for this parametric analysis. The highest specific CO_2 emission of 84.82 kg/MWh was observed at a condenser pressure of 0.143 bar while the lowest specific CO_2 emission of 80.34 kg/MWh was observed at a condenser pressure of 0.063 bar.

4.3 Performance assessment of calcium looping integrated natural gas fired combined cycle power plants

In this section, the performance of the proposed NGFCPP3 and NGFCPP2 configurations are compared with dual NGFCPP1. A framework for evaluating all the developed configurations was built on the basis of energy, exergy, environmental and cost analyses. A primary objective of this study is to come up with an efficient calcium looping integrated natural gas fired combined cycle power plant for CO_2 capture and electricity generation. The identified efficient natural gas fired combined cycle power plant configuration is further studied using sensitivity analyses to see the effect of carbonator reactor temperature, isentropic efficiency of gas turbine and condenser pressure on the plant performance.

4.3.1 Plant performance

The results from the performance assessment based on the overall energy, exergy and environmental parameters were analyzed and discussed in this sub-section. Table 4.8, Table 4.9 and Table 4.10 represent the overall comparative evaluation of all the developed power plant configurations. The environmental reference state taken for the study is 1.013 bar and 33 ^{0}C. The result in Table 4.8 and Table 4.9 shows that the amount of energy and exergy input supplied to all the three power plant configurations were same i.e., 551.88 MW and 584.99 MW. A significant amount of energy i.e., 205 MW in case of NGFCPP1 and 102 MW in case of NGFCPP2 and NGFCPP3 is consumed by the air compressor of GPGU's. The net energy and exergy efficiency of NGFCPP3 (without CU) was found to be 31.69 % and 29.90 % as compared to the energy and exergy efficiency of NGFCPP1 having an energy and exergy efficiency of 36.24 % and 34.19 %. Similarly, the NGFCPP2 having an energy and exergy efficiency of 30.22 % and 28.51 % was also found to be lower than NGFCPP1. The lower energy and exergy efficiency of NGFCPP3 and NGFCPP2 as compared to NGFCPP1 was mainly due to the replacement of a GPGU by calcium looping based CO_2 capture unit. The GPGU that works on the basis of the Brayton cycle is generally more energy efficient than SPGU that works on the basis of Rankine cycle (Layton et al., 2012). Thus, the replacement of GPGU with CCaLU or DCaLU resulted in low electrical energy production in the integrated power plants.

Table 4.8 Plant performance of NGFCPP1, NGFCPP2 and NGFCPP3 on energy basis

Parameters	NGFCPP1	NGFCPP2	NGFCPP3	
			Without CU	With CU
Energy input from natural gas combustion (MW)	551.88	551.88	551.88	551.88
Gross power output (MW)	446.16	305.09	305.09	305.09
Electricity consumption by compressor of GPGU (MW)	205	102.5	102.5	102.5
Total electricity consumption (MW)	246.14	138.32	131	131
Electricity consumption by CU (MW)				12.04
Net power output (MW)	200.02	166.77	174.89	162.85
Net energy efficiency (%)	36.24	30.22	31.69	29.51
Energy efficiency penalty (%)		6.02	4.55	6.73

It was also observed that the NGFCPP3 (without CU) has less energy and exergy penalty of 4.55% and 4.29% as compared to the NGFCPP2 having an energy and exergy penalty of 6.02% and 5.68%. This is because of the elimination of the ASS in NGFCPP3 that consumes a considerable amount of electricity produced by the power plant. Thus, the result reveals that the proposed integration strategy in NGFCPP3 holds a higher degree of energy utilization as compared to the NGFCPP2. Since the CO_2 compression is an essential process for carbon sequestration, the energy and exergy efficiency were also calculated for the NGFCPP3 by integrating a CU. The results revealed that the energy and exergy penalty of NGFCPP3 (with CU) were 6.73% to 6.35%. Therefore, a better energy integrating strategy needs to be identified to further reduce the energy consumption of CU.

Table 4.9 Plant performance of NGFCPP1, NGFCPP2 and NGFCPP3 on exergy basis

Parameters	NGFCPP1	NGFCPP2	NGFCPP3	
			Without CU	With CU
Exergy input from natural gas combustion (MW)	584.99	584.99	584.99	584.99
Gross power output (MW)	446.16	305.09	305.09	305.09
Electricity consumption by compressor of GPGU (MW)	102.5	102.5	102.5	102.5
Total electricity consumption (MW)	246.14	138.32	131	131
Electricity consumption by CU (MW)				12.04
Net power output (MW)	200.02	166.77	174.89	162.85
Net exergy efficiency (%)	34.19	28.51	29.90	27.84
Exergy efficiency penalty (%)		5.68	4.29	6.35

The environmental analysis in terms of CO_2 emissions for all configurations was given in Table 4.10. The result shows that at the same carbonator reactor temperature (600 ^{0}C), the overall CO_2 capture efficiency and specific CO_2 emissions in NGFCPP2 were 93.9% and 41.45 kg/MWh as compared to NGFCPP2, having a CO_2 capture efficiency and specific CO_2 emissions of 91.3% and 57.02 kg/MWh. This correspondingly results in the lifetime CO_2 emission of 1210982.4 Mg in NGFCPP2 and 1747094.4 Mg in NGFCPP3. However, the CO_2 obtained as the end product in NGFCPP3 was 99.9% pure when compared to 96.8% CO_2 purity in the case of NGFCCPP2.

Table 4.10 Plant performance of NGFCPP1, NGFCPP2 and NGFCPP3 based on environmental analysis

Environmental performance indicators	NGFCPP1	NGFCPP2	NGFCPP3	
			Without CU	With CU
Total amount of CO_2 generated in the power plant (kg/s)	31.92	31.72	31.92	31.92
Total amount of captured by the calcium looping unit (kg/s)		29.8	29.15	29.15
CO_2 capture efficiency (%)		93.9	91.32	91.32
Purity of captured CO_2 (%)		96.8	99.99	99.99
Specific CO_2 emission (kg/MWh)	574.51	41.45	57.02	61.23
Annual CO_2 emission (kg x 10^3)	805303.3	48439.3	69883.78	69883.78
Lifetime CO_2 emission of the power plant (kg x 10^3)	20132582.4	1210982.4	1747094.4	1747094.4

4.3.2 Exergy analysis of major units

In this analysis, the exergy efficiency, exergy destruction and exergetic improvement potential were taken as the main parameters to identify the location of efficiency losses and to determine the maximum scope of improvement possible in the NGFCPP3 configuration. The exergetic efficiency, exergy destruction and improvement potential of all the units in NGFCPP3 configuration are presented in Fig. 4.12. It was observed that the highest exergetic destruction was associated with DCaLU, which holds the highest exergetic destruction of 43%. This includes 30% and 13% of exergy destruction in combustor and calcium looping system respectively. Followed by this, the second highest exergy destruction of 34%, was found in the GPGU2. A major reason for the high exergy losses in these units are due to chemical reaction irreversibility in combustors

and reactors and the excess air supplied to the power plant. The CU having the lowest exergy destruction of 2% signifies that the thermal losses were significantly lower than other units.

The exergy analysis also helps to quantify the energy savings by calculating the exergetic efficiency and improvement potential. The calculated exergy efficiency and improvement potential for the proposed configuration are presented in Fig. 4.12B. The results indicate that the SPGU has exergetic efficiency of 75.22%, which was highest compared to all individual units. This shows that the SPGU effectively converts thermal energy into electrical energy with minimal exergy destruction. However, the exergetic improvement potential of 19.6 MW indicates that a considerable amount of energy can be recovered from the SPGU. On the other hand, besides having the lowest exergy efficiency of 54.2%, the CU has a very low exergetic improvement potential compared to other units because of its significantly less energy intensive operation requirement. The result also quantifies the maximum potential of improvement in the NGFCPP3 that can be explored in the DCaLU and GPGU2. The exergetic improvement potential of DCaLU and GPGU2 was found to be 70.71 MW and 43.66 MW respectively.

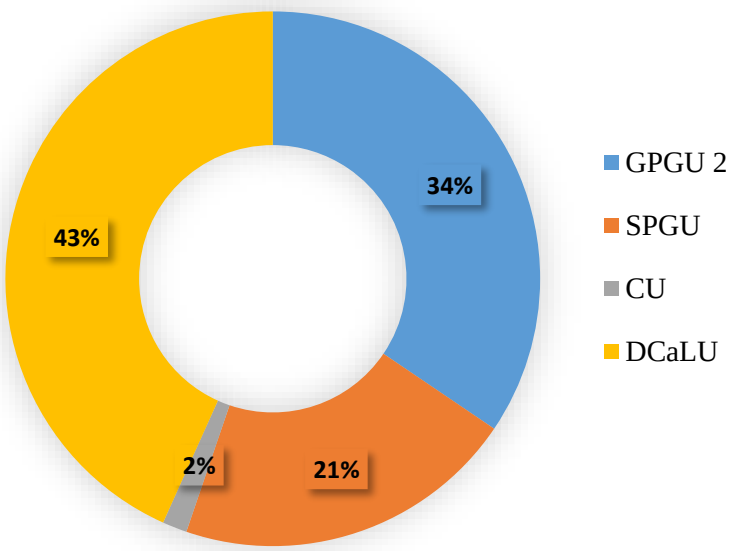

(A)

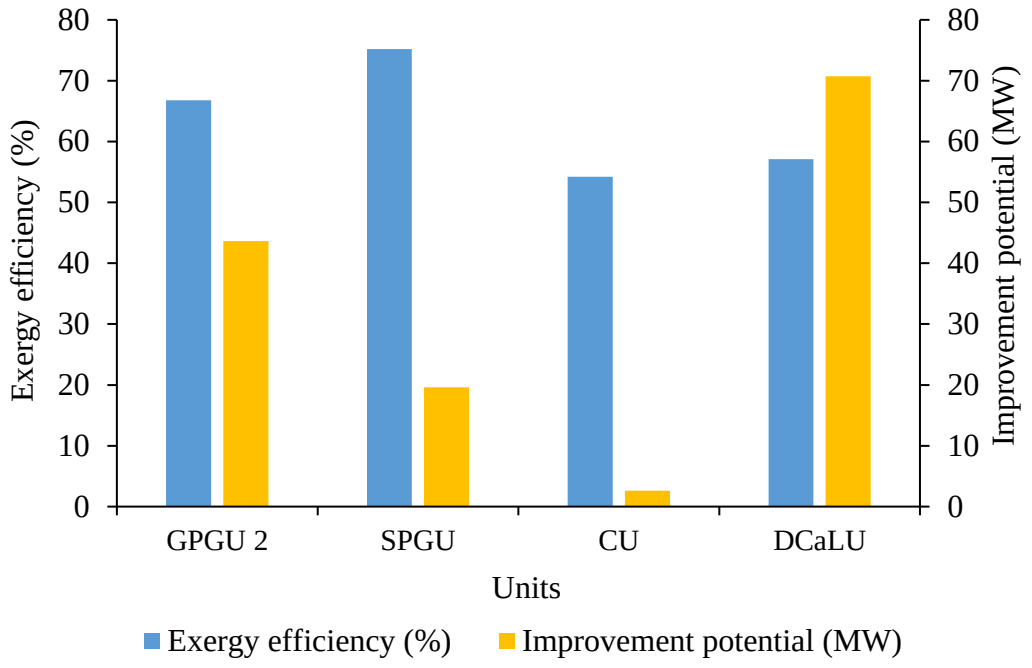

(B)

Fig. 4.12 Distribution of (A) Exergy destruction (B) Exergy efficiency and improvement potential in NGFCPP3

4.3.3 Cost and exergoeconomic analysis

The cost analysis plays a very vital role in determining the operational feasibility of the power plants. The TCR, LCOE and CA were used as main performance indicators to analyze the comparative assessment of the developed configurations from a cost perspective. The outcome of cost analysis in terms of these estimated performance indicators is presented in Table 4.11.

The result indicates that with the integration of DCaLU and CCaLU, the TCR in the NGFCPP3 and NGFCPP2 configurations increases to 866.97 M€ and 976.19 M€ as compared to NGFCCPP1 having a TCR of 262.36 M€. The higher TCR of NGFCPP2 compared to the NGFCCPP3 was because of the cost incurred by the ASS integrated into the NGFCPP2. The LCOE and LPCD were also calculated for the proposed configurations and compared as shown in Table 4.11. The results reveal that the NGFCPP2 configuration has higher LCOE and CA of 143.12 €/MWh and 0.19 €/kg as compared to the NGFCPP3 having a LCOE of 129.11

€/MWh and 0.16 €/kg. This shows that the NGFCPP3 is economically more competitive than NGFCPP2 from the electricity generation from the CO_2 mitigation perspective. Furthermore, the LCOE of NGFCPP3 as compared to NGFCPP1 is quite high. This is primarily due to the addition of DCaLU in place of GPGU1. As a result of this modification, more capital was required and an energy penalty was incurred, but at the same time, 91% of the CO_2 generated during combustion was captured.

Table 4.11 Cost performance indicators of NGFCPP1, NGFCPP2 and NGFCPP3

Cost parameters	NGFCPP1	NGFCPP2	NGFCPP3
TCR (M€)	262.36	976.19	866.97
LCOE (€/MWh)	44.95	143.12	129.11
CA (€/kg)		0.19	0.16

The results from exergoeconomic analysis of NGFCPP3 configuration as shown in Fig. 4.13 reveal that the HRSG1, HRSG2 and cooling water system with BOP unit have exergoeconomic factors of 20.47%, 17.61% and 17.16% respectively.

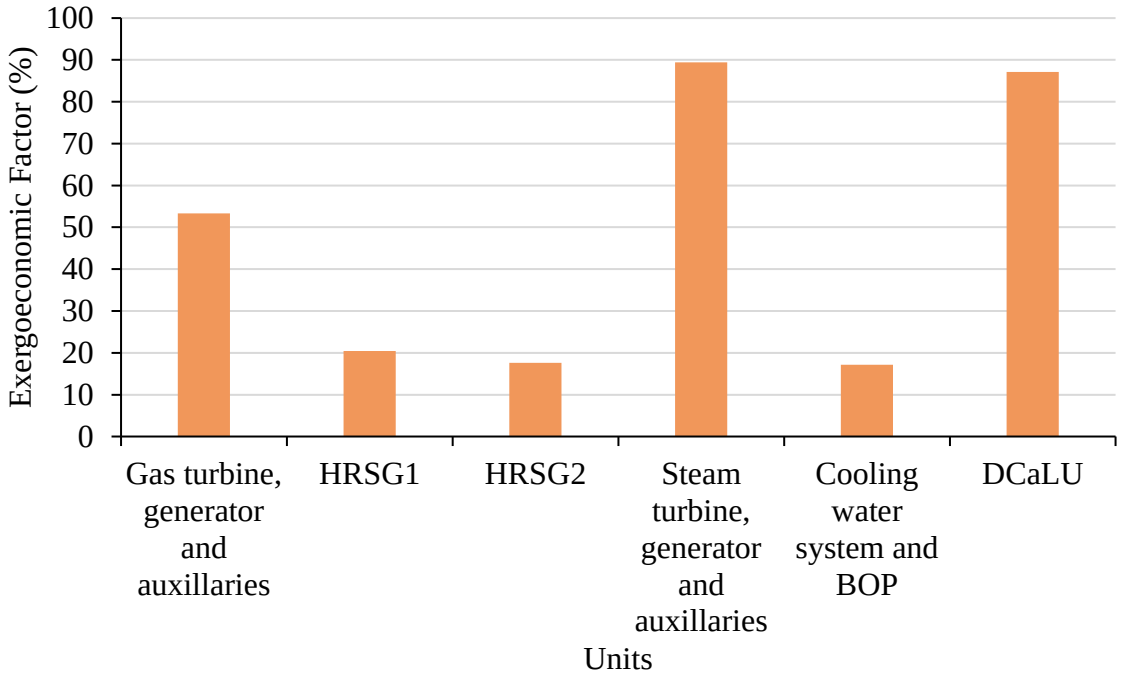

Fig. 4.13 Exergoeconomic factor of different units in NGFCPP3

Thus, reducing energy destruction in these units can result in an increase in capital expenditure savings. On the other hand, the exergoeconomic factor of 89.42% and 87.13% in steam turbine, generator and auxiliaries and DCaLU correspondingly indicates that the necessary studies are needed to be carried out to reduce its relevant expenditure. The gas turbine, generator and auxiliaries with an exergoeconomic factor is nearly 50% reveals that neither the capital cost of the unit nor cost of the exergy destruction are dominating to each other.

4.3.4 Sensitivity analysis

A sensitivity analysis in NGFCPP3 was carried out to assess the performance of the plant by varying the carbonator temperature, condenser pressure and isentropic efficiency of the turbines. The results obtained from these sensitivity analyses were discussed in this section.

4.3.4.1 Effect of carbonator reactor temperature on the performance of NGFCPP3

The carbonator reactor temperature was varied and its outcome on the performance of NGFCPP3 was analyzed by observing its effect on specific CO_2 emissions, CO_2 capture efficiency, RCa.C and net energy efficiency. Fig. 4.14A shows the variation of specific CO_2 emission and CO_2 capture efficiency with respect to the carbonator reactor temperature. The results indicate that as the carbonator reactor temperature was increased from 580 ^{0}C to 640 ^{0}C, the CO_2 capture efficiency was reduced from 94.88% to 74.22%. On the other hand, the specific CO_2 emission increased considerably from 32.30 kg/MWh to 165.72 kg/MWh. This behaviour in carbonator temperature was due to the inhibition of carbonation reaction with the increase in temperature (Charitos et al., 2010; Yin et al., 2015).

Fig. 4.14B illustrates the variation of RCa.C and net energy efficiency with respect to the carbonator reactor temperature. The net energy efficiency was found to be nearly constant at 31.69% with the variation of carbonator reactor temperature. This reveals that the net energy efficiency of NGFCPP3 (without CU) is an independent parameter with respect to the change in carbonator temperature. The variation of RCa.C indicates the CaO sorption rates with respect to the carbonator reactor temperature. The highest RCa.C, i.e., 23.77, was found to be at the carbonator reactor temperature of 580 ^{0}C, while the lowest RCa.C, i.e., 7.06 was found to be at the carbonator reactor temperature of 640 ^{0}C.

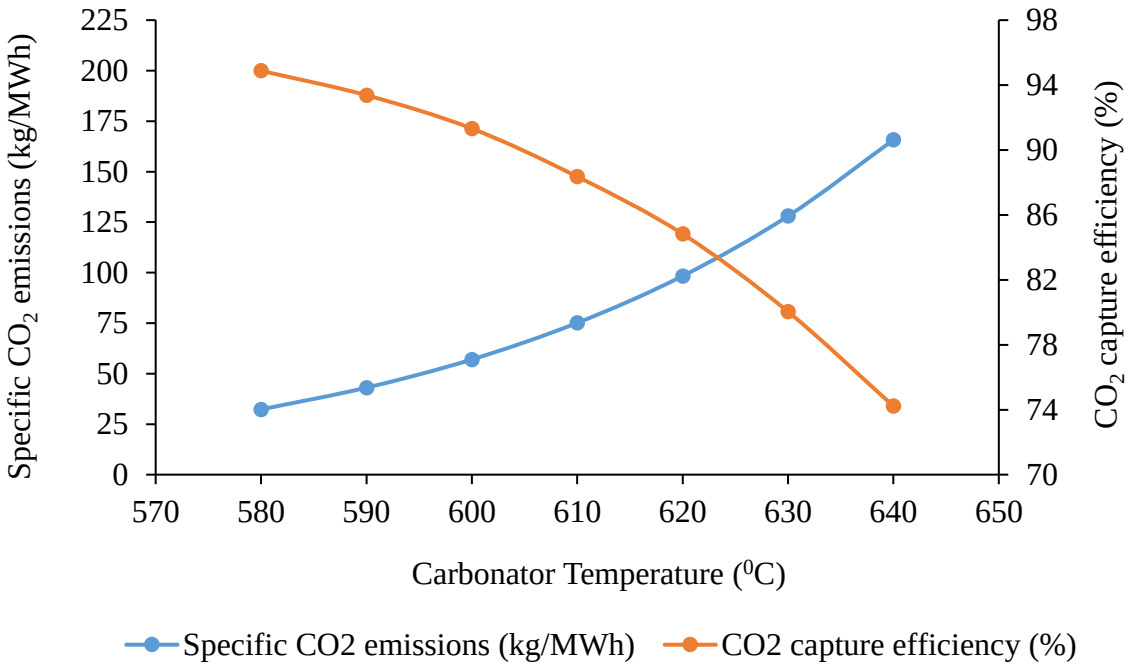

(A)

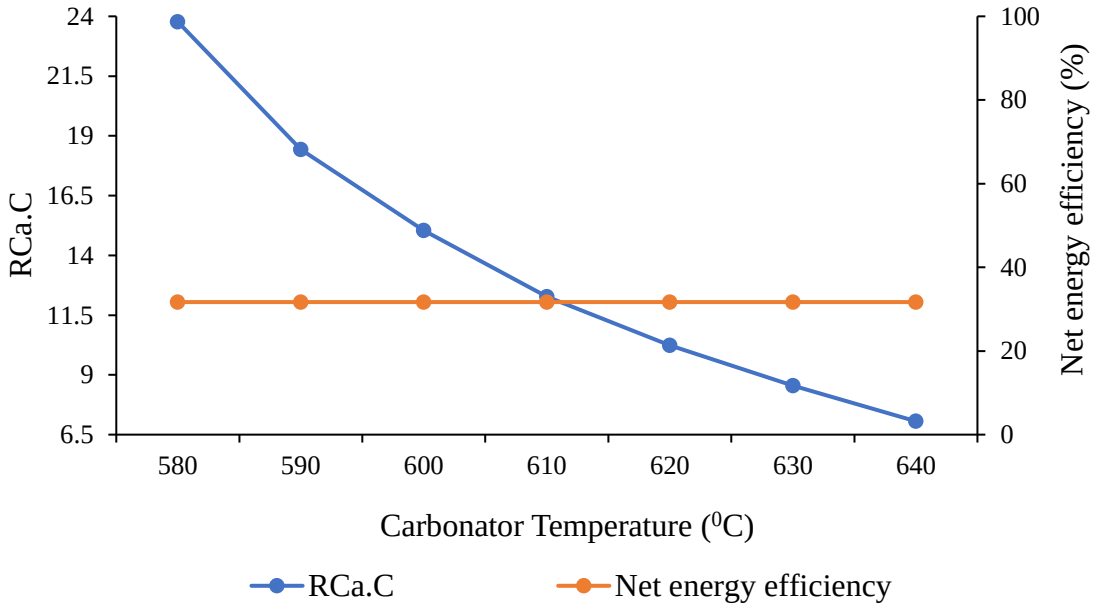

(B)

Fig. 4.14 Effect of carbonator temperature on (A) specific CO_2 emissions and CO_2 capture efficiency (B) net energy efficiency and CaO circulation rate per unit of CO_2 in flue gas

4.3.4.2 Effect of isentropic efficiency of gas turbine on the performance of NGFCPP3

The variation of net energy efficiency, net exergy efficiency and specific CO_2 emission for different values of isentropic gas turbine efficiency is presented in Fig. 4.15. The results indicate that the net energy efficiency and net exergy efficiency increases in a linear proportion with respect to the isentropic efficiency of gas turbine. The highest energy and exergy efficiency were found to be 35.05% and 33.07% at an isentropic gas turbine efficiency of 91% while lowest energy and exergy efficiency were found to be 28.33 % and 26.72 % at an isentropic gas turbine efficiency of 71%. The results reveal that with the increase in isentropic efficiency of gas turbines, the thermal losses of the gas turbine reduce and thus lead to higher work output and efficiency. It also shows that with the increase in work output, the specific CO_2 emission also decreases steadily. The specific CO_2 emission ranges between 63.79 kg/MWh and 51.55 kg/MWh indicates the possible amount of CO_2 emission reduction per unit of electricity generation that can be attained between a range of 71% and 91% of isentropic gas turbine efficiency. Improving the geometry of gas turbine's casing and blade are some of the ways that can enhance the isentropic efficiency of gas turbines (Kadhim et al., 2018; Pakatchian et al., 2015)

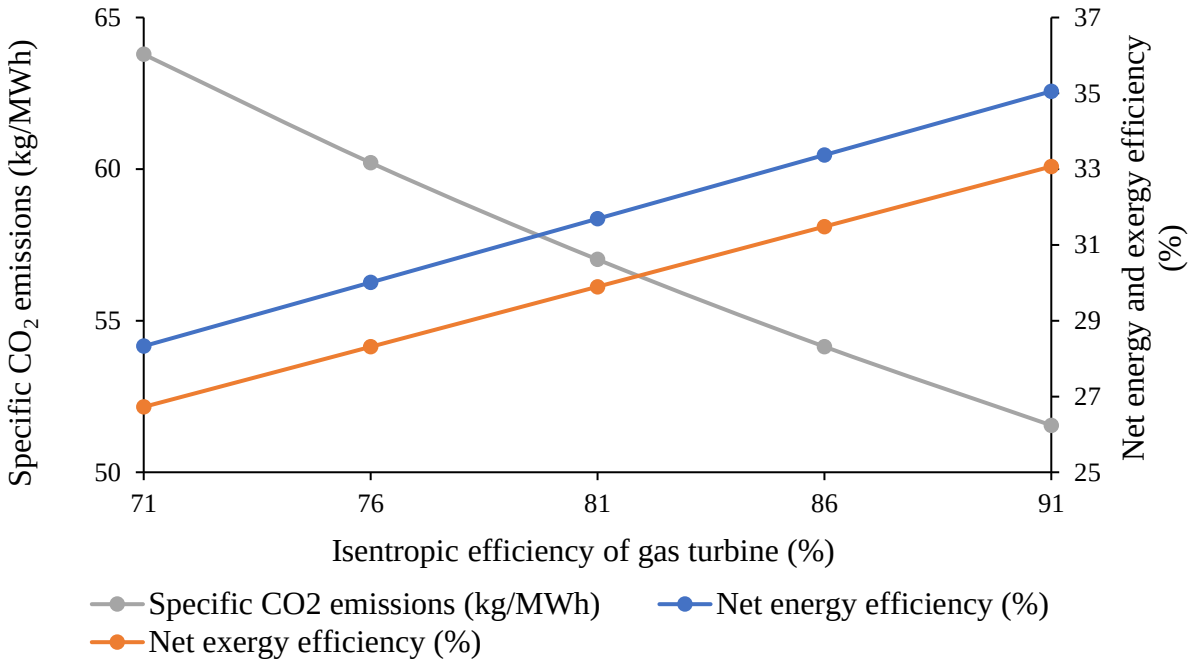

Fig. 4.15 Effect of isentropic efficiency of gas turbine on specific CO_2 emission, net energy and exergy efficiency

4.3.4.3 Effect of condenser pressure on the performance of NGFCPP3

The variation in the performance of NGFCPP3 with respect to the change in condenser pressure is illustrated in Fig. 4.16. The net energy efficiency, net exergy efficiency, specific CO_2 emission and the net electrical energy consumption of the power plant were taken as the main parameters for this analysis. It should be noted that when the condenser pressure was changed, the total heat input and mass flowrate of water/steam was kept constant. The result reveals that the net energy efficiency increases from 30.82 % to 32.94 % and net exergy efficiency from 29.08 % to 31.07 % with the decrease of condenser pressure. The main reason for this is the higher gas expansion in turbines that ultimately leads to higher net work output. The specific CO_2 emission was also calculated at various values of condenser pressure considered in this parametric analysis. The highest specific CO_2 emission of 58.62 kg/MWh was observed at a condenser pressure of 0.143 bar, while the lowest specific CO_2 emission of 54.86 kg/MWh was observed at a condenser pressure of 0.063 bar.

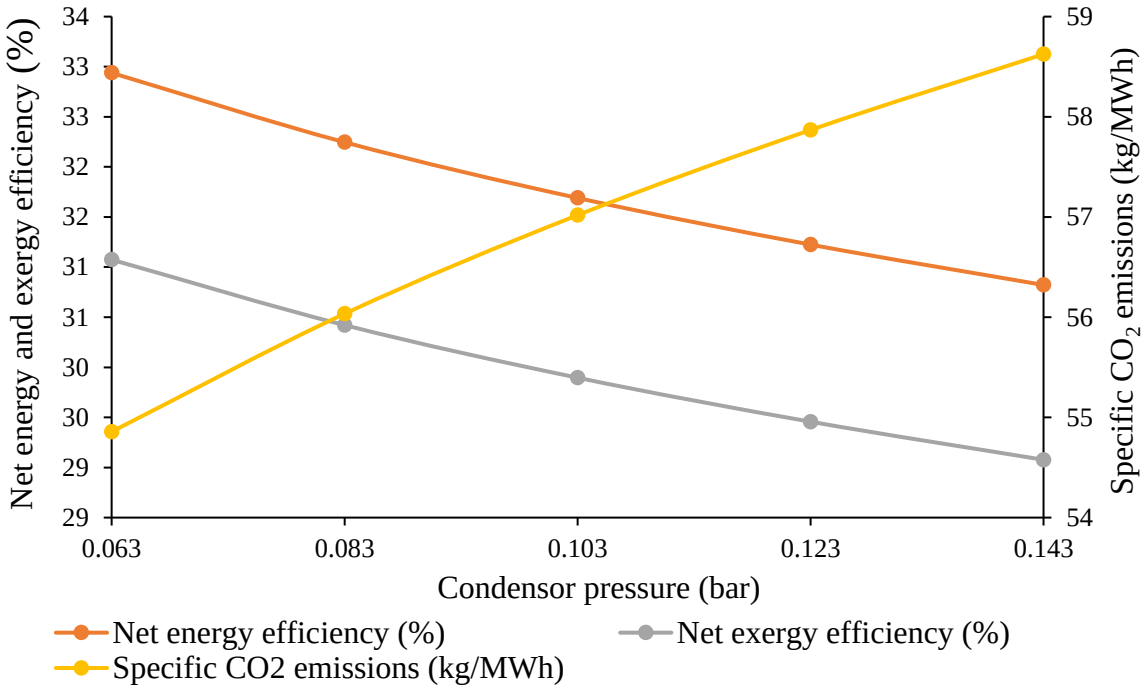

Fig. 4.16 Effect of condenser pressure on specific CO_2 emission, net energy efficiency and net exergy efficiency

4.4 Performance assessment of H_2 production unit coupled with calcium looping integrated coal fired power plant (HCFPP1 and HCFPP2)

In this section, the performance of the proposed single and double calcium looping integrated coal fired power plants (referred as HCFPP1 and HCFPP2 respectively) for cogeneration were analyzed on the basis of overall energy, exergy and environmental parametric indicators. Table 4.12 and Table 4.13 represent the overall comparative evaluation of the two developed power plant configurations on energy and exergy basis while Table 4.14 represents the same on environmental basis. The environmental reference state taken for the study is 1.013 bar and 33 ^{0}C. The results in Table 4.12 and Table 4.13 show that the amount of energy and exergy input supplied to both the power plant configurations were same i.e., 1511.45 MW and 1651.08 MW.

Table 4.12 Plant performance of HCFPP1 and HCFPP2 on energy basis

Parameters	HCFPP1	HCFPP2	
		Without CU	With CU
Energy input from coal combustion (MW)	1511.45	1511.45	1511.45
Gross power output (MW)	570.26	570.37	570.37
Total Electricity consumption (MW)	137.54	94.06	94.06
Electricity consumption by CU (MW)			55.30
Net power output (MW)	432.72	476.31	421.02
Energy obtained from the generated H_2	89.18	89.18	89.18
Net electrical efficiency (%)	28.63	31.51	27.86
Overall energy efficiency (%)	34.53	37.41	33.76
Overall energy gain(-) or penalty(+) (%)		-2.88	0.77

The results reveal that net electrical power output in HCFPP1 and HCFPP2 was found to be 432.72 MW and 476.31 MW respectively. The higher net electrical power output in HCFPP2 was mainly due to the elimination of ASS in the process of CO_2 capture as compared to the HCFPP1. The overall net energy and exergy efficiency of HCFPP2 (without CU) was found to be 37.41% and 34.16%. The HCFPP1 has an overall energy and exergy efficiency of 34.53% and 31.52%. As compared to the performance of HCFPP1 configuration without CU, the HCFPP2 configuration without CU has net energy and exergy gain of 2.88% and 2.64% and the same configuration with integration CU has net energy and exergy penalty of 0.77% and 0.71%. Thus, the results reveal that the proposed strategy in HCFPP2 holds a superior degree of energy utilization when integrated with calcium looping gasification based H_2 production unit as compared to the HCFPP1 configuration.

Table 4.13 Plant performance of HCFPP1 and HCFPP2 on exergy basis

Parameters	HCFPP1	HCFPP2	
		Without CU	With CU
Exergy input from coal combustion (MW)	1651.08	1651.08	1651.08
Gross power output (MW)	570.26	570.37	570.37
Total electricity consumption (MW)	137.54	94.06	94.06
Electricity consumption by CU (MW)			55.30
Net power output (MW)	432.72	476.31	421.02
Exergy obtained from the generated H_2	87.99	87.99	87.99
Net electrical efficiency (%)	26.20	28.84	25.49
Overall exergy efficiency (%)	31.52	34.16	30.82
Overall exergy gain(-) or penalty(+) (%)		-2.64	0.71

Since the foremost objective of any CO_2 capture system is to lower the CO_2 emissions significantly, an analysis as shown in Table 4.14 was also carried out to assess the performance of

the proposed configuration on environmental basis. It was assumed that both power plant configurations have an overall plant life period of 25 years and operate 7008 hours annually. The carbonator reactor temperature in both HCFPP1 and HCFPP2 configurations was adjusted to capture around 91.05% of CO_2 generated in the overall plant. From the environmental analysis, it was observed that the specific CO_2 emission of HCFPP1 was higher i.e., 85.11 kg/MWh as compared to HCFPP2 (without CU) that was having a specific CO_2 emission of 78.57 kg/MWh. The purity of CO_2 obtained from the HCFPP1 configuration was also found to be low, i.e., 83.76% as compared to HCFPP2 configuration having a CO_2 purity of 97.2%.

Table 4.14 Plant performance of HCFPP1 and HCFPP2 based on environmental analysis

Environmental performance indicators	HCFPP1	HCFPP2	
		Without CU	With CU
Total CO_2 generated from overall power plant (kg/s)	137.9	137.9	137.9
Total amount of CO_2 captured by the plant (kg/s)	125.54	125.56	125.56
CO_2 capture efficiency (%)	91.05	91.05	91.05
Purity of captured CO_2 (%)	83.76	97.20	97.20
Specific CO_2 emission (kg/MWh)	85.11	78.57	87.09

4.4.1 Exergy analysis of major units

The exergy analysis was performed to investigate the efficiency losses due to thermodynamic irreversiblities in the major units of the HCFPP2 configuration. The analysis not only identifies the location of efficiency losses but also helps to determine the maximum scope of improvement possible in the system. The exergetic efficiency, exergy destruction and improvement potential of different units in HCFPP2 configuration are presented in Fig. 4.17 and Fig. 4.18. The results show that the most energy intensive operational units of the configuration were DCaLU, SPGU and H_2 Production Unit (HPU) having an exergy destruction of 76.24%, 9.42% and 7.84%. In DCaLU, the combustor accounts an exergy destruction of 54.43% and

calcium looping system holds an exergy destruction of 21.8%. On the other hand, the exergy efficiency of the same units was found to be 63.57%, 93.56% and 73.49% respectively.

This reveals that while the SPGU and HPU were converting the input thermal energy into useful work more effectively than DCaLU. A major reason for this exergy destruction is because of the irreversiblities of the chemical reactions that occur in the combustor and the reactors of calcium looping unit (Wang et al., 2013; Som et al., 2008). Thus, the highest percentage of improvement potential of 81.92% as shown in Fig. 4.18B was found to be in the DCaLU only. It was observed from Fig. 4.17 and Fig. 4.18A that the SPGU has the highest exergetic efficiency of 93.56% and an exergy destruction of 9.42% only. This reveals that the SPGU is converting a considerable amount of its input thermal energy into useful work. The results also indicate that the air preheater (HE3), CU and H_2 Compression Unit (HCU) although holds quite lower exergetic efficiency of 42.43%, 51.33% and 50.74% as compared to other units, a scope of minimum exergetic improvement potential of 5.33%, 3.64% and 1.16% was observed.

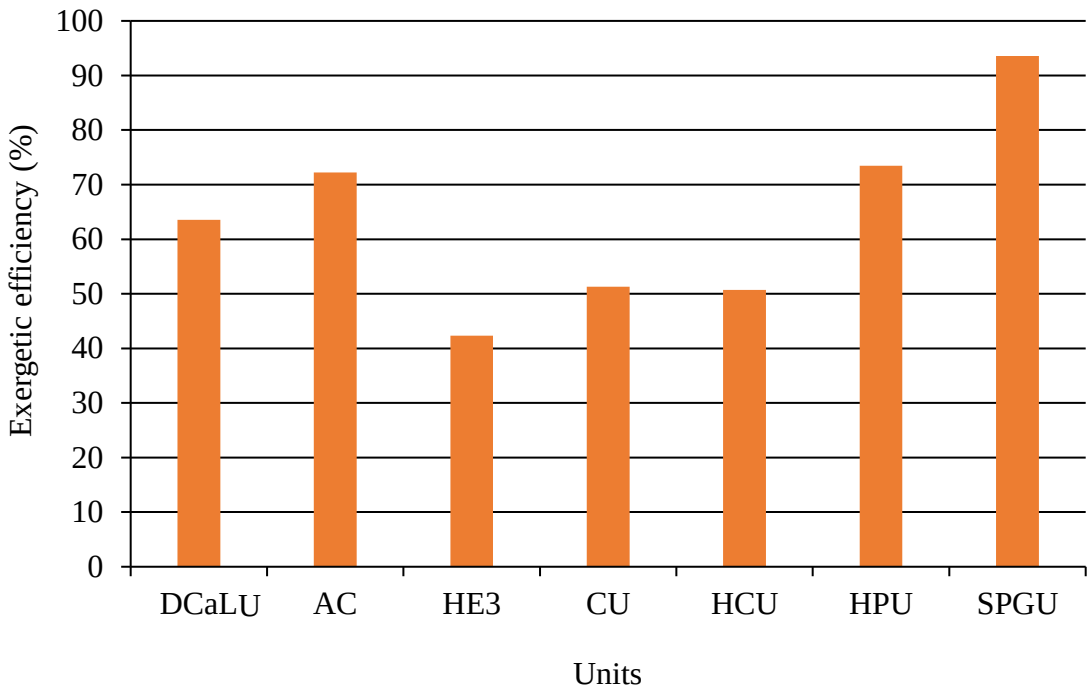

Fig. 4.17 Exergy efficiency of main units in HCFPP2

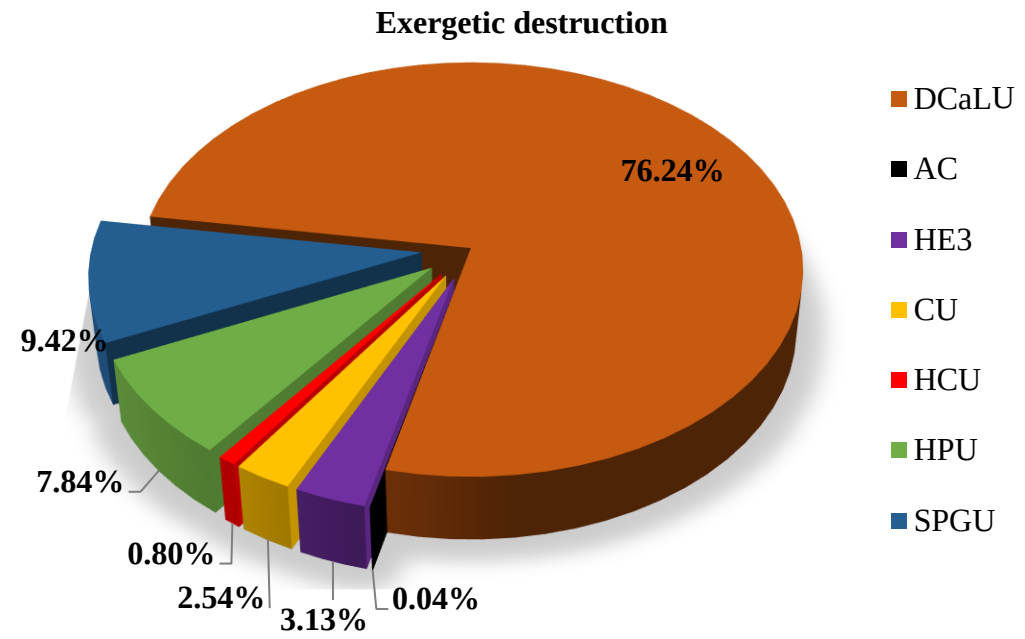

(A)

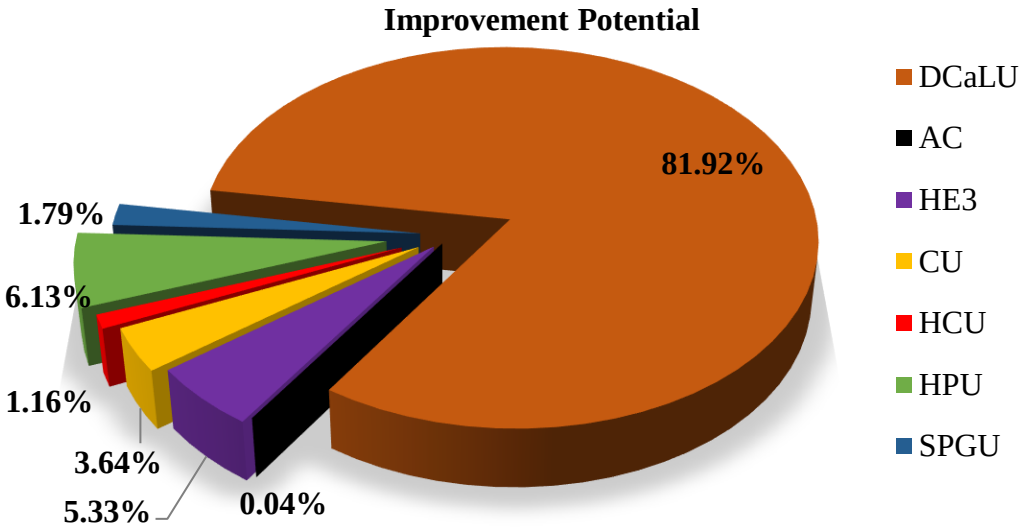

(B)

Fig. 4.18 (A) – Distribution of exergy destruction, (B) – Improvement potential in HCFPP2

4.4.2 Cost and exergoeconomic analysis

Having exhibited the energy, exergy and environmental competitiveness of the HCFPP1 and HCFPP2, it is essential to benchmark their cost performance indicators as well. The calculated cost indicators for both the configurations are presented in Table 4.15. The comparative assessment of HCFPP1 and HCFPP2 reveals that the TCR of HCFPP2 was 1074.28 M€ as compared to the TCR of HCFPP1 i.e., 1170.61 M€. The higher capital requirement of the HCFPP1 was because of the ASS unit that accounts for around 18% of the TCR. It has been observed from the literature that the LCOE of ammonia and amine based CO_2 capture system when integrated with coal power plant were around 95 €/MWh and 105 €/MWh respectively (Versteeg and Rubin., 2011; Mantripragada and Rubina., 2014). In this aspect, the LCOE of HCFPP1 and HCFPP2 were found to be 69.40 €/MWh and 58.51 €/MWh only. The estimated cost of H_2 from the plant was determined on the basis of LPCH. The results revealed that the LPCH of HCFPP2 was 2.11 €/kg only as compared to HCFPP1 having a LPCH of 2.34 €/kg. The overall results obtained from the analysis reveals that the HCFPP2 is economically superior to HCFPP1.

The exergoeconomic factor evaluated for all the units in HCFPP2 was shown in Fig. 4.19. The results indicate that the HCU with the lowest exergoeconomic factor of 10.91% holds the higher potential of cost savings by reducing the cost of exergy destruction rate. Similar performance was observed for the cooling water system and BOP. The HPU holds an exergoeconomic factor of 51.91% and shows that cost of exergy destruction and capital investment rate also almost in balance with each other. The high exergoeconomic factor of 93.16%, 92.53% and 67.90% in the corresponding steam turbine, generator and auxiliaries, calcium looping plant and high and low pressure steam exchangers reveals that although the exergy destruction in these units is high, the cost of operation and maintenance is even higher.

Table 4.15 Cost performance indicators of HCFPP1 and HCFPP2

Parameters	HCFPP1	HCFPP2
TCR (M€)	1170.61	1074.28
LCOE (€/MWh)	69.40	58.51
LPCH (€/kg)	2.34	2.11

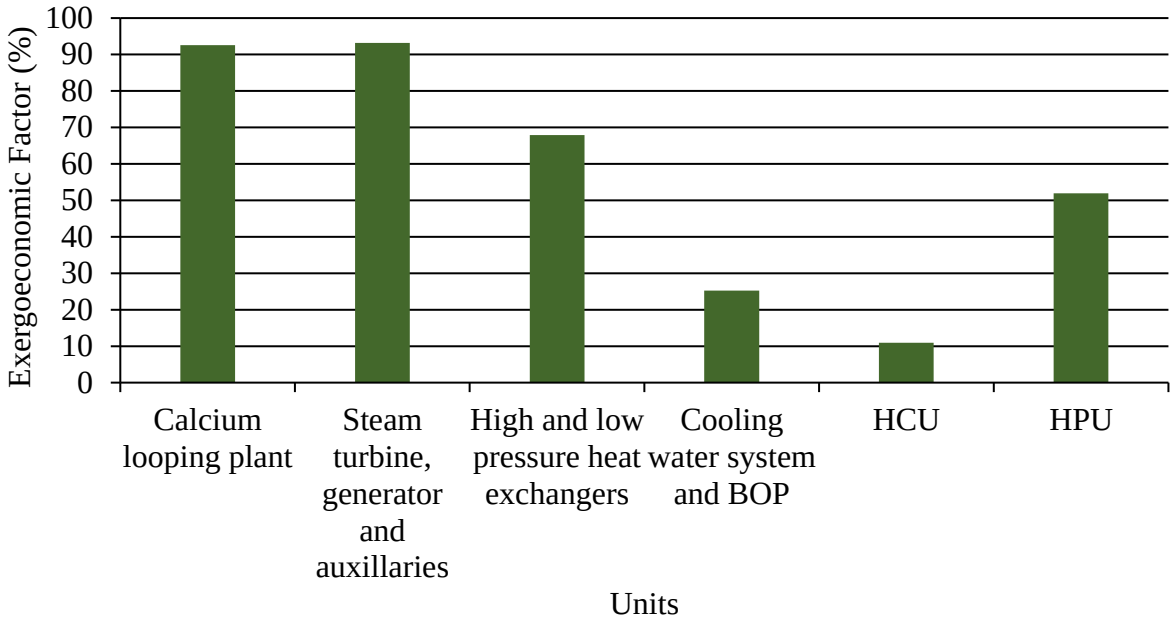

Fig. 4.19 Exergoeconomic factor of different units in HCFPP2

4.5 Performance assessment of natural gas fired combined cycle power plant integrated with calcium looping and DME production units (DNGFCPP1 and DNGFCPP2)

The performance of the proposed DNGFCPP1 and DNGFCPP2 configurations were evaluated by using the energy and environmental parameters such as total energy input, gross electrical power output, net electrical output, DME efficiency, net electrical efficiency, net energy efficiency, etc. The computational results of both the configurations are shown in Table 4.16 and Table 4.17. The computational results reveal that the total energy input to the system increases as the energy generation scheme was integrated with CO_2 utilization. The overall energy input for DNGFCPP2 and DNGFCPP1 were 3346.17 MW and 1306.73 MW, respectively. It indicates that the DNGFCPP2 configuration is highly energy intensive as compared to DNGFCPP1 configuration. The total electrical power consumption in DNGFCPP2 was 404.84 MW, which was significantly higher when compared against DNGFCPP1's energy requirement of 236.17 MW. The higher electrical energy consumption in DNGFCPP2 is mainly due to complete utilization of CO_2 that was captured using DCaLU. This complete utilization of CO_2 in DPU was achieved by recycling the unreacted gases (CO_2, CH_4, H_2) and by-products (CO, CH_3OH, H_2O) from the DSU. In the DPU, these recycled gases were mixed with feed natural gas and CO_2 from DCaLU. This increases the processing load in DPU. In particular, the exit stream from the DRR at atmospheric

pressure increases the load on the compression train. This in turns reduces the overall net electrical power generated by the DNGFCPP2 to 59.12 MW as compared to the DNGFCPP1 configuration having a net electrical power output of 69.7 MW, respectively. The above presented data and discussion elaborate the reasons for electrical energy penalty associated with DNGFCPP2 and DNGFCPP1 configurations.

The electrical efficiencies of DNGFCPP1 and DNGFCPP2 were observed to be 5.34% and 1.77%. However, the performance of the DNGFCPP1 and DNGFCPP2 cannot be determined solely on the basis of electrical energy efficiency as most of the input energy was used for DME production and not for electrical power generation. The DME can be used as an alternative fuel such as diesel. Hence, the thermal energy of DME was also considered as another end output in this work. Therefore, the energy of DME along with the net electrical power output was considered to assess the overall performance of the proposed configurations. Subsequently, the net electrical efficiency and DME efficiency were included while calculating the overall energy efficiency. Thus, the DNGFCPP1 and DNGFCPP2 have overall energy efficiencies of 45.31% and 52.83%, respectively.

Table 4.16 Plant performance of DNGFCPP1 and DNGFCPP2 on energy basis

Parameter	DNGFCPP1	DNGFCPP2
Total energy input to the plant (MW)	1306.73	3346.17
Gross electrical power output from the overall plant (MW)	305.89	463.96
Overall electrical power requirement of the compressors, pumps and auxiliaries (MW)	236.17	404.84
Energy obtained from total produced DME (MW)	522.30	1708.68
Net electrical power output from the overall plant (MW)	69.72	59.12
Electrical efficiency of the plant (%)	5.34	1.77
Overall energy efficiency of the plant (%)	45.31	52.83
Net energy efficiency penalty(+)/gain(-) of the overall plant (%)		-7.52

The environmental analysis in terms of CO_2 emissions for both the configurations were given in Table 4.17. CO_2 utilization efficiency of 25.7% in DNGFCPP1 indicates that all the captured CO_2 from DCaLU was not completely utilized for DME generation, and a considerable amount of it was released into the atmosphere. On the other hand, 91.3% of the total captured CO_2 by DCaLU was utilized in DNGFCPP2 configuration and thus corresponds to 89.6% of overall CO_2 utilization efficiency. Subsequently, the comparative analysis of specific CO_2 emission reveals that the DNGFCPP2 was having the low CO_2 emission rate of 5.64 kg/MWh only as compared to DNGFCPP1 having a specific CO_2 emission of 49.90 kg/MWh. This clearly indicates that DNGFCPP2 is a more environmentally efficient configuration than DNGFCPP1.

Table 4.17 Plant performance of DNGFCPP1 and DNGFCPP2 on environmental basis

Parameter	DNGFCPP1	DNGFCPP2
Total CO_2 generated from overall power plant (kg/s)	42.43	31.92
Total amount of CO_2 captured by the calcium looping unit (kg/s)	29.15	29.15
Total amount of CO_2 utilized for DME production (kg/s)	10.91	28.61
CO_2 capture efficiency (%)	68.70	91.32
CO_2 utilization efficiency (%)	25.7	89.63
Purity of captured CO_2 (%)	99.99	99.99
Specific CO_2 emission (kg/MWh)	49.90	5.64
Annual CO_2 emission (kg x 10^3)	207027	69883

4.5.1 Exergy analysis of natural gas fired combined cycle power plants integrated with calcium looping and DME production units

The previous section describes the competitiveness of the DNGFCPP2 against the DNGFCPP1 on the basis of overall energy and environmental analysis. Similarly, the exergy analysis was also carried out to compare the overall exergetic performance of the proposed power plant configurations. The computational results are presented in Table 4.18. The overall exergy

efficiency of DNGFCPP1 and DNGFCPP1 configurations are 47.02%, and 62.78%, respectively, at the corresponding total exergy input of 1385.13, and 3125.06 MW. Thus, an exergy efficiency gain of 15.76% was achieved for the DNGFCPP2 as compared to the exergy efficiency of the DNGFCPP1. From the above studies, it was observed that the DNGFCPP2 configuration has higher exergy efficiency as compared to DNGFCPP1 configuration.

Table 4.18 Plant performance of DNGFCPP1 and DNGFCPP2 on exergy basis

Parameter	DNGFCPP1	DNGFCPP2
Total exergy input to the plant (MW)	1358.13	3125.06
Exergy output from DME production (MW)	581.61	1902.68
Exergy output from electrical power (MW)	69.72	59.12
Overall exergy efficiency of the plant (%)	47.02	62.78
Net exergy efficiency penalty(+)/gain(-) of the overall plant (%)		-15.76

Subsequently, the exergetic performance of all units were investigated by calculating exergy input, output, destruction and efficiency. The process units with high exergy destruction have the scope for energy savings. This can be realized by improving the performance of the process in terms of design, operation, and heat integration. The exergetic efficiency, exergy destruction, and improvement potential of all the units in DNGFCPP2 configuration is presented in Fig. 4.20. It was found out that the SPGU has exergetic efficiency of 75.22%, which was highest as compared to all other units. Therefore, it has very low exergetic improvement potential to explore. On the other hand, the highest exergetic destruction was associated with the DPU having an exergy destruction of around 81%. Apart from the exergy losses in the CSP and DMESR reactor, the chemical irreversiblities in DRR system also plays a considerable role for this exergy destruction. It shares 33.96% of exergy destruction in DPU. This was mainly due to its high operating temperature. The exergy destruction of DCaLU was found to be 6%, with 4% of it coming from the combustor and 2% from calcium looping system. The results from Fig. 4.20B

shows that there is a large potential for exergetic performance improvement of 2024.39 MW in the DPU. The exergetic performance of this unit may be further improved by synthesizing a novel catalyst that can give the same conversion at low reactor temperature. Exergy destruction can be further reduced by exploring the heat integration option between the condensers present in DPU and the heat exchangers of DSU. In order to improve the overall performance of the integrated plant, this kind of improvement potential analysis of different units helps to focus attention on the promising units such as DRR, where a small improvement in design gives significant impact on energy and exergy efficiency.

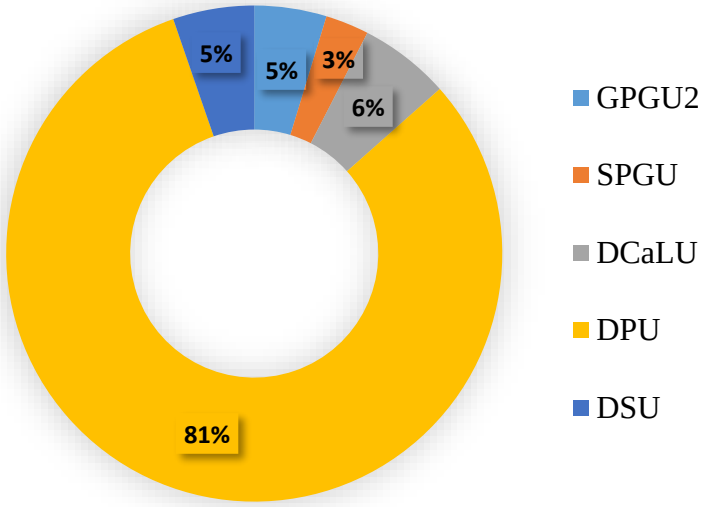

(A)

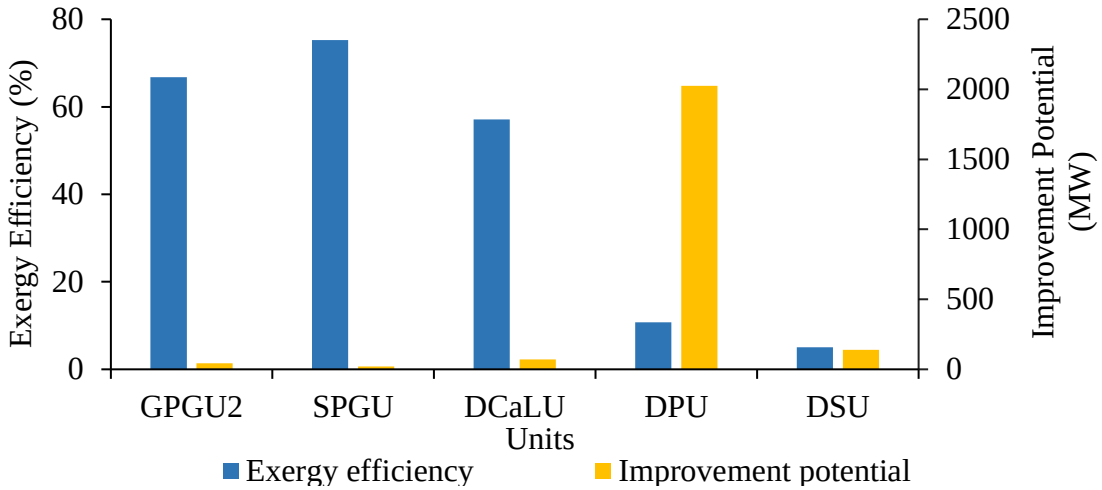

(B)

Fig. 4.20 (A) Exergy destruction (B) Exergy efficiency and improvement potential of DNGFCPP2

4.5.2 Cost and exergoeconomic analysis

In this analysis, capital costs of various units and components were estimated initially by using the ratio and proportion correlation method. These units and components costs were further used to calculate the TCR as well as operational and maintenance cost. The total installation cost was assumed to be 80% of the total units and components cost, whereas the total contingency and owner's cost were assumed to be 15% of the engineering, procurement, and construction cost. At the end, the TCR, LCOE, LPCD, CA, and PP were calculated by using the above estimated parameters. These were used as performance indicators to analyze the proposed configurations from a cost perspective. The outcome of cost analysis in terms of measurable performance indicators is presented in Table 4.19.

The results indicate that the TCR of the DNGFCPP1 and DNGFCPP2 were 1058.95 M€ and 1896.39 M€, respectively. The capital cost requirement of natural gas fired combined cycle power plant increases as the plant integrates more sustainable CO_2 mitigation options. Therefore, a high capital requirement was needed for DNGFCPP2 as compared to DNGFCPP1 configuration. The LCOE and LPCD have also been calculated for the proposed configurations and compared as shown in Table 4.19. Among the configurations, the DNGFCPP1 configuration has the higher LCOE of 1392.54 €/MWh as compared to the LCOE of DNGFCPP2 of 1038.39 €/MWh. This shows that DNGFCPP2 is economically more competitive than DNGFCPP1 configuration from the electricity generation perspective. The LPCD on the other hand reveals that the cost of DME produced in the DNGFCPP1 and DNGFCPP2 were 0.37 and 0.20 €/kg, respectively. The LPCD in DNGFCPP2 decreased because of the renewable energy integration with DPU. The LPCD obtained from the proposed configuration was less as compared to the other electricity and DME cogeneration configuration which is in the range of 0.29 and 1.43 €/kg (Clausen et al., 2010; Martin., 2016). The overall results from cost analysis indicates that the cost associated with DNGFCPP2 from DME and electricity cogeneration aspect is quite less as compared to the DNGFCPP1.

The exergoeconomic factors for various units of NGFCPP3 configuration calculated and presented in Fig. 4.21. This study reveals that the cooling water system and BOP in DPU, DSU, compression train in DPU, DMESR, cooling water system and BOP in SPGU, HRSG1 and HRSG2 modules have the exergy destruction cost rate in the range between 0.64% and 20.47%. These units

have higher exergy destruction cost rate. Thus, the potential of cost savings by reducing the exergy destruction in these modules is higher than the other modules. Exploring the opportunities for the same may lead to the overall performance improvement of the plant even at the expense of further capital investment.

Table 4.19 Cost performance indicators of DNGFCPP1 and DNGFCPP2

Parameters	DNGFCPP1	DNGFCPP2
TCR (M€)	1058.95	1896.39
LCOE (€/MWh)	1392.54	1038.39
LPCD (€/kg)	0.37	0.20

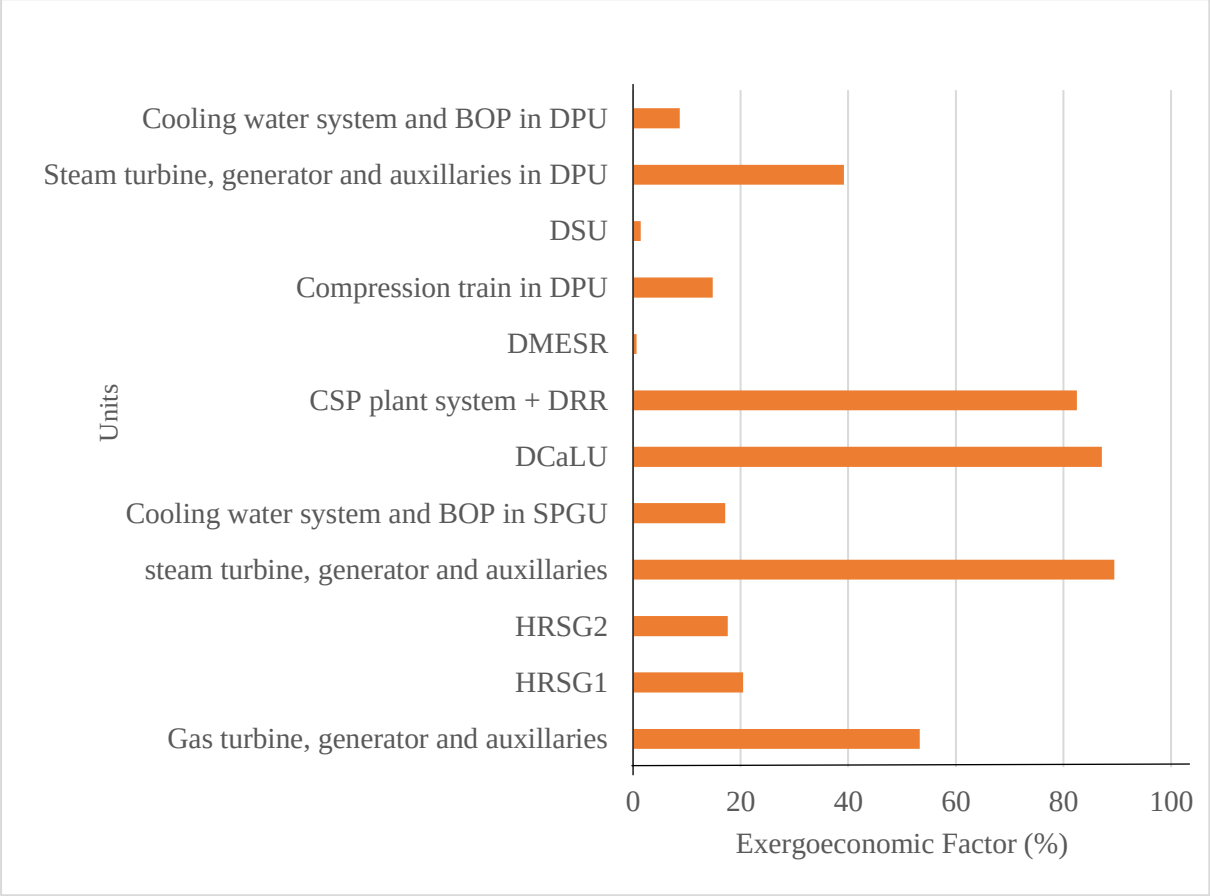

Fig. 4.21 Exergoeconomic factor of different components and units in DNGFCPP2

4.6 Performance assessment of various developed double calcium looping integrated power plant configurations

A demonstration of the proposed double calcium looping based simulation schemes of biomass, coal and natural gas fired power plants considering different case studies i.e., CCS, CCU and CCHC were presented in the above sections. A comparative assessment of the main parameters such as energy efficiency, exergy efficiency, specific CO_2 emissions and TCR for all these power plants is presented in Table 4.20.

Table 4.20 Comparative performance of all the proposed configurations

Parameters	BFPP3	CFPP3	HCFPP2	NGFCPP3	DNGFCPP2
Energy Efficiency penalty(+)/gain (-) (%)	0.1	0.52	-2.88	4.55	-7.52
Exergy Efficiency penalty(+)/gain (-) (%)	0.1	0.48	-2.64	4.29	-15.76
Specific CO_2 emissions (kg/MWh)	312.56	82.94	78.57	57.02	5.64
TCR (M€)	7.57	998.52	1074.28	866.97	1896.39

The results reveal that the proposed CCU and CCHC based configurations i.e., DNGFCPP2 and HCFPP2 have better net energy and exergy efficiencies compared to their respective conventional power plants integrated with only CCS based configurations i.e., NGFCPP3, CFPP3 and BFPP3. This indicates that CCU and CCHC technologies are more suitable thermodynamically than the CCS technology. The specific CO_2 emissions of DNGFCPP2 with 5.64 kg/MWh was found to be the lowest. While NGFCPP3 and HCFPP2 with specific CO_2 emissions of 57.02 kg/MWh and 78.57 kg/MWh were the second and third lowest, respectively, their difference from DNGFCPP2 is considerable. The BFPP3 holds the highest specific CO_2 emissions among all the configurations. Based on all the results, it can be deduced that DNGFCPP2 as the most environmental favorable among all the configurations. However, from the economic

perspective, the results also reveal that the DNGFCPP2 holds the higher TCR of 1896.39 M€ than other configurations. Therefore, it can be deduced from the overall discussion that all the proposed configurations have their distinctive abilities and have a role for providing a solution to restrict GHG emissions. A key selection factor among the proposed configurations is also based on the factors such as type of fuel and sequestration option available, demand of electricity, DME and H_2 and the scale of capital investment availability for the installation and operation of the plant etc. in the given region.

CHAPTER 5

CONCLUSIONS AND RECOMMENDATIONS

Chapter 5

Conclusions and recommendations

Rapid industrialization in many countries releasing massive volumes of CO_2 for producing energy from fossil fuels results in climate change. The complete switching from fossil fuel based power generation to renewable energy is unlikely in the near future in developing countries such as India, China, Brazil, Argentina, etc. Therefore, it is very much necessary to explore the CO_2 free energy harvesting from fossil fuels. A suitable CO_2 capture scheme and its integration with thermal power plants based on several deciding factors such as environmental effects, geographical advantages, technology readiness level and economics can pave the way its feasibility. Keeping these aspects as motivating factors, the present research work contributes to the area of steady state simulation of sustainable power generation options in biomass fired power plant, coal fired power plant and natural gas fired combined cycle power plant by adopting an effective CCS, CCHC and CCU strategies in accordance with Indian scenario.

In this work, all the power plant configurations were developed in four steps. In the first step, available data from the literature was used to validate individual unit models using aspenONE software such as the ORC, coal, natural gas fired combined cycle power plant, DCaLU, DPU and VAR cycle. These tested models were then integrated to develop effective power plant configurations with suitable CCS, CCHC, CCU technologies. Thirdly, these simulated models were configured as per the indigenous fuel and environmental conditions. Finally, a comprehensive energy, exergy, environment and cost analysis was carried out to assess the performance of the proposed configurations.

The important research findings of the present research work are as follows:

1. Based on the energy, exergy, cost and environmental studies, it is concluded that the proposed novel double calcium looping based power plant configurations (BFPP3, CFPP3 and NGFCPP3) were better than their respective conventional calcium looping integrated power plant configurations.

2. The results also showed that when compared with a single calcium looping based coal gasification process, double calcium looping can be a more effective approach to capture CO_2, generate H_2 and power.

3. As part of a DME based CO_2 utilization strategy, the findings from the proposed DNGFCPP2 scheme shows that it was a better alternative than DNGFCPP1 due to its solar energy integration. Such an integration strategy can prove to be a more viable option in regions where CCS options are not available or economically not feasible. Also, the exergy efficiencies are greater than the energy efficiencies by large margins because, the specific exergy of DME is higher than its LHV while the other parameters i.e., mass flow rate, steam turbine work output and total heat input mentioned in the energy and exergy efficiency equations remains same.

4. Cogeneration of H_2 and DME in the corresponding HCFPP2 and DNGFCPP2 configurations along with power production increases the overall energy and exergy efficiency.

5. The specific CO_2 emissions was found to be the lowest in case of DNGFCPP2. This is because of the integration of solar power with DPU, which results in almost complete utilization of CO_2.

6. Since the limestone ores are largely available in countries like India at a low cost, the proposed double calcium looping integrated power plant can be a more viable option.

At the end, it can be concluded that the performance of proposed configurations was found to be environmentally sustainable as the sorbent used for CO_2 capture is non-toxic in nature and abundantly available. However, in the proposed configurations, CO_2 capture process moderately decreased the overall energy and exergy efficiency, as compared to conventional power plant configurations. The proposed theoretical analysis can be further enhanced by considering all possible realistic scenarios to get the more accurate estimates for setting up the pilot to medium scale power plants.

The recommendations for future work is given below:

- The assumptions adopted to simplify the energy, exergy, cost and environmental analysis can be systematically relaxed to improve the visibility of this work at the industry level.

- As all practical problems cannot be foreseen in the theoretical works, experimental investigations at pilot scale is necessary to check the real time feasibility. Hence, the detailed experimental studies will give more insights on these proposed configurations.

- Investigation of the appropriate chemistries and kinetics, interaction between the combustion products and calcium sorbents can get more realistic estimates for reaction environment.

- Development of a low-cost synthetic calcium sorbents using economically benign techniques can increase the performance of the proposed configurations.

- A detailed economic and life cycle assessment towards environmental and economical sustainability would reveal more information such as global worming potential, cumulative energy demand, etc.

References

Aaron D, Tsouris C. Separation of CO_2 from flue gas: a review. Separation science and technology. 2005;40(1-3):321-48.

Abanades JC, Murillo R, Fernandez JR, Grasa G, Martínez I. New CO_2 capture process for hydrogen production combining Ca and Cu chemical loops. Environmental science and technology. 2010;44(17):6901-4.

Ahmadi P, Dincer I, Rosen MA. Development and assessment of an integrated biomass-based multi-generation energy system. Energy. 2013;56:155-66.

Algieri A, Morrone P. Techno-economic analysis of biomass fired ORC systems for single-family combined heat and power (CHP) applications. Energy procedia. 2014;45:1285-94.

Al-Sulaiman FA, Dincer I, Hamdullahpur F. Energy and exergy analyses of a biomass trigeneration system using an organic Rankine cycle. Energy. 2012;45(1):975-85.

Anheden M, Svedberg G. Exergy analysis of chemical-looping combustion systems. Energy conversion and management. 1998;39(16-18):1967-80.

Annual Report. Ministry of Mines (2016-17). Government of India. 2017.

Arasto A, Chiaramonti D, Kiviluoma J, Waldheim L, Maniatis K, Sipilä K. Bioenergy's role in balancing the electricity grid and providing storage options: An EU perspective. IEA Bioenergy. 2017.

Aroonwilas A, Veawab A. Integration of CO_2 capture unit using single-and blended-amines into supercritical coal-fired power plants: Implications for emission and energy management. International journal of greenhouse gas control. 2007;1(2):143-50.

Assche LV, Compernolle T. Economic feasibility studies for carbon capture and utilization technologies: a tutorial review. Clean technologies and environmental policy. 2021:1-25.

Benitez-Guerrero M, Valverde JM, Sanchez-Jimenez PE, Perejon A, Perez-Maqueda LA. Calcium-Looping performance of mechanically modified Al_2O_3-CaO composites for energy storage and CO_2 capture. Chemical engineering journal. 2018;334:2343-55.

Berstad D, Anantharaman R, Blom R, Jordal K, Arstad B. NGCC post-combustion CO_2 capture with Ca/carbonate looping: Efficiency dependency on sorbent properties, capture unit performance and process configuration. International journal of greenhouse gas control. 2014;24:43-53.

Berstad D, Anantharaman R, Jordal K. Post-combustion CO_2 capture from a natural gas combined cycle by CaO/$CaCO_3$ looping. International journal of greenhouse gas control. 2012;11:25-33.

Bhatt MS. Enhancement of energy efficiency and loading of steam turbines through retrofitting 2-d designs with 3-d designs. Journal of scientific and industrial research. 2011;70(1):64-70.

Blamey J, Paterson NP, Dugwell DR, Fennell PS. Mechanism of particle breakage during reactivation of CaO-based sorbents for CO_2 capture. Energy and fuels. 2010;24(8):4605-16.

Bolland O, Saether S. New concepts for natural gas fired power plants which simplify the recovery of carbon dioxide. Energy conversion and management. 1992;33(5–8):467-75.

Brigagão GV, de Medeiros JL, Ofélia de Queiroz FA. A novel cryogenic vapor-recompression air separation unit integrated to oxyfuel combined-cycle gas-to-wire plant with carbon dioxide enhanced oil recovery: energy and economic assessments. Energy conversion and management. 2019;189:202-14.

Buhre BJ, Elliott LK, Sheng CD, Gupta RP, Wall TF. Oxy-fuel combustion technology for coal-fired power generation. Progress in energy and combustion science. 2005;31(4):283-307.

Castillo JC. Cost estimation of using an absorption refrigeration system with geothermal energy for industrial applications in El Salvador. Geothermal training in Iceland: reports of the united nations university geothermal training progamme. 2007.

Chao C, Deng Y, Dewil R, Baeyens J, Fan X. Post-combustion carbon capture. Renewable and sustainable energy reviews. 2021;138:110490.

Charitos A, Hawthorne C, Bidwe AR, Sivalingam S, Schuster A, Spliethoff H, Scheffknecht G. Parametric investigation of the calcium looping process for CO_2 capture in a 10 kW_{th} dual fluidized bed. International journal of greenhouse gas control. 2010;4(5):776-84.

Charon O. Recent developments and future trends in oxy-combustion applications. 17^{th} IFRF topic oriented technical meeting, les vaux de cernay, France. 2000.

Chauvel A, Fournier G, Raimbault C. Manual of process economic evaluation. Editions TECHNIP. 2003.

Chen S, Wang D, Xue Z, Sun X, Xiang W. Calcium looping gasification for high-concentration hydrogen production with CO_2 capture in a novel compact fluidized bed: simulation and operation requirements. International journal of hydrogen energy. 2011;36(8):4887-99.

Chi S, Rochelle GT. Oxidative degradation of monoethanolamine. Industrial and engineering chemistry research. 2002;41(17):4178-86.

CIL. Coal price notification. Coal India limited; 2018. Link: https://www.coalindia.in/media/documents/Price_Notification_dated_08.01.2018_effective_from_0000_Hrs_of_09.01.2018_09012018.pdf .

Clausen LR, Elmegaard B, Houbak N. Technoeconomic analysis of a low CO_2 emission dimethyl ether (DME) plant based on gasification of torrefied biomass. Energy. 2010;35(12):4831-42.

Connell DP, Lewandowski DA, Ramkumar S, Phalak N, Statnick RM, Fan LS. Process simulation and economic analysis of the calcium looping process (CLP) for hydrogen and electricity production from coal and natural gas. Fuel. 2013;105:383-96.

Coppola A, Salatino P, Montagnaro F, Scala F. Reactivation by water hydration of the CO_2 capture capacity of a calcium looping sorbent. Fuel. 2014;127:109-15.

Dai Y, Wang J, Gao L. Parametric optimization and comparative study of organic rankine cycle (ORC) for low grade waste heat recovery. Energy conversion and management. 2009;50(3):576-82.

Dean CC, Blamey J, Florin NH, Al-Jeboori MJ, Fennell PS. The calcium looping cycle for CO_2 capture from power generation, cement manufacture and hydrogen production. Chemical engineering research and design. 2011;89(6):836-55.

Desjardins J. Every coal power plant in the world (1927-2019). Energy archives, visual capitalist. 2019. Link: https://www.visualcapitalist.com/every-coal-power-plant-1927-2019/.

Diego ME, Arias B, Abanades JC. Analysis of a double calcium loop process configuration for CO_2 capture in cement plants. Journal of cleaner production. 2016;117:110-21.

Dieter H, Beirow M, Schweitzer D, Hawthorne C, Scheffknecht G. Efficiency and flexibility potential of calcium looping CO_2 capture. Energy procedia. 2014;63:2129-37.

DinAli MN, Dincer I. Development of a new trigenerational integrated system for dimethyl-ether, electricity and fresh water production. Energy conversion and management. 2019a;185:850-65.

DinAli MN, Dincer I. Performance assessment of a new solar energy based cogeneration system for dimethyl-ether and electricity production. Solar energy. 2019b;190:337-49.

DinAli MN, Dincer I. Renewable energy based dimethyl-ether production system linked with industrial waste heat. Journal of energy resources technology. 2019c;141(12):122003.

Duan L, Feng T, Jia S, Yu X. Study on the performance of coal-fired power plant integrated with Ca-looping CO_2 capture system with recarbonation process. Energy. 2016;115:942-53.

Dugué J. The use of oxygen for industrial combustion. 17th IFRF topic oriented technical meetings, international flame research foundation document no. D121/y/6. 2000.

Dutta A, Farooq S, Karimi IA, Khan SA. Assessing the potential of CO_2 utilization with an integrated framework for producing power and chemicals. Journal of CO_2 utilization. 2017;19:49-57.

Edie. Edie newsroom. 14 Jan 2021. Link: https://www.edie.net/news/8/Inside-the-world-s-first-fully-commercial-carbon-capture-and-utilisation-plant/.

EIA India. Country analysis executive summary: India. 30 Sep 2020. Link: https://www.eia.gov/international/content/analysis/countries_long/India/india.pdf .

EIA. International energy outlook 2019 with projections to 2050. Office of energy analysis US department of energy: Washington, DC, USA. 2019.

Er-Rbib H, Bouallou C, Werkoff F. Production of synthetic gasoline and diesel fuel from dry reforming of methane. Energy procedia. 2012;29:156-65.

Escudero AI, Espatolero S, Romeo LM. Oxy-combustion power plant integration in an oil refinery to reduce CO_2 emissions. International journal of greenhouse gas control. 2016;45:118-29.

Espatolero S, Cortés C, Romeo LM. Optimization of boiler cold-end and integration with the steam cycle in supercritical units. Applied energy. 2010;87:1651-60.

ET markets. The economic times. 2020. Link: economictimes.indiatimes.com/commoditysummary/symbol-NATURALGAS.cms .

Fennell P, Anthony B. Calcium and chemical looping technology for power generation and carbon dioxide (CO_2) capture. Elsevier. 2015.

Fernández JR, Abanades JC. Overview of the Ca–Cu looping process for hydrogen production and/or power generation. Current opinion in chemical engineering. 2017;17:1-8.

Florin NH, Harris AT. Enhanced hydrogen production from biomass with in situ carbon dioxide capture using calcium oxide sorbents. Chemical engineering science. 2008;63(2):287-316.

Forristall R. Heat transfer analysis and modeling of a parabolic trough solar receiver implemented in engineering equation solver. National renewable energy lab, Golden, CO (United States). 2003.

Franz J, Maas P, Scherer V. Economic evaluation of pre-combustion CO_2 capture in IGCC power plants by porous ceramic membranes. Applied energy. 2014;130:532-42.

Fytianos G, Ucar S, Grimstvedt A, Hyldbakk A, Svendsen HF, Knuutila HK. Corrosion and degradation in MEA based post-combustion CO_2 capture. International journal of greenhouse gas control. 2016;46:48-56.

Gaber C, Schluckner C, Wachter P, Demuth M, Hochenauer C. Experimental study on the influence of the nitrogen concentration in the oxidizer on NOx and CO emissions during the oxy-fuel combustion of natural gas. Energy. 2021;214:118905.

Gądek W, Kalisz S. Review of ash deposition coefficients for selected biomasses. Renewable energy sources: engineering, technology, innovation: ICORES 2017, springer international publishing. 2018:119-26.

GAIL. GAIL (India) limited. Jhajjar hissar pipeline project [E-Tender no. 8000000830, bid document no: 05/51/23L6/GAIL/017]. 2009.

Gangadharan P, Kanchi KC, Lou HH. Evaluation of the economic and environmental impact of combining dry reforming with steam reforming of methane. Chemical engineering research and design. 2012;90(11):1956-68.

Goto K, Yogo K, Higashii T. A review of efficiency penalty in a coal-fired power plant with post-combustion CO_2 capture. Applied energy. 2013;111:710-20.

Hagi H, Nemer M, Le Moullec Y, Bouallou C. Assessment of the flue gas recycle strategies on oxy-coal power plants using an exergy-based methodology. Chemical engineering transactions. 2013;35:343-8.

Hanak DP, Anthony EJ, Manovic V. A review of developments in pilot-plant testing and modelling of calcium looping process for CO_2 capture from power generation systems. Energy and environmental science. 2015;8(8):2199-249.

Hanak DP, Biliyok C, Yeung H, Białecki R. Heat integration and exergy analysis for a supercritical high-ash coal-fired power plant integrated with a post-combustion carbon capture process. Fuel. 2014;134:126-39.

Hanak DP, Manovic V. Calcium looping combustion for high-efficiency low-emission power generation. Journal of cleaner production. 2017a;161:245-55.

Hanak DP, Manovic V. Calcium looping with supercritical CO_2 cycle for decarbonisation of coal-fired power plant. Energy. 2016;102:343-53.

Hanak DP, Manovic V. Economic feasibility of calcium looping under uncertainty. Applied energy. 2017b;208:691-702.

Hanak DP, Michalski S, Manovic V. From post-combustion carbon capture to sorption-enhanced hydrogen production: A state-of-the-art review of carbonate looping process feasibility. Energy conversion and management. 2018;177:428-52.

Harris ZM, Milner S, Taylor G. Biogenic carbon—capture and sequestration. Greenhouse gas balances of bioenergy systems, academic press. 2018:55-76.

Harvey A. History of power: the evolution of the electric generation industry. Power. 1 Oct 2022. Link: https://www.powermag.com/history-of-power-the-evolution-of-the-electric-generation-industry/.

Hinderink AP, Kerkhof FP, Lie AB, Arons JD, Van Der Kooi HJ. Exergy analysis with a flowsheeting simulator—I. Theory; calculating exergies of material streams. Chemical engineering science. 1996;51(20):4693-700.

Hu Y, Ahn H. Process integration of a calcium-looping process with a natural gas combined cycle power plant for CO_2 capture and its improvement by exhaust gas recirculation. Applied energy. 2017;187:480-8.

Hu Y, Liu W, Chen H, Zhou Z, Wang W, Sun J, Yang X, Li X, Xu M. Screening of inert solid supports for CaO-based sorbents for high temperature CO_2 capture. Fuel. 2016;181:199-206.

Ibrahim TK, Mohammed MK, Awad OI, Abdalla AN, Basrawi F, Mohammed MN, Najafi G, Mamat R. A comprehensive review on the exergy analysis of combined cycle power plants. Renewable and sustainable energy reviews. 2018;90:835-50.

IEA. Bioenergy power generation. International energy agency, Paris. 2020a. Link: https://www.iea.org/reports/bioenergy-power-generation.

IEA. Energy technology perspectives. International energy agency. 2015. Link: https://www.iea.org/etp/.

IEA. Global energy review. International energy agency, Paris. 2021. Link: https://www.iea.org/reports/global-energy-review-2021.

IEA. Hydrogen. International energy agency, Paris. 2020b. Link: https://www.iea.org/reports/hydrogen.

IEA. Key world energy statistics. International energy agency, Paris. 2020c. Link: https://www.iea.org/reports/key-world-energy-statistics-2020.

IEA. World energy outlook. Flagship report, international energy agency. 2019. Link: https://www.iea.org/reports/worldenergy-outlook-2019.

IEAGHG. A brief history of CCS and current status. Report 2013/16. 2013. Link: https://ieaghg.org/docs/General_Docs/Reports/2013-16_Information_Sheets_for_CCS_All_sheets.pdf.

IEO. International energy outlook 2016 with projections to 2040. Washington DC, USA. 2016.

Ivanova S, Vanhaecke E, Libs S, Louis B, Pham-Huu C, Ledoux MJ. Centre national de la recherche scientifique CNRS, universite louis pasteur (Strasbourg I). Dehydration of methanol to dimethyl ether using catalysts based on a zeolite supported on silicon carbide, patent US 9,073,837, United States. 2015.

Jansen D, Gazzani M, Manzolini G, van Dijk E, Carbo M. Pre-combustion CO_2 capture. International journal of greenhouse gas control. 2015;40:167-87.

Jenkins BM, Bhatnagar AP. On the electric power potential from paddy straw in the Punjab and the optimal size of the power generation station. Bioresource technology. 1991;37(1):35-41.

Kadhim HT, Jabbar FA, Rona A, Bagdanavicius A. Improving the performance of gas turbine power plant by modified axial turbine. International journal of mechanical and mechatronics engineering. 2018;12 (6): 690-96.

Kanoğlu M, Çengel YA, Dinçer İ. Efficiency evaluation of energy systems. Springer science and business media. 2012.

Kaur S. Public preferences for setting up a biomass power plant to combat open-field burning of rice crop residues: a case study of district sangrur, punjab, India. Biomass and Bioenergy. 2020;138:105577.

Keeling CD, Bacastow RB, Bainbridge AE, Ekdahl Jr CA, Guenther PR, Waterman LS, Chin JF. Atmospheric carbon dioxide variations at mauna loa observatory, hawaii. Tellus. 1976;28(6):538-51.

Keeling CD. The concentration and isotopic abundances of carbon dioxide in the atmosphere. Tellus. 1960;12(2):200-03.

Khallaghi N, Hanak DP, Manovic V. Techno-economic evaluation of near-zero CO_2 emission gas-fired power generation technologies: A review. Journal of natural gas science and engineering. 2020;74:103095.

Khushi food products. Kalyan, Maharashtra, India. Accessed March 20, 2021. Link: https://www.indiamart.com/proddetail/natural-sugarcane-bagasse-20642930833.html.

Kim M, Kim K, Kim TH, Kim J. Economic and environmental benefit analysis of a renewable energy supply system integrated with carbon capture and utilization framework. Chemical engineering research and design. 2019;147:200-13.

Komaki A, Gotou T, Uchida T, Yamada T, Kiga T, Spero C. Operation experiences of oxyfuel power plant in callide oxyfuel project. Energy procedia. 2014;63:490-6.

Koohestanian E, Shahraki F. Review on principles, recent progress, and future challenges for oxy-fuel combustion CO_2 capture using compression and purification unit. Journal of Environmental chemical engineering. 2021;9(4):105777.

Kotas TJ. The exergy method of thermal plant analysis. Oxford: butterworth-heinemann; 1985:267-8.

Koytsoumpa EI, Bergins C, Kakaras E. The CO_2 economy: review of CO_2 capture and reuse technologies. The journal of supercritical fluids. 2018;132:3-16.

Kung HH. Methanol production and use chemical industries. Evanston, IL: northwestern university. 1994.

Lako P. Coal-fired power technologies. Coal-fired power options on the brink of climate policies. 2004.

Lakshmi GS, Singh B, Kamal A, Sharma S, Kumar VK. Energy statistics. twenty sixth issue. Central statistics office, government of India. 2019.

Layton A, Reap J, Bras B, Weissburg M. Correlation between thermodynamic efficiency and ecological cyclicity for thermodynamic power cycles. PLoS One. 2012;7(12):e51841.

Lebarbier VM, Dagle RA, Kovarik L, Lizarazo-Adarme JA, King DL, Palo DR. Synthesis of methanol and dimethyl ether from syngas over $Pd/ZnO/Al_2O_3$ catalysts. Catalysis science and technology. 2012;2(10):2116-27.

Lee JH, Park HS, Jung JY, Kim JS, Jung YL, Park SW. A numerical investigation on the isentropic efficiency of steam turbine nozzle stage with different nozzle vane thickness and mass flow rate. Transactions of the korean society of mechanical engineers B. 2017;41(10):685-91.

Lee S. Dimethyl ether synthesis and conversion to value-added chemicals. Accessed January 20, 2021. Link: https://sunggyuleephd.com/dme/.

Leung DY, Caramanna G, Maroto-Valer MM. An overview of current status of carbon dioxide capture and storage technologies. Renewable and sustainable energy reviews. 2014;39:426-43.

Lewis CW. Biomass through the ages. Biomass. 1981;1(1):5-15.

Li F, Fan LS. Clean coal conversion processes–progress and challenges. Energy and environmental science. 2008;1(2):248-67.

Li Y, Zhao C, Ren Q, Duan L, Chen H, Chen X. Effect of rice husk ash addition on CO_2 capture behavior of calcium-based sorbent during calcium looping cycle. Fuel processing technology. 2009;90(6):825-34.

Lin SY, Suzuki Y, Hatano H, Harada M. Developing an innovative method, HyPr-RING, to produce hydrogen from hydrocarbons. Energy conversion and management. 2002;43(9-12):1283-90.

Liu W, An H, Qin C. Performance enhancement of calcium oxide sorbents for cyclic CO_2 capture: a review. Energy and fuels. 2012;26(5):2751-67.

Looney B. Statistical review of world energy. British petroleum. 2020;69:66.

Loria P, Bright MB. Lessons captured from 50 years of CCS projects. The electricity journal. 2021 Aug 1;34(7):106998.

Lugo-Leyte R, Zamora-Mata JM, Toledo-Velazquez M, Salazar-Pereyra M, Torres-Aldaco A. Methodology to determine the appropriate amount of excess air for the operation of a gas turbine in a wet environment. Energy. 2010;35(2):550-5.

Luu MT, Milani D, Wake M, Abbas A. Analysis of di-methyl ether production routes: process performance evaluations at various syngas compositions. Chemical engineering science. 2016;149:143-55.

Ma X, Li Y, Huang X, Feng T, Mu M. Sorption-enhanced reaction process using advanced Ca-based sorbents for low-carbon hydrogen production. Process safety and environmental protection. 2021;155:325-42.

MacDowell N, Florin N, Buchard A, Hallett J, Galindo A, Jackson G, Adjiman CS, Williams CK, Shah N, Fennell P. An overview of CO_2 capture technologies. Energy and environmental science. 2010;3(11):1645-69.

Madejski P, Chmiel K, Subramanian N, Kuś T. Methods and techniques for CO_2 capture: Review of potential solutions and applications in modern energy technologies. Energies. 2022;15(3):887.

Manovic V, Anthony EJ. Carbonation of CaO-based sorbents enhanced by steam addition. Industrial and engineering chemistry research. 2010;49(19):9105-10.

Mantripragada HC, Rubin ES. Calcium looping cycle for CO_2 capture: Performance, cost and feasibility analysis. Energy procedia. 2014;63:2199-206.

Manzolini G, Macchi E, Gazzani M. CO_2 capture in integrated gasification combined cycle with SEWGS–part B: economic assessment. Fuel. 2013;105:220-27.

Markewitz P, Kuckshinrichs W, Leitner W, Linssen J, Zapp P, Bongartz R, Schreiber A, Müller TE. Worldwide innovations in the development of carbon capture technologies and the utilization of CO_2. Energy and environmental science. 2012;5(6):7281-305.

Martin M. Optimal year-round production of DME from CO_2 and water using renewable energy. Journal of CO_2 utilization. 2016;13:105-13.

Martínez I, Murillo R, Grasa G, Fernández JR, Abanades JC. Integrated combined cycle from natural gas with CO_2 capture using a Ca–Cu chemical loop. AIChE journal. 2013;59(8):2780-94.

Mehrpooya M, Sharifzadeh MM, Mousavi SA. Evaluation of an optimal integrated design multi-fuel multi-product electrical power plant by energy and exergy analyses. Energy. 2019;169:61-78.

Metz B, Davidson O, De Coninck HC, Loos M, Meyer L. IPCC special report on carbon dioxide capture and storage. Cambridge: Cambridge University Press. 2005.

Míguez JL, Porteiro J, Pérez-Orozco R, Patiño D, Rodríguez S. Evolution of CO_2 capture technology between 2007 and 2017 through the study of patent activity. Applied energy. 2018;211:1282-96.

Mikulčić H, Skov IR, Dominković DF, Alwi SR, Manan ZA, Tan R, Duić N, Mohamad SN, Wang X. Flexible carbon capture and utilization technologies in future energy systems and the utilization pathways of captured CO_2. Renewable and sustainable energy reviews. 2019;114:109338.

Miser T. A short history of evolving uses of natural gas. Power engineering. 2015;2:119.

Mishra RS, Singh H. Detailed parametric analysis of solar driven supercritical CO_2 based combined cycle for power generation, cooling and heating effect by vapor absorption refrigeration as a bottoming cycle. Thermal science and engineering progress. 2018;8:397-410.

MNRE. Annual Report 2019-2020. Ministry of new and renewable energy, India. 2020. Link: https://mnre.gov.in/img/documents/uploads/file_f-1597797108502.pdf .

Moioli S, Giuffrida A, Gamba S, Romano MC, Pellegrini L, Lozza G. Pre-combustion CO_2 capture by MDEA process in IGCC based on air-blown gasification. Energy procedia. 2014;63:2045-53.

Montagnaro F, Salatino P, Scala F, Chirone R. An assessment of water and steam reactivation of a fluidized bed spent sorbent for enhanced SO_2 capture. Powder technology. 2008;180(1-2):129-34.

Montagnaro F, Salatino P, Scala F, Wu YH, Anthony EJ, Jia LF. Assessment of sorbent reactivation by water hydration for fluidized bed combustion application. Journal of energy resources of technology. 2006;128:90–8.

Montagnaro F, Scala F, Salatino P. Reactivation by water hydration of spent sorbent for fluidized-bed combustion application: influence of hydration time. Industrial and engineering chemistry research. 2004;43(18):5692-701.

Motwani KH, Jain SV, Patel RN. Cost analysis of pump as turbine for pico hydropower plants–a case study. Procedia engineering. 2013;51:721-6.

Mustafa MA, Abdelhady S, Elweteedy AA. Analytical study of an innovated solar power tower (PS10) in Aswan. International Journal of energy engineering. 2012;2(6):273-8.

Negi BS, Pandey KK, Sehgal N. Renewables, shale gas and gas import-striking a balance for India. Energy procedia. 2017;105: 3720-26.

Neto S, Szklo A, Rochedo PR. Calcium looping post-combustion CO_2 capture in sugarcane bagasse fuelled power plants. International journal of greenhouse gas control. 2021;110:103401.

Olaleye AK, Wang M, Kelsall G. Steady state simulation and exergy analysis of supercritical coal-fired power plant with CO_2 capture. Fuel. 2015;151:57-72.

Outlook. British petroleum, 2019 edition. London, UK. 2019.

Ozcan DC, Macchi A, Lu DY, Kierzkowska AM, Ahn H, Müller CR, Brandani S. Ca–Cu looping process for CO_2 capture from a power plant and its comparison with Ca-looping, oxy-combustion and amine-based CO_2 capture processes. International journal of greenhouse gas control. 2015;43:198-212.

Ozcan H, Dincer I. Comparative performance assessment of three configurations of magnesium–chlorine cycle. International journal of hydrogen energy. 2016;41(2):845-56.

Ozdil NFT, Segmen MR, Tantekin A. Thermodynamic analysis of an organic rankine cycle (ORC) based on industrial data. Applied thermal engineering. 2015;91:43-52.

Pakatchian MR, Saeidi H, Dashti AR. Axial flow compressor of MGT-70 gas turbine blade shape optimization based on operating condition. International gas turbine congress. Tokyo, Japan. 2015:249-55.

Park SH, Lee CS. Applicability of dimethyl ether (DME) in a compression ignition engine as an alternative fuel. Energy conversion and management. 2014;86:848-63.

Parsons RH. The early days of the power station industry. Cambridge university press. 29 Jan 2015.

Perejón A, Romeo LM, Lara Y, Lisbona P, Martínez A, Valverde JM. The calcium-looping technology for CO_2 capture: On the important roles of energy integration and sorbent behavior. Applied energy. 2016;162:787-807.

Pfaff I, Kather A. Comparative thermodynamic analysis and integration issues of CCS steam power plants based on oxy-combustion with cryogenic or membrane based air separation. Energy procedia. 2009;1(1):495-502.

Pillai BBK, Surywanshi GD, Patnaikuni VS, Anne SB, Vooradi R. A novel calcium looping–integrated NGCC power plant configuration for carbon capture and utilization—comprehensive performance analysis. International journal of energy research. 2022;46(2):900-22.

Pillai BBK, Surywanshi GD, Patnaikuni VS, Anne SB, Vooradi R. Performance analysis of a double calcium looping-integrated biomass-fired power plant: exploring a carbon reduction opportunity. International journal of energy research. 2019;43(10):5301-18.

Prasertsri W, Frauzem R, Suriyapraphadilok U, Gani R. Sustainable DME synthesis-design with CO_2 utilization. Computer aided chemical engineering. 2016;38:1081-86.

Quoilin S, Van Den Broek M, Declaye S, Dewallef P, Lemort V. Techno-economic survey of organic rankine cycle (ORC) systems. Renewable and sustainable energy reviews. 2013;22:168-86.

Rackley SA. Carbon capture and storage. 2010.

Rafiee A, Khalilpour KR, Milani D, Panahi M. Trends in CO_2 conversion and utilization: A review from process systems perspective. Journal of environmental chemical engineering. 2018;6(5):5771-94.

Rahman MM, Ibrahim TK, Abdalla AN. Thermodynamic performance analysis of gas-turbine power-plant. International journal of physical sciences. 2011;6(14):3539-50.

Ramachandran R, Menon RK. An overview of industrial uses of hydrogen. International journal of hydrogen energy. 1998;23(7):593-8.

Ravikumar D, Keoleian G, Miller S. The environmental opportunity cost of using renewable energy for carbon capture and utilization for methanol production. Applied energy. 2020;279:115770.

Reddy VS, Kaushik SC, Tyagi SK. Exergetic analysis of solar concentrator aided natural gas fired combined cycle power plant. Renewable energy. 2012;39(1):114-125.

Romano MC, Chiesa P, Lozza G. Pre-combustion CO_2 capture from natural gas power plants, with ATR and MDEA processes. International journal of greenhouse gas control. 2010;4(5):785-97.

Roussanaly S, Vitvarova M, Anantharaman R, Berstad D, Hagen B, Jakobsen J, Novotny V, Skaugen G. Techno-economic comparison of three technologies for pre-combustion CO_2 capture from a lignite-fired IGCC. Frontiers of chemical science and engineering. 2020;14(3):436-52.

Safarian S, Aramoun F. Energy and exergy assessments of modified organic rankine cycles (ORCs). Energy reports. 2015;1:1-7.

Sahoo U, Kumar R, Pant PC, Chaudhary R. Resource assessment for hybrid solar-biomass power plant and its thermodynamic evaluation in India. Solar energy. 2016;139:47-57.

Schakel W, Oreggioni G, Singh B, Strømman A, Ramírez A. Assessing the techno-environmental performance of CO_2 utilization via dry reforming of methane for the production of dimethyl ether. Journal of CO_2 utilization. 2016;16:138-49.

Schurer AP, Cowtan K, Hawkins E, Mann ME, Scott V, Tett SF. Interpretations of the Paris climate target. Nature geoscience. 2018;11(4):220-1.

Shah K, Moghtaderi B, Zanganeh J, Wall T. Integration options for novel chemical looping air separation (ICLAS) process for oxygen production in oxy-fuel coal fired power plants. Fuel. 2013;107:356-70.

Shaikh AR, Wang Q, Han L, Feng Y, Sharif Z, Li Z, Cen J, Kumar S. Techno-economic analysis of hydrogen and electricity production by biomass calcium looping gasification. Sustainability. 2022;14(4):2189.

Shimizu T, Hirama T, Hosoda H, Kitano K, Inagaki M, Tejima K. A twin fluid-bed reactor for removal of CO_2 from combustion processes. Chemical engineering research and design. 1999;77(1):62-8.

Sifat NS, Haseli Y. A critical review of CO_2 capture technologies and prospects for clean power generation. Energies. 2019;12(21):4143.

Singh U, Rao AB, Chandel MK. Economic implications of CO_2 capture from the existing as well as proposed coal-fired power plants in India under various policy scenarios. Energy procedia. 2017;114:7638-50.

Singh U, Sharma N. Soft-computing approach to predict cost and performance of natural gas combined cycle (NGCC) plants using carbon dioxide capture. INAE Letters. 2016;1(2):65-76.

Som SK, Datta A. Thermodynamic irreversibilities and exergy balance in combustion processes. Progress in energy and combustion science. 2008;34(3):351-76.

Sun Y, Ritchie T, Hla SS, McEvoy S, Stein W, Edwards JH. Thermodynamic analysis of mixed and dry reforming of methane for solar thermal applications. Journal of natural gas chemistry. 2011;20(6):568-76.

Supap T, Idem R, Tontiwachwuthikul P, Saiwan C. Analysis of monoethanolamine and its oxidative degradation products during CO_2 absorption from flue gases: A comparative study of GC-MS, HPLC-RID, and CE-DAD analytical techniques and possible optimum combinations. Industrial and engineering chemistry research. 2006;45(8):2437-51.

Suresh MV, Reddy KS, Kolar AK. 3-E analysis of advanced power plants based on high ash coal. International journal of energy research. 2010a;34(8):716-35.

Suresh MV, Reddy KS, Kolar AK. 4-E (Energy, Exergy, Environment, and Economic) analysis of solar thermal aided coal-fired power plants. Energy for sustainable development. 2010b;14(4):267-79.

Taghavifar H, Nemati A, Walther JH. Combustion and exergy analysis of multi-component diesel-DME-methanol blends in HCCI engine. Energy. 2019;187:115951.

Tapia JF, Lee JY, Ooi RE, Foo DC, Tan RR. Planning and scheduling of CO_2 capture, utilization and storage (CCUS) operations as a strip packing problem. Process safety and environmental protection. 2016;104:358-72.

Telesca A, Calabrese D, Marroccoli M. Spent limestone sorbent from calcium looping cycle as a raw material for the cement industry. Fuel. 2014;118:202-205.

Therminol. Heat transfer fluids by eastman. Eastman corporate headquarters. 2022. Link: https://www.eastman.com/Literature_Center/T/TF9141.pdf.

Thimsen D, Wheeldon J, Dillon D. Economic comparison of oxy-coal carbon dioxide (CO_2) capture and storage (CCS) with pre-and post-combustion CCS. Oxy-fuel combustion for power generation and carbon dioxide (CO_2) capture. Woodhead publishing. 2011:17-34.

Townsend A, Gillespie A. Scaling up the CCS market to deliver net-zero emissions. 2020 Thought leadership. Global CCS Institute. 2020.

Uday limestone. India. Accessed March 20, 2021. Link: https://www.indiamart.com/proddetail/rawlimestone-lumps-16215477362.html.

Uysal C, Kurt H, Kwak HY. Exergetic and thermos economic analyses of a coal-fired power plant. International journal of thermal sciences. 2017;117:106-20.

Van Dijk HA, Cohen D, Hakeem AA, Makkee M, Damen K. Validation of a water–gas shift reactor model based on a commercial FeCr catalyst for pre-combustion CO_2 capture in an IGCC power plant. International journal of greenhouse gas control. 2014;29:82-91.

Vankeirsbilck I, Vanslambrouck B, Gusev S, De Paepe M. Organic Rankine cycle as efficient alternative to steam cycle for small scale power generation. International conference on heat transfer, fluid mechanics and thermodynamics. 2011.

Versteeg P, Rubin ES. A technical and economic assessment of ammonia-based post-combustion CO_2 capture at coal-fired power plants. International journal of greenhouse gas control. 2011;5(6):1596-605.

Voldsund M, Jordal K, Anantharaman R. Hydrogen production with CO_2 capture. International journal of hydrogen energy. 2016;41(9):4969-92.

Vorrias I, Atsonios K, Nikolopoulos A, Nikolopoulos N, Grammelis P, Kakaras E. Calcium looping for CO_2 capture from a lignite fired power plant. Fuel. 2013;113:826-36.

Wang D, Chen S, Xu C, Xiang W. Energy and exergy analysis of a new hydrogen-fueled power plant based on calcium looping process. International journal of hydrogen energy. 2013;38(13):5389-400.

Wang J, Dai Y, Gao L. Exergy analyses and parametric optimizations for different cogeneration power plants in cement industry. Applied energy. 2009;86(6):941-48.

Wang W, Wang Y. Dry reforming of ethanol for hydrogen production: thermodynamic investigation. International journal of hydrogen energy. 2009;34(13):5382-89.

Wang X, Demirel Y. Feasibility of power and methanol production by an entrained-flow coal gasification system. Energy fuels. 2018;32(7):7595-610.

Wang Y, Zhao L, Otto A, Robinius M, Stolten D. A review of post-combustion CO_2 capture technologies from coal-fired power plants. Energy procedia. 2017;114:650-65.

Whitesides RW. Process equipment cost estimating by ratio and proportion. Course notes, PDH Course G127. 2005.

Wu F, Argyle MD, Dellenback PA, Fan M. Progress in O_2 separation for oxy-fuel combustion–A promising way for cost-effective CO_2 capture: A review. Progress in energy and combustion science. 2018;67:188-205.

Wu F, Dellenback PA, Fan M. Highly efficient and stable calcium looping based pre-combustion CO_2 capture for high-purity H_2 production. Materials today energy. 2019;13:233-8.

Wu W, Chen SC, Kuo PC, Chen SA. Design and optimization of stand-alone triple combined cycle systems using calcium looping technology. Journal of cleaner production. 2017;140:1049-59.

Wu Y, Blamey J, Anthony EJ, Fennell PS. Morphological changes of limestone sorbent particles during carbonation/calcination looping cycles in a thermogravimetric analyzer (TGA) and reactivation with steam. Energy and fuels. 2010;24:2768–76.

Xie W, Huang J, Liu J. Assessing thermal behaviors and kinetics of (co-) combustion of textile dyeing sludge and sugarcane bagasse. Applied thermal engineering. 2018;131:874-883.

Xin K, Hashish M, Roghair I, van Sint Annaland M. Process simulation and economic analysis of pre-combustion CO_2 capture with deep eutectic solvents. Frontiers in energy research. 2020;8:323.

Xiong YQ, Luo P, Hua B. Energy consumption analysis of air separation process for oxy-fuel combustion system. Advanced materials research. 2014;1033:146-50.

Xu J, Sun E, Li M, Liu H, Zhu B. Key issues and solution strategies for supercritical carbon dioxide coal fired power plant. Energy. 2018;157:227-46.

Yang K, Zhang H, Wang Z. Study of zeotropic mixtures of ORC (organic rankine cycle) under engine various operating conditions. Energy. 2013;58:494-510.

Yin F, Shah K, Zhou C. Novel calcium-looping-based biomass-integrated gasification combined cycle: thermodynamic modeling and experimental study. Energy and fuels. 2016;30(3): 1730-40.

Zhai R, Li C, Qi J, Yang Y. Thermodynamic analysis of CO_2 capture by calcium looping process driven by coal and concentrated solar power. Energy conversion and management. 2016;117:251-63.

Zhang X, Liu Y. Performance assessment of CO_2 capture with calcination carbonation reaction process driven by coal and concentrated solar power. Applied thermal engineering. 2014;70(1):13-24.

Zhao M, Shi J, Zhong X, Tian S, Blamey J, Jiang J, Fennell PS. A novel calcium looping absorbent incorporated with polymorphic spacers for hydrogen production and CO_2 capture. Energy and environmental science. 2014;7(10):3291-5.

Zhao Z, Su S, Si N, Hu S, Wang Y, Xu J, Jiang L, Chen G, Xiang J. Exergy analysis of the turbine system in a 1000 MW double reheat ultra-supercritical power plant. Energy. 2017;119:540-8.

Zheng C, Liu Z. Oxy-fuel combustion: fundamentals, theory and practice. Elsevier: academic Press. 2017

Zhou X, Yang X, Li J, Zhao J, Li C, Du M, Yu Z, Fang Y. Pressurized catalytic calcium looping hydrogen generation from coal with in-situ CO_2 capture. Energy conversion and management. 2019;198:111899.

Zhu Y, Li W, Li J, Li H, Wang Y, Li S. Thermodynamic analysis and economic assessment of biomass-fired organic rankine cycle combined heat and power system integrated with CO_2 capture. Energy conversion and management. 2020;204:112310.

Publications in Present Work

International Journals

(i) Based on the thesis

1. **Pillai BBK**, Surywanshi GD, Patnaikuni VS, Anne SB, Vooradi R. A novel calcium looping–integrated NGCC power plant configuration for carbon capture and utilization—Comprehensive performance analysis. International Journal of Energy Research. 2022 Feb;46(2):900-922. [SCI Impact Factor: 5.164]

2. **Pillai BBK**, Surywanshi GD, Patnaikuni VS, Anne SB, Vooradi R. Performance analysis of a double calcium looping-integrated biomass-fired power plant: Exploring a carbon reduction opportunity. International Journal of Energy Research. 2019 Aug;43(10):5301-5318. [SCI Impact Factor: 5.164]

(ii) Other/ co-authored journals

1. Surywanshi GD, **Pillai BBK**, Patnaikuni VS, Vooradi R, Anne SB. Energy and exergy analyses of chemical looping combustion-based 660 MWe supercritical coal-fired power plant. International Journal of Exergy. 2020;31(1):14-33. [SCI Impact Factor: 1.383]

2. Surywanshi GD, **Pillai BBK**, Patnaikuni VS, Vooradi R, Anne SB. Formic acid synthesis–a case study of CO_2 utilization from coal direct chemical looping combustion power plant. Energy Sources, Part A: Recovery, Utilization, and Environmental Effects. 2022 Mar 31. [SCI Impact Factor: 2.406]

3. Surywanshi GD, **Pillai BBK**, Patnaikuni VS, Vooradi R, Anne SB. 4-E analyses of chemical looping combustion based subcritical, supercritical and ultra-supercritical coal-fired power plants. Energy Conversion and Management. 2019 Nov 15;200:112050.;44(1):2220-35. [SCI Impact Factor: 9.709]

Conference Presentations

1. **Pillai BBK**, Surywanshi GD, Patnaikuni VS, Anne SB, Vooradi R, Energy analysis of sugarcane bagasse based biomass power plant integrated with calcium looping technology, 10th International Energy, Exergy and Environment Symposium (IEEES-10), Katowice, Poland, July 1-4, 2018.

2. **Pillai BBK**, Patnaikuni VS, Anne SB, Vooradi R, Integration of a calcium looping system for CO_2 capture in an Indian natural gas fired combined cycle power plant : A feasibility study, 2nd International Conference on Functional Materials and Chemical Engineering (ICFMCE 2018), Abu Dhabi, Nov 20-22, 2018.

3. **Pillai BBK**, Surywanshi GD, Patnaikuni VS, Anne SB, Vooradi R, Energy and Exergy Analysis of a Natural Gas Fired Combined Cycle Power Plant Integrated with Calcium Looping for CO_2 Capture in Indian Climatic Conditions, 2nd International Conference on New Frontiers in Chemical, Energy and Environmental Engineering (INCEEE- 2019), NIT Warangal, India, 15-16 February, 2019.

4. **Pillai BBK**, Surywanshi GD, Patnaikuni VS, Anne SB, Vooradi R. Integration of NGCC power plant with dry reforming of natural gas for Dimethyl ether production: CO_2 utilization approach, 11th International Energy, Exergy and Environment Symposium (IEEES-11), Chennai, July 14-18, 2019.